



Calhoun: The NPS Institutional Archive

Theses and Dissertations

Thesis Collection

2004-03

Interdicting electrical power grids

Alvarez, Rogelio E.

Monterey, California. Naval Postgraduate School

<http://hdl.handle.net/10945/1715>



Calhoun is a project of the Dudley Knox Library at NPS, furthering the precepts and goals of open government and government transparency. All information contained herein has been approved for release by the NPS Public Affairs Officer.

Dudley Knox Library / Naval Postgraduate School
411 Dyer Road / 1 University Circle
Monterey, California USA 93943

<http://www.nps.edu/library>



NAVAL POSTGRADUATE SCHOOL

MONTEREY, CALIFORNIA

THESIS

INTERDICTING ELECTRICAL POWER GRIDS

by

Rogelio E. Alvarez

March 2004

Thesis Advisor:
Second Reader:

Javier Salmeron
R. Kevin Wood

Approved for public release; distribution is unlimited

THIS PAGE INTENTIONALLY LEFT BLANK

REPORT DOCUMENTATION PAGE			Form Approved OMB No. 0704-0188	
Public reporting burden for this collection of information is estimated to average 1 hour per response, including the time for reviewing instruction, searching existing data sources, gathering and maintaining the data needed, and completing and reviewing the collection of information. Send comments regarding this burden estimate or any other aspect of this collection of information, including suggestions for reducing this burden, to Washington headquarters Services, Directorate for Information Operations and Reports, 1215 Jefferson Davis Highway, Suite 1204, Arlington, VA 22202-4302, and to the Office of Management and Budget, Paperwork Reduction Project (0704-0188) Washington DC 20503.				
1. AGENCY USE ONLY (Leave blank)		2. REPORT DATE March 2004	3. REPORT TYPE AND DATES COVERED Master's Thesis	
4. TITLE AND SUBTITLE: Interdicting Electrical Power Grids			5. FUNDING NUMBERS 2002-GT-R-057	
6. AUTHOR(S) Rogelio E. Alvarez			8. PERFORMING ORGANIZATION REPORT NUMBER	
7. PERFORMING ORGANIZATION NAME(S) AND ADDRESS(ES) Naval Postgraduate School Monterey, CA 93943-5000			10. SPONSORING/MONITORING AGENCY REPORT NUMBER	
9. SPONSORING /MONITORING AGENCY NAME(S) AND ADDRESS(ES) U.S. Department of Justice Office of Justice Programs 810 Seventh St., NW Washington, DC 20531			11. SUPPLEMENTARY NOTES The views expressed in this thesis are those of the author and do not reflect the official policy or position of the Department of Defense or the U.S. Government.	
12a. DISTRIBUTION / AVAILABILITY STATEMENT Approved for public release; distribution is unlimited			12b. DISTRIBUTION CODE	
13. ABSTRACT (maximum 200 words) This thesis explores Benders decomposition for solving interdiction problems on electric power grids, with applications to analyzing the vulnerability of such grids to terrorist attacks. We refine and extend some existing optimization models and algorithms and demonstrate the value of our techniques using standard reliability test networks from IEEE. Our implementation of Benders decomposition optimally solves any problem instance, in theory. However, run times increase as Benders' cuts are added to the master problem, and this has prompted additional research to increase the decomposition's efficiency. We demonstrate empirical speed ups by dropping slack cuts, solving a relaxed master problem in some iterations, and using integer but not necessarily optimal master-problem solutions. These mixed strategies drastically reduce computation times. For example, in one test case, we reduce the optimality gap, and the time that it takes to achieve this gap, from 16% in 75 hours to 5% in 16 minutes.				
14. SUBJECT TERMS Electric Power Grids; Network Interdiction; Mixed Integer Programming			15. NUMBER OF PAGES 121	
			16. PRICE CODE	
17. SECURITY CLASSIFICATION OF REPORT Unclassified	18. SECURITY CLASSIFICATION OF THIS PAGE Unclassified	19. SECURITY CLASSIFICATION OF ABSTRACT Unclassified	20. LIMITATION OF ABSTRACT UL	

NSN 7540-01-280-5500

Standard Form 298 (Rev. 2-89)
Prescribed by ANSI Std. Z39-18

THIS PAGE INTENTIONALLY LEFT BLANK

Approved for public release; distribution is unlimited

INTERDICTING ELECTRIC POWER GRIDS

Rogelio E. Alvarez
Lieutenant Commander, United States Navy
B.S., United States Naval Academy, 1991

Submitted in partial fulfillment of the
requirements for the degree of

MASTER OF SCIENCE IN OPERATIONS RESEARCH

from the

**NAVAL POSTGRADUATE SCHOOL
March 2004**

Author: Rogelio E. Alvarez

Approved by: Javier Salmeron
Thesis Advisor

R. Kevin Wood
Second Reader

James N. Eagle
Chairman, Department of Operations Research

THIS PAGE INTENTIONALLY LEFT BLANK

ABSTRACT

This thesis explores Benders decomposition for solving interdiction problems on electric power grids, with applications to analyzing the vulnerability of such grids to terrorist attacks. We refine and extend some existing optimization models and algorithms and demonstrate the value of our techniques using standard reliability test networks from IEEE.

Our implementation of Benders decomposition optimally solves any problem instance, in theory. However, run times increase as Benders' cuts are added to the master problem, and this has prompted additional research to increase the decomposition's efficiency. We demonstrate empirical speed ups by dropping slack cuts, solving a relaxed master problem in some iterations, and using integer but not necessarily optimal master-problem solutions. These mixed strategies drastically reduce computation times. For example, in one test case, we reduce the optimality gap, and the time that it takes to achieve this gap, from 16% in 75 hours to 5% in 16 minutes.

THIS PAGE INTENTIONALLY LEFT BLANK

DISCLAIMER

The reader is cautioned that computer programs developed in this research may not have been exercised for all cases of interest. While every effort has been made to ensure that the programs are free of computational and logic errors, they cannot be considered fully validated. Any application of these programs without the additional verification is at the risk of the planner.

THIS PAGE INTENTIONALLY LEFT BLANK

TABLE OF CONTENTS

I.	INTRODUCTION.....	1
A.	THE ELECTRIC POWER GRID IN THE U.S.	1
B.	THESIS OUTLINE.....	4
II.	PRELIMINARIES	5
A.	INTRODUCTION TO DCOPF	5
B.	THE INTERDICTION MODEL WITHOUT SYSTEM RESTORATION	8
1.	Interdiction Model.....	8
2.	Heuristic Approach.....	9
3.	The MIP Approach	10
a.	Overview	10
b.	Derivation	10
C.	INTERDICTION MODEL WITH SYSTEM RESTORATION	13
1.	System Restoration	13
2.	Interdiction Model.....	14
3.	Heuristic Approach.....	15
a.	Description	15
4.	The MIP Model.....	16
a.	Overview	16
b.	Derivation	17
D.	BENDERS DECOMPOSITION	17
E.	DECOMPOSITION ALGORITHM	20
III.	VALIDATING THE DC POWER FLOW MODEL	25
A.	INTRODUCTION.....	25
B.	DCOPF VS. ACPF IN THE ABSENCE OF INTERDICTION.....	26
C.	DCOPF VS. ACPF AFTER INTERDICTION	29
IV.	BENDERS DECOMPOSITION FOR THE PROBLEM WITHOUT SYSTEM RESTORATION	33
A.	SMALL TEST CASE PROBLEM DERIVATION	33
1.	Description	33
2.	Mathematical Formulation	34
B.	BENDERS DECOMPOSITION: GENERAL INTERDICTION PROBLEM WITHOUT SYSTEM RESTORATION	42
C.	RESULTS.....	42
V.	BENDERS DECOMPOSITION FOR THE PROBLEM WITH SYSTEM RESTORATION	45
A.	FORMULATION	45
B.	RESULTS.....	46
VI.	ALGORITHM REFINEMENTS AND RESULTS	49
A.	INTRODUCTION.....	49

B.	RELAXING THE MASTER PROBLEM.....	51
C.	CUT-DROPPING STRATEGIES.....	57
1.	Dropping All Non-active Cuts.....	57
2.	Dropping Non-LP Active Cuts	59
3.	Dropping the First Slack Cut	59
4.	Keeping the n -Most Active Cuts	60
D.	SUB-OPTIMAL INTEGER SOLUTIONS.....	61
E.	COMBINED STRATEGY	63
VII.	CONCLUSIONS AND RECOMMENDATIONS FOR FURTHER RESEARCH.....	65
A.	CONCLUSIONS.....	65
B.	RECOMMENDATIONS FOR FURTHER RESEARCH	66
	LIST OF REFERENCES.....	69
	APPENDICES.....	71
APPENDIX A:	MIP MODEL WITHOUT SYSTEM RESTORATION	71
A.1	The Interdiction Model (I-DCOPF)	71
A.2	The Dual Interdiction Model, DI-DCOPF.....	73
A.3	Linearization of DI-DCOPF	75
A.4	The Master Problem	79
APPENDIX B:	MIP MODEL WITH SYSTEM RESTORATION	81
B.1	Constructing Time Periods, and Additional Notation.....	81
B.2	The Interdiction Model, I-DCOPF-R.....	83
B.3	The Dual Interdiction Model, DI-DCOPF-R.....	85
B.4	Linearization of DI-DCOPF-R	86
B.5	The Master Problem	90
APPENDIX C:	LINEARIZATION OF CROSS-PRODUCTS.....	93
	INITIAL DISTRIBUTION LIST	97

LIST OF FIGURES

Figure 1.	Framework for a heuristic interdiction algorithm.	10
Figure 2.	Power disruption and energy disruption.	14
Figure 3.	Interdiction algorithm framework with restoration.	16
Figure 4.	Benders Decomposition Algorithm flowchart.	22
Figure 5.	IEEE RTS One Area case one-line diagram without interdiction.	27
Figure 6.	Effects of interdiction to IEEE RTS One Area case.	30
Figure 7.	Three-bus example.	33
Figure 8.	Convergence of Benders decomposition for the three-bus case.	41
Figure 9.	IEEE RTS One Area case without system restoration: Convergence.	43
Figure 10.	IEEE RTS One Area case without system restoration: Time versus Iteration.	44
Figure 11.	IEEE RTS One Area case with system restoration: Convergence. ...	46
Figure 12.	IEEE RTS One Area case with system restoration: Cumulative time.	47
Figure 13.	IEEE RTS Two Area case with system restoration: Solution trajectory.	48
Figure 14.	Benders Decomposition Algorithm (with refinements) flowchart.	50
Figure 15.	Relaxed master problem strategy: Convergence (I).	52
Figure 16.	Relaxed master problem strategy: Time versus iteration (I).	53
Figure 17.	Relaxed master problem strategy: Convergence (II).	54
Figure 18.	Relaxed master problem strategy: Time versus iteration (II).	55
Figure 19.	Relaxed master problem strategy: Convergence and Time versus Iteration (III).	56
Figure 20.	Dropping non-active cuts: Convergence.	59
Figure 21.	Keeping the n -most active cuts: Convergence.	61
Figure 22.	Master problem sub-optimal solution strategy: Convergence.	62
Figure 23.	Combined strategy, n -most active cuts with relaxed-MP.	64

THIS PAGE INTENTIONALLY LEFT BLANK

LIST OF TABLES

Table 1.	ACPF versus DCOPF: IEEE RTS One Area case (no interdiction).	29
Table 2.	PWS's ACPF versus DCOPF: IEEE RTS One Area case, scenario $M=6$.	31
Table 3.	Overall comparison of power flows provided by DCOPF and PWS.	32
Table 4.	Combined strategies: n -most active cuts with relaxed-MP.	63

THIS PAGE INTENTIONALLY LEFT BLANK

ACKNOWLEDGMENTS

I would like to acknowledge the faculty at the Naval Postgraduate School, who provided me with the knowledge to embark on this work. Specifically, Professor Javier Salmeron, who played a major role in my decision to work on this optimization project and provided the ground work and direction to see it through. His tireless dedication and patience made it all possible. You have been an outstanding advisor; I couldn't have done it without you.

Secondly, I would like to thank Professor Kevin Wood whose professionalism, demanding nature and analytic insight ensured the highest quality end product was achieved. His reputation and expertise were assurance that a great thesis would result.

Finally, I would like to thank my family, who supported me during this challenging time, specially my wife Jacqueline who held together our home while I embarked on this study, and my mother Isabel whose encouragement and prayers have guaranteed all my life's successes. Thank you all.

THIS PAGE INTENTIONALLY LEFT BLANK

EXECUTIVE SUMMARY

This thesis extends existing optimization models and methods for analyzing the vulnerability of electric power grids to terrorist attacks.

Electric power systems are critical to the United States' economy and security. After the events of September 11, 2001, and the United States' ensuing war against terrorism, the fear of retaliation against critical infrastructures has become a major concern for security analysts. The vulnerability of the electric power systems to physical disruptions heads the list of concerns, because the U.S. transmission grid has not expanded as quickly as demand has over the last decade, and thus the system has become "brittle." This brittleness (vulnerability) became more evident on 14 August 2003 when a relatively modest number of system malfunctions caused a blackout of the northeastern region of the country, and raises this question: How much worse might the blackout have been had it resulted from a well-planned terrorist attack?

This thesis first considers certain modeling issues of the problem of optimal interdiction, and then focuses on techniques for solving the proposed models. This should help us identify the most critical components of the U.S. power grid, and ultimately help determine effective protective measures to improve the system's robustness.

We refine and extend the existing optimization models and algorithms of Salmeron et al. that identify critical system components (e.g., transmission lines) by creating maximally disruptive attack plans for terrorists, who are assumed to have limited offensive resources. Most importantly, this thesis exploits bi-level structures embedded in the interdiction models to enable faster solutions through the use of Benders decomposition.

We first validate the DC power-flow model that underlies in the interdiction models. By manipulating a few equations, the inherent nonlinearities in these models are substituted by linear forms, converting those models into (linear)

mixed-integer problems (MIPs). We explore Benders decomposition for solving the MIPs, and successfully apply it to two standard reliability test networks from IEEE.

Although we solve the IEEE test cases to optimality, we notice that the efficiency of the Benders' master problem deteriorates as (a) the number of components in the test cases increases, and (b) the number of Benders' cuts in the master problem grows. We investigate several techniques in order to improve the algorithm's speed. First, we demonstrate faster convergence by solving the mixed-integer master problem exactly every k^{th} iteration only, and solving its easier, linear-programming relaxation otherwise. Importantly, the algorithm thus modified always maintains a valid upper (optimistic) bound, just as the original does. Since relaxed (non-integer) master-problem solutions cannot be used by the subproblems to compute lower (pessimistic) bounds, we exploit sub-optimal integer solutions to the master problem every m^{th} iteration to improve the lower bound. In one of our two test networks, this combined techniques reduce computational time by one third. We also show that limiting the number of cuts in the master problem can speed convergence, and study several strategies for keeping or deleting cuts. Results are mixed, but improvements can be dramatic. For example, in the second of our test networks, by limiting the number of cuts to 500 and solving a relaxed master problem nine of every ten iterations, we achieve an optimality gap under 5% in 16 minutes; this compares to a 16% gap in 75 hours using the original decomposition algorithm

GLOSSARY

The following briefly defines the general concepts related to electric power networks and interdiction. Some of these definitions are from (or strongly based on) the glossaries provided by Energy Information Administration (EIA 2003), Elec-Saver (2003) and SIEMENS(2004).

AC Power: *Power* associated with *alternating current* circuits.

Admittance: Property that allows the flow of electrical *current* through reactive circuit elements under the action of a potential difference. Admittance is the reciprocal of *impedance*. Admittance equations establish the relationship between *current*, *impedance* and *voltage*.

Alternating Current: *Current* that periodically reverses direction.

Bus (or Busbar): A heavy, rigid electrical conductor that makes a common connection between several electrical circuits.

Capacitance: The property of a circuit that allows it to store an electrical charge.

Case: A set of data to be analyzed, along with the results of the analysis. Data consists of *power* grid components (*lines*, *buses*, *generators*, *substations*, etc), physical data (i.e., such as line *impedances*, generating capacities, etc.), non-physical data (e.g., interdiction *resource*, optimization parameters, etc.). Results include the *interdicted* components, associated *generation* and *power* flows, and *load* shedding for every *period*, among others.

Costumer Sector: A type of *load* with specific requirements (e.g., amount of *power* demand and cost for failing to provide it).

Current: The flow of electrons in a circuit. Current is measured in amperes.

DC Power: *Power* associated with *direct current* circuits.

Direct Current: *Current* that flows in one direction

Disruption: The cost of *power* shed (in dollars per hour) or the cost of *energy shed* (in dollars), as a consequence of interdiction.

Energy: The result of integrating *power* over time.

Energy Shed: Amount of *energy* that cannot be supplied to the load (one or several *customer sectors*) over the course of a given *period*.

Generation (of electricity): The production of electric energy through the transformation of other forms of energy. The amount of electric energy produced.

Generating Unit (or Generator): Any combination of physically connected generator(s), reactor(s), boiler(s), combustion turbine(s), or other prime mover(s) operated together to produce electric *power*.

Impedance: The total opposition to *alternating current*. Impedance is the vector sum of *resistance* and *reactance*. The unit for impedance is the ohm.

Inductance: The property of an electrical circuit that causes it to oppose changes in *current*.

Interdiction Plan: Specific subset of the electric system equipment that might be interdicted by terrorists. Optimal or near-optimal *interdiction plans* are identified in for given *interdiction-resource scenarios*.

Interdiction Resource: A numerical value associated with a mathematical expression that represents the capacity of terrorists to carry out attacks. For example if such an expression has the form: $(3 \times \text{total number of attacks to buses}) + (1 \times \text{total number of attacks to lines}) \leq 5$, then “5” is the interdiction resource.

Line: See “Transmission Line.”

Load: Demand for electric *power*, measured in *watts*, at a specific point in time.

One-line Diagram: Schematic drawing of an electrical *power* system that uses graphical symbols to represent electrical equipment such as *buses*, *generators*, *loads*, *transmission lines* and *transformers*. It may incorporate numerical values for the system, such as line *power* flows, generating unit outputs, *bus* voltages, etc.

Phase angle: The angle by which the sine curve of the voltage in a circuit element (or a combination of elements) leads or lags the sine curve of the *current* in that circuit element(s).

Period (of restoration): Each of the stages that an electric power network undergoes following an attack, as *interdicted* components are repaired or replaced over time.

Power (transmission): The transfer rate for *energy*. Unit of measurement is watts. Power is sometimes used loosely to refer to electricity.

Power Shed: Amount of *power* that cannot be supplied to a *load* or loads (one or several *customer sectors*) at a specific point in time.

Reactance: Opposition to the flow of *alternating current*. Measured in *ohms*.

Reactive Power: Power associated with *inductance* or *capacitance*.

Resistance: The propensity of a circuit to oppose *current* flow. It is measured in *ohms*.

Scenario: A particular value of the *interdiction resource*. In our formulation, we analyze the worst-possible *Interdiction Plans* for a given scenario.

Slack Bus: (Also called swing bus.) A bus whose (initially unspecified) power generation must be determined in order to match supply and demand in the network.

Substation: Facility with equipment that switches, changes, or regulates electric voltage and *current*.

Transformer: A static electrical device which, by electromagnetic induction, regenerates AC *power* from one circuit into another and/or changes the voltage of *alternating current*.

Transmission: The movement or transfer of electric energy over an interconnected group of lines and associated equipment between points of supply and points at which it is transformed for delivery to consumers, or is delivered to other electric systems. Transmission is considered to end when the energy is transformed for distribution to the consumer.

Transmission Line (High-voltage): The high-voltage (≥ 69 kV in the U.S.) conductors used to carry electrical *energy* from one location to another.

Transmission System (also referred to as Electric Power Grid and Electric Network in this thesis): An interconnected group of electric *transmission lines* and associated equipment for moving or transferring electric energy in bulk between points of supply and points at which it is transformed for delivery over a lower-voltage distribution system to consumers, or is delivered to other electric systems.

I. INTRODUCTION

This research continues the development of mathematical models and optimization methods for planning electrical power grids that are robust to terrorist attacks. We focus on solving an interdiction model, which is represented as a mixed-integer program (MIP), through the use of Benders decomposition.

A. THE ELECTRIC POWER GRID IN THE U.S.

The electric power grid in the United States (U.S.) consists of over 10,000 generating units with a total production in excess of 760 giga-watts (GW), and over 700,000 miles of transmission lines, all controlled by approximately 100 control centers. (Actually, only modest interconnection capacity exists between three main sub-systems in this grid, namely the Eastern interconnection, the Western interconnection and the Texas interconnection. Therefore, “the U.S. power grid” may be viewed as three, nearly independent systems.)

In the past, utilities have been concerned with the grid’s vulnerabilities to isolated natural disasters and unscheduled, technical outages caused by equipment failures. To date, protecting the electric grid against multiple, nearly simultaneous failures has not been a high priority for utilities because of the expense involved and the relatively low frequency of such events. However, in the current era, a set of nearly simultaneous failures might be the precise objective of a terrorist attack. “Low frequency” may no longer be so slow.

As a result of the threat that terrorism currently poses to critical infrastructure of all types in the U.S., understanding the physical vulnerability of the electric grid has become more important not only for the electric power industry, but also for national security (NSTAC 1997). In fact, a National Security Assessment (1997) states that man-made physical destruction is the greatest threat facing the electric power infrastructure.

The U.S. electric power grid is plagued by a number of inherent weaknesses. Among the most significant of these weaknesses are the traversals

of sparsely populated areas, which readily expose the system to malicious attacks, and the decreasing reserve in transmission capacity.

The U.S. transmission network is built with some redundancy and multiple protective devices; however, current reserve levels in transmission capacity may be insufficient to back up multiple failures in some key components, as exemplified by the 14 August 2003 power-system failure (which cost our national economy between \$7 and \$10 billion dollars; ICF Consulting 2003). Not surprisingly, this failure brings additional speculation about terrorist threats to the U.S. power grid (Germain 2003), and raises important questions about the resilience of the U.S. power grid and the possibility of widespread loss of power to customers.

The August 14th blackout could be financially insignificant when compared to the effects of a coordinated terrorist attack on several key facilities during a period of peak load. ICF Consulting (2003), which analyzed the cost of the August 14th blackout, states that a terror-induced blackout could prove significantly more costly and have debilitating impacts on the affected region as well as the entire country. Additionally, a simulated terrorist attack on the Pacific Northwest's power grid was recently conducted under the project name "Blue Cascades." An analysis of that simulated attack showed that a real attack, if successful, could wreak havoc on the nation's economy, shutting down power and productivity in a domino effect that would last for weeks (Allen 2003).

The discussion above motivates the development of optimization models to represent the problem of terrorists attacking a power grid. By studying how to attack power grids, one can gain insight on how to protect them.

This research follows Salmeron et al. (2003, 2004), who develop bi-level mathematical models to identify maximally disruptive attacks for terrorists, who are assumed to have full access to power-system data, but limited offensive resources. Salmeron et al. initially introduce a static interdiction model and then extend it to capture the dynamics of system operation as the grid is repaired after an attack (which can make slow-to-repair grid components more attractive

targets). An attack is optimal in the first model if it maximizes the total, instantaneous, unserved demand for power; in the extended model, it is optimal if it maximizes the total cost of unserved demand for energy. These models have been tested using standard reliability test systems (RTSs) drawn from IEEE (1999-I, 1999-II).

This thesis makes no attempt to extend the modeling approach for power flows used by Salmeron et al. Thus, some values representing power-system behavior (such as reactive power flows, line losses, voltage magnitudes, transformer tap positions, etc.) are still disregarded and/or are assumed fixed in this work. However, we assess the accuracy of that approach by comparing results from our approximating “DC power-flow model” with those provided by a full AC power-flow model. We use the AC model embedded in the PowerWorld Simulator (PowerWorld 2003) to carry out this comparison.

Salmeron et al. (2003) propose heuristic algorithms for finding an approximate solution to their interdiction models. These heuristic solutions are generally within 10% of optimality but in some instances that gap can reach 25%. The possibility of large gaps was discovered after publication of the referenced paper, when the authors were able to solve equivalent Mixed Integer Linear Program (MIP) formulations exactly (Salmeron et al. 2004). These MIP formulations have been reviewed and consolidated in the framework of this thesis

In theory, a MIP can be solved exactly by standard techniques such as “branch-and-bound” (e.g., Wolsey 1998, pp. 95-107). However, these techniques cannot always solve the large-scale problems found in practice, and this motivates the search for alternative techniques with better scalability. Benders decomposition (Benders 1962) is a well-known method for solving large-scale MIP models, and this thesis investigates its use to solve the interdiction problem efficiently. Previous application of Benders decomposition to interdiction problems can be found in Cormican (1995) and Israeli and Wood (2002).

B. THESIS OUTLINE

Subsequent chapters in this thesis are organized as follows: Chapter II introduces the DC power-flow model that is the basis for the interdiction model. It also defines the interdiction model and presents the heuristic and MIP approaches developed previous to this work to solve the problem. Finally, Chapter II introduces Benders decomposition and its associated algorithm in the framework of our interdiction problem. Chapter III validates the DC power-flow model through comparison with an AC power-flow model. We compare power flows for different interdiction plans on IEEE's "One Area RTS." Chapter IV details the application of Benders decomposition to our interdiction model. A three-bus example demonstrates the decomposition process, which is then applied to the interdiction problem without system restoration. Computational results are presented. Chapter V presents the Benders decomposition for the interdiction model with system restoration over time. Chapter VI discusses refinements to the algorithm and provides computational results. Chapter VII summarizes results and recommends topics for future work. Appendices A and B show the full derivation of the interdiction models, which are introduced in Chapter II and further described in Chapters IV and V. Appendix C describes the linearization of cross products for the three-bus problem developed in Chapter IV.

II. PRELIMINARIES

This chapter introduces the DC Optimal Power Flow model (DCOPF) that is the basis for the development of two interdiction models: without system restoration (see Section B), and including system restoration (see Section C). Both Sections B and C describe heuristic and MIP approaches explored prior to this research for solving the interdiction models. Section D introduces Benders decomposition in the context of our models.

A. INTRODUCTION TO DCOPF

At the heart of the interdiction models is a DC power-flow model (DCPF), so we first provide some background on this and related models. DCPF simplifies the so-called “full AC power-flow model” (ACPF), which is generally accepted as a valid representation of power flows under steady-state conditions and symmetry (Frauendorfer et al. 1993). The DCPF representation entails various assumptions which may be acceptable in the context of security analysis (Wood and Wollenberg 1996). For example, DCPF disregards reactive power effects and assumes nominal voltage magnitudes at the buses.

DCPF can be used to construct an optimization problem, DCOPF, which optimizes a merit function subject to DCPF constraints. The merit function typically measures generating costs. In contrast, our DCOPF not only minimizes generation costs, but also the penalty associated with unmet demand (“load shed”), because we cannot guarantee that all demand will be met in the presence of interdiction. The DCOPF formulation from Salmeron et al. (2003) is presented below for completeness. (Definitions of terms can be found in the glossary.)

Sets:

$i \in I$, set of buses

$g \in G$, set of generating units

- $l \in L$, set of transmission lines
 $c \in C$, set of consumer sectors
 $s \in S$, set of substations
 $i \in I_s$, subset of buses at substation s
 $g \in G_i$, subset of generating units connected to bus i
 $l \in L_i^{Bus}$, subset of lines connected to bus i
 $l \in L_s^{Sub}$, subset of lines connected to substation s (including transformers, which are represented by lines)
 $G^* \subseteq G$, $L^* \subseteq L$, $I^* \subseteq I$, $S^* \subseteq S$, interdictable generators, lines, buses, and substations, respectively. These are “interdictable components.”

Parameters (units, if applicable):

- $o(l), d(l)$, origin and destination buses of line l respectively (more than one line with the same $o(l)$, $d(l)$ may exist).
 $i(g)$, bus for generator g , i.e., $g \in G_{i(g)}$
 $s(i)$, substation $s \in S$ associated with bus $i \in I_s$
 d_{ic} , load of consumer sector c at bus i (MW)
 \bar{P}_l^{Line} , transmission capacity for line l (MW)
 \bar{P}_g^{Gen} , maximum output from generator g (MW)
 r_l, x_l , resistance, and reactance of line l respectively (Ω). (We assume $x_l \gg r_l$)
 B_l , series susceptance, calculated as $B_l = x_l / (r_l^2 + x_l^2)$ ($1/\Omega$)

h_g , generation cost for unit g (\$/MWh)

f_{ic} , load-shedding cost for customer sector c at bus i (\$/MWh)

Decision variables (units):

P_g^{Gen} , generation from unit g (MW)

P_l^{Line} , power flow on line l (MW)

S_{ic} , load shed (unmet) for customer sector c at bus i (MW)

θ_i , phase angle at bus i (radians)

Remark: All units are converted to per unit (p.u.) values for a base load of 100 MW. (Remark: We use this same value in all implemented models.) For example, to convert r_l to per-unit values, we consider the transmission line (l) nominal voltage rating E_l (in kV). Then:

$$r_l \text{ (per unit)} = r_l \text{ (ohms)} \times 100 \text{ (MW)} / (\text{line rating(kV)})^2 =$$

$$\frac{100r_l}{E_l^2} \left(\frac{\text{MVA } \Omega}{(\text{kV})^2} \right) = \frac{100r_l}{E_l^2} \left(\frac{\cancel{\text{MVA}} \Omega}{(\cancel{\text{K}}^2 \cancel{\text{KV}})} \right) = \frac{100r_l}{E_l^2} \left(\frac{\text{A } \Omega}{\text{V}} \right) = \frac{100r_l}{E_l^2} \text{ p.u. (since } 1\text{V}=1\text{A} \times 1\Omega)$$

The same process is carried out for reactance (x_l) conversions. For the rest of MW magnitudes, we use per-unit values after dividing by the 100 MW base load.

The formulation of DCOPF is:

$$(\text{DCOPF}): \min_{P^{Gen}, P^{Line}, S, \theta} \sum_g h_g P_g^{Gen} + \sum_i \sum_c f_{ic} S_{ic}$$

s.t.

$$P_l^{Line} = B_l (\theta_{o(l)} - \theta_{d(l)}) \quad \forall l \in L \quad (2.1)$$

$$\sum_g P_g^{Gen} - \sum_{l|o(l)=i} P_l^{Line} + \sum_{l|d(l)=i} P_l^{Line} = \sum_c (d_{ic} - S_{ic}) \quad \forall i \quad (2.2)$$

$$-\bar{P}_l^{Line} \leq P_l^{Line} \leq \bar{P}_l^{Line} \quad \forall l \in L \quad (2.3)$$

$$\underline{P}_g^{Gen} \leq P_g^{Gen} \leq \bar{P}_g^{Gen} \quad \forall i, \forall g \in G_i \quad (2.4)$$

$$0 \leq S_{ic} \leq d_{ic} \quad \forall i, c \quad (2.5)$$

This model assumes fixed (nominal) voltage magnitudes and does not represent shunts, reactive power flows, power losses, DC lines, transformer tap positions, phase transformers, and other features that could destroy the linear structure of the approximation. Discrepancies in power flows in DCOPF and a full ACPF are discussed in Chapter III.

B. THE INTERDICTION MODEL WITHOUT SYSTEM RESTORATION

1. Interdiction Model

After some manipulation, DCOPF above can be stated in standard form as:

$$\begin{aligned} \text{(DCOPF): } \min_y & c^T y \\ \text{s.t. } & Ay = b \\ & y \geq 0 \end{aligned} \quad (2.6)$$

where y represents generation outputs, load shedding, power flows and phase angles variables, along with slack variables associated with constraints (2.3)-(2.5).

The interdiction model extends (2.6) in order to choose the most disruptive, resource-constrained interdiction plan, $\delta \in \Delta$, where Δ is a set of binary vectors representing possible terrorist attack plans. An interdiction plan is represented by the binary vector δ , where δ_e is 1 if component e of the power grid is attacked and is 0 otherwise. We assume that terrorists attempt to maximize the minimum post-interdiction “disruption” which is measured as the generating cost plus the load-shedding cost (penalty) evaluated by DCOPF.

A simple representation of the max-min Interdiction of the DCOPF (I-DCOPF) model is shown below:

$$\begin{aligned}
(\text{I-DCOPF}) : \max_{\delta \in \Delta} \min_y c y \\
\text{s.t. } g(\delta, y) = 0 \\
y \geq 0
\end{aligned} \tag{2.7}$$

where $g(\delta, y)$ represents a set of constraints, some of which involve functions that are nonlinear in (δ, y) (see Appendix A.1). For a given interdiction plan, $\hat{\delta}$, the inner minimization is still a DCOPF model which is, of course, linear in y .

Prior to this thesis, model (2.7) was tackled by (a) using a heuristic algorithm and by (b) reformulating (2.7) as a MIP which was solved with a standard solver. This thesis contributes to (b) by refining the MIP formulation that serves as basis for the Benders decomposition approach. In order to place this thesis' contributions in context, the following two subsections summarize approaches (a) and (b).

2. Heuristic Approach

A heuristic algorithm introduced by Salmeron et al. (2003) solves model (2.7) approximately, and has been tested using small- and medium-scale networks drawn from the IEEE Reliability Test Data (1999-I, 1999-II). This heuristic solves DCOPF for a given grid configuration (i.e., for a given interdiction plan). Then it assigns “values” to interdictable electrical components in the grid (lines, buses, substations, etc.) based on present and previous flow patterns associated with the components. Finally, the heuristic maximizes the value of the components to be interdicted while excluding previously explored solutions. This process is repeated for a pre-specified number of iterations. This decomposition-based approach has been empirically proven to obtain good, but not necessarily optimal, interdiction plans. Figure 1 depicts the basic cycle of the algorithm. Additional details on the heuristic can be found in the cited reference.

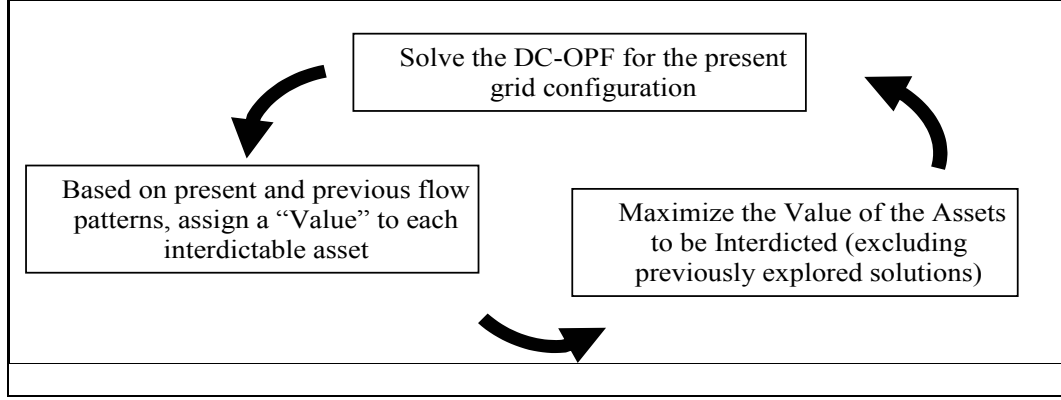


Figure 1. Framework for a heuristic interdiction algorithm. (From Salmeron et al. 2003.)

The inability to prove optimality of the heuristic solution (unless all possible solutions are enumerated explicitly) has led to the search for alternative representations of (2.7) that are amenable to solution by MIP techniques, such as branch-and-bound, as described in the following section.

3. The MIP Approach

a. Overview

The development of a MIP model enables validation of the heuristic solution and the development of exact decomposition algorithms that are frequently used solve large-scale problems. (Typically the solutions are approximate, but then large-scale systems are almost never solved exactly by any technique.) The derivation of the MIP begins with the linearization of constraints in $g(\delta, y) = 0$, followed by the dualization of the inner minimization problem in (2.7). This procedure converts the max-min problem into a nonlinear maximization problem which is linearized through additional steps. Both of these linearization techniques are fully explained in Salmeron et al. (2004), but are briefly described in the following for continuity.

b. Derivation

The nonlinearities in the expression of $g(\delta, y) = 0$ in model (2.7) are associated with admittance equations in the presence of interdiction variables δ . These have the form:

$$P_l^{Line} = (1 - \delta_l^{Line})(1 - \delta_{o(l)}^{Bus})(1 - \delta_{d(l)}^{Bus}) \left(\prod_{s|l \in L_s} (1 - \delta_s^{Sub}) \right) B_l (\theta_{o(l)} - \theta_{d(l)}), \forall l \in L \quad (2.8)$$

Note that in the interdiction model, the original admittance equation (DC.1) for every interdictable line l is modified as (2.8) to account for potential interdiction (directly or indirectly) of the line, in which case the admittance equation should not be enforced. This leads to nonlinearities in the form of multiple cross-products.

Following Salmeron et al. (2004), (2.8) can be fully linearized. For example, one can convert the nonlinear constraint $P = B(\theta_a - \theta_b)(1 - \delta_1)(1 - \delta_2)$ into the following two linear inequalities:

$$\begin{aligned} P - B(\theta_a - \theta_b) &\leq M(\delta_1 + \delta_2) \\ P - B(\theta_a - \theta_b) &\geq -M(\delta_1 + \delta_2) \end{aligned} \quad (2.9)$$

Here, $M = \bar{P} + B\bar{\theta}$, where $\bar{\theta}$ is an upper bound on the maximum phase angle difference between buses a and b . (2.9) enforces $P = B(\theta_a - \theta_b)$ when all the related δ -variables are 0, and eliminates the constraint when any of these δ variables is 1. The resulting model is still called I-DCOPF in this thesis, and is specified in detail in Appendix A.1.

We proceed by taking the dual of the inner minimization in (2.7), assuming constraints in $g(\delta, y) = 0$ have been linearized as described above. This converts the max-min problem into a simple maximization. The resulting model is called DI-DCOPF (“Dual of I-DCOPF,” although only the inner minimization is dualized). The full formulation is given in Appendix A.2. This model’s objective function consists of a linear function of continuous vector π , along with nonlinear costs involving cross-products of type $\delta\pi$. The new variables π correspond to duals of each of the balance and bound constraints in I-DCOPF. The terms associated with the $\delta\pi$ products arise from the line and generator capacity constraints.

The resulting problem can be stated, in brief, as:

$$\begin{aligned}
 (\text{DI-DCOPF}): \quad & \max_{\delta \in \Delta} \max_{\pi} b^{\pi} \pi + b^v v \\
 \text{s.t.} \quad & A\pi \leq c \quad (y) \\
 & v \in V(\delta, \pi)
 \end{aligned} \tag{2.10}$$

Here, b^{π} and b^v are appropriately dimensioned coefficient vectors, π is a vector of dual variables to constraints in I-DCOPF and v is a vector where each component is the result of a cross product of a variable δ and a variable π . Variables in parentheses, here and elsewhere, are dual variables for the associated constraints; in this case the variables are y .

To linearize a cross-product involving a δ -variable and a π -variable, we create an intermediate variable, e.g., $v_{jk} = \delta_j \pi_k$, with the property that, $\delta_j = 0 \Rightarrow v_{jk} = 0$, and $\delta_j = 1 \Rightarrow v_{jk} = \pi_k$. Since the sign of π_k is known (assume $\pi_k \geq 0$ for demonstration purposes), we add the following linear constraints, represented as $v \in V(\delta, \pi)$, to ensure the above relationships between δ_j , π_k , and v_{jk} hold:

$$v_{jk} = \delta_j \pi_k \equiv \begin{cases} v_{jk} \leq \bar{\pi}_k \delta_j \\ v_{jk} \leq \pi_k \\ v_{jk} \geq \pi_k - \bar{\pi}_k (1 - \delta_j) \\ 0 \leq \pi_k \leq \bar{\pi}_k \\ v_{jk} \geq 0, \end{cases} \tag{2.11}$$

where $\bar{\pi}_k$ is an appropriate upper bound on π_k .

Let us drop the (j, k) subindices for simplicity. Then, the following scheme depicts the validity of the representation in (2.11):

$$v \in V(\delta, \pi) \equiv \left\{ \begin{array}{l} v \leq \bar{\pi}\delta \\ v \leq \pi \\ v \geq \pi - \bar{\pi}(1-\delta) \\ 0 \leq \pi \leq \bar{\pi} \\ v \geq 0 \end{array} \right\} \rightarrow \left\{ \begin{array}{l} \delta = 0 \Rightarrow \left\{ \begin{array}{l} v \leq 0 \\ v \leq \pi \\ v \geq \pi - \bar{\pi} \\ 0 \leq \pi \leq \bar{\pi} \\ v \geq 0 \end{array} \right\} \Rightarrow \left\{ \begin{array}{l} v = 0 \\ \pi \in [0, \bar{\pi}] \end{array} \right. \\ \delta = 1 \Rightarrow \left\{ \begin{array}{l} v \leq \bar{\pi} \\ v \leq \pi \\ v \geq \pi \\ 0 \leq \pi \leq \bar{\pi} \\ v \geq 0 \end{array} \right\} \Rightarrow \left\{ \begin{array}{l} v = \pi \\ \pi \in [0, \bar{\pi}] \end{array} \right. \end{array} \right. \quad (2.12)$$

Remark: When $\pi \leq 0$, the linearization is carried out as:

$$v_{jk} = \delta_j \pi_k \equiv \left\{ \begin{array}{l} v_{jk} \geq -\bar{\pi}_k \delta_j \\ v_{jk} \geq \pi_k \\ v_{jk} \leq \pi_k + \bar{\pi}_k (1 - \delta_j) \\ -\bar{\pi}_k \leq \pi_k \leq 0 \\ v_{jk} \leq 0 \end{array} \right. \quad (2.13)$$

Finally, generation phase angles, power flows and load shedding are jointly denoted by the dual variable y .

The dualization and linearization described above allow us to represent the interdiction problem as a MIP. The resulting model is called LDI-DCOPF (Linearization of DI-DCOPF; see Appendix A.3).

C. INTERDICTION MODEL WITH SYSTEM RESTORATION

1. System Restoration

The model described in Section B is a static representation of power disruptions at a given point in time. That model does not represent the consequences of the variability in repair times of damaged system components and the increased cost of load shedding resulting from repair-time delays. Unless the outage duration of each interdictable component is the same, the interdiction model presented in Section B cannot capture this effect. For

example, Salmeron et al. (2003) show that if the interdicator's decisions are driven by the goal of maximizing short-term power shedding (or its hourly cost), the resulting interdiction plan might be far from optimal had his or her goal been maximizing total energy shed (or its cost) until the system repair is completed. This issue is especially important when transformers and other difficult-to-replace equipment are subject to interdiction.

Figure 2 depicts of the ideas above using two graphs.

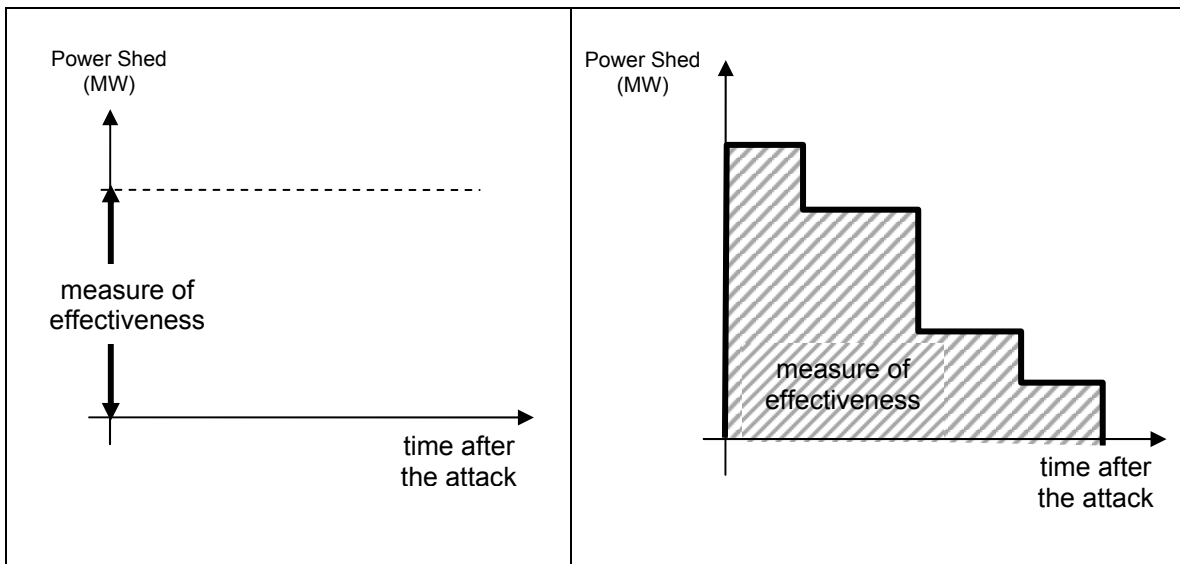


Figure 2. Power disruption and energy disruption. The model without restoration provides the optimal interdiction plan according to instantaneous picture of power shed (left). The model with restoration over time accounts for energy disruption (right). (From Salmeron et al. 2004.)

2. Interdiction Model

Salmeron et al. (2004) show how I-DCOPF (2.7) can be extended to handle the time associated with repairs. This resulting model seeks to maximize total cost of energy shed, accounting for the fact that the system will be progressively restored over time. The interdiction model with system restoration can be stated in brief as:

$$\begin{aligned}
& \max_{\delta \in \Delta} \min_y \sum_{t \in T} D_t c y_t \\
& \text{s.t. } g_t(\delta, y_t) = 0, \forall t \in T \\
& \quad y_t \geq 0, \forall t \in T
\end{aligned} \tag{2.14}$$

This model uses interdiction constructs to couple instances of DCOPF, one for each system state that represents a stage or “time-period” of system repair: Note the time subindex t , where T is the set of time periods based on repair times of all components in the system (see Appendix B.1). That index is added to all of the inner decision variables to account for power flows in the grid and other decision variables that change over time. D_t represents the duration of time period t , y_t is the same y described in (2.6) but for every time period t , and g_t is the resulting set of nonlinear equations in (δ, y_t) . Note the time-dependent constraints $g_t(\delta, y_t) = 0$ not only ensure that some components are out of service right after interdiction, but also guarantee that components will be in service again after their posted repair time. Thus, the constraints $g_t(\delta, y_t) = 0$ for different periods t are coupled by the variables δ . The full model derivation, described in detail in Salmeron et al. (2004), consists of the inner DCOPF model with system restoration (referred to as DCOPF-R) and the associated interdiction model (referred to as I-DCOPF-R); see Appendix B.1 for additional definitions and notation, and Appendix B.2 for the formulation.

As in the case without system restoration, a solution to the interdiction model with system restoration can be obtained through a heuristic algorithm or through a MIP reformulation of the problem, as described in the following paragraphs.

3. Heuristic Approach

a. Description

The Heuristic for a model with system restoration over time (schematically depicted in Figure 3) follows the approach of that for a model without system restoration.

For a fixed interdiction vector δ (i.e., $\delta = \hat{\delta}$), the inner DCOPF-R subproblem provides the joint flow patterns for a number of system stages (restoration periods). The subproblem decomposes into $|T|$ sub-subproblems (because when $\hat{\delta}$ is fixed, the subproblem is no longer coupled by time periods). Each subproblem consists of an instance of DCOPF with some subset of system components being “out of service.” Components that are out of service are determined “on the fly” as the algorithm solves a DCOPF model for every time period.

Salmeron et al. (2004) redefine the concept of a component’s value in this dynamic model by factoring the time it would be out of service if interdicted.

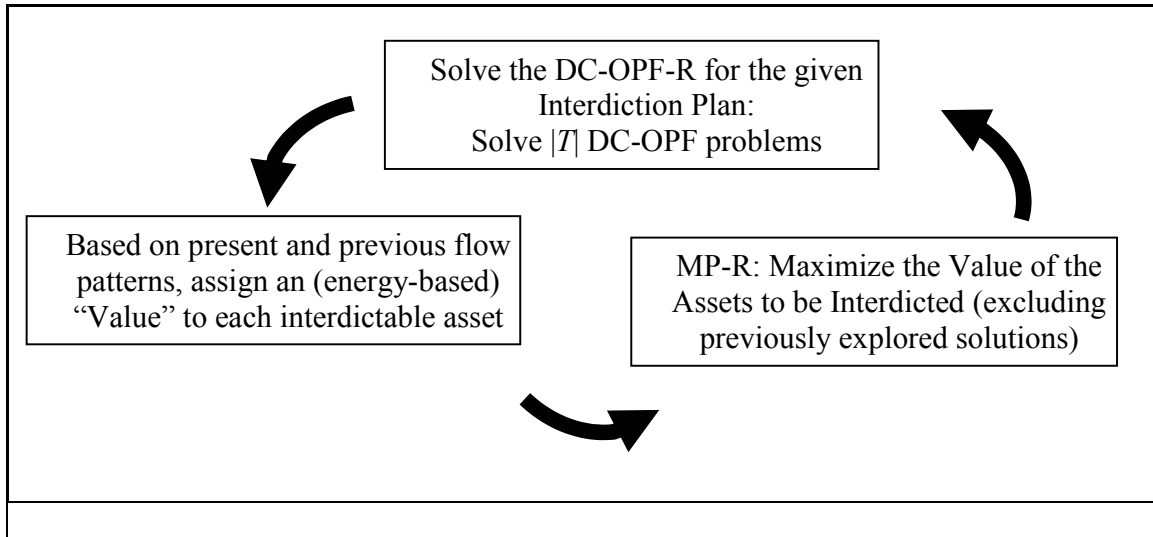


Figure 3. Interdiction algorithm framework with restoration. DCOPF-R decomposes into $|T|$ sub-subproblems, each being an instance of DCOPF with some components “out of service.” (From Salmeron et al. (2004).)

4. The MIP Model

a. Overview

The structure of I-DCOPF-R allows us to convert it into a standard MIP through a process of dualization and linearization, just as in the case without system restoration.

b. Derivation

As the new interdiction model is a variant of the model without system restoration, where the inner model has a similar structure to a power flow model (replicated over time), the development of the MIP formulation is performed as in Section B: First, admittance equations are linearized (Appendix B.2). Next, the inner minimization problem is dualized (Appendix B.3). Finally, cross-products in the objective function are linearized. The resulting MIP, called LDI-DCOPF-R, is specified in Appendix B.4.

D. BENDERS DECOMPOSITION

Benders Decomposition is a well-known technique for solving MIPs (Benders 1962). This technique has proven effective in solving large-scale optimization problems (e.g., facility location problems, two-stage stochastic optimization problems, etc.) including interdiction problems (Cormican 1995, Israeli and Wood 2002). Benders decomposition is well suited when the assignment of a subset of variables, so-called “complicating variables,” yields easily solvable, disconnected and convex subproblems, such as the network-flow problems in Geoffrion and Graves (1974) and Brown and McBride (1984); these MIPs could probably not have been solved directly, i.e., using branch and bound. Based on the successful application of Benders decomposition to these similar problems, we implement it to solve LDI-DCOPF and LDI-DCOPF-R.

Since the development of Benders decomposition is similar for both models, we focus on LDI-DCOPF. The MIP formulation of this model embeds a bi-level structure that makes Benders decomposition suitable for solving the problem: The first level is the interdictors’ level, which is modeled through binary decision variables. The second level is an instance of DCOPF (actually, its dual), where some components of the original power grid have been removed through the first-level decision variables. Because DCOPF is linear, it satisfies Benders’ theoretical requirement for convexity in the subproblem.

Our interdiction problem (LDI-DCOPF) may be stated, in brief, as:

$$\begin{aligned}
(\text{P}): \quad & z^* = \max_{\delta, v, \pi} c^v v + c^\pi \pi \\
\text{s.t.} \quad & A^v v + A^\pi \pi + B\delta = b \quad (y) \\
& \pi \geq 0 \\
& v \geq 0 \\
& \delta \in \Delta
\end{aligned} \tag{2.15}$$

Note: This problem is referred to as LDI-DCOPF elsewhere in this thesis, but for simplicity in this section, we refer to it as problem (P).

Note: non-positive π 's and v 's have been converted to non-negative π 's and v 's.

In our Benders decomposition scheme, the interdiction vector δ plays the role of the vector of “complicating variables.”

Rewriting (P) as:

$$\begin{aligned}
(\text{P}): \quad & \max_{\delta \in \Delta} \max_{v, \pi} c^v v + c^\pi \pi \\
\text{s.t.} \quad & A^v v + A^\pi \pi = b - B\delta \quad (y) \\
& v \geq 0 \\
& \pi \geq 0
\end{aligned} \tag{2.16}$$

the dual of the inner maximization above is:

$$\begin{aligned}
& \min_y y(b - B\delta) \\
\text{s.t.} \quad & yA^v \geq c^v \quad (v) \\
& yA^\pi \geq c^\pi \quad (\pi)
\end{aligned} \tag{2.17}$$

where y represents the vector of dual variables corresponding to the constraints of the primal problem in (2.16). We assume the polytope $H = \{y \mid yA^v \geq c^v, yA^\pi \geq c^\pi\}$ always contains a feasible solution, and its optimal solution is not unbounded. We will show later that these assumptions are valid.

Since the solution to (2.17) will lie at one of the extreme points of the feasible region H , we can rewrite (2.17) as:

$$\min_{i \in I} y_i(b - B\delta) \quad (2.18)$$

where $I = \{1, 2, \dots, k\}$ indexes the set of extreme points of H which is $\{y_1, y_2, \dots, y_{|I|}\}$.

Since $\min_{i \in I} y_i(b - B\delta) \leq y_i(b - B\delta), \forall i \in I$, we can rewrite (P) as:

$$\begin{aligned} \text{(P): } \quad & \max_{\delta \in \Delta, z \in \mathbb{R}} z \\ \text{s.t. } & z \leq y_i(b - B\delta) \quad \forall i \in I \end{aligned} \quad (2.19)$$

If we relax (2.19) by considering a subset of constraints $i \in I$, indexing these constraints by $i = 1, 2, \dots, k$, at a given iteration k of our Benders Decomposition Algorithm (BDA), we have the following “master problem” (MP) to solve:

$$\begin{aligned} \text{(MP}_k\text{): } \quad & \hat{z}_k = \max_{\delta \in \Delta, z \in \mathbb{R}} z \\ \text{s.t. } & z \leq y_i(b - B\delta) \quad i = 1, 2, \dots, k \end{aligned} \quad (2.20)$$

(MP_k) is a relaxation of (P), and therefore its optimal objective function value, \hat{z}_k , constitutes an upper bound on z^* , the optimal objective value to (P).

If the solution to (MP_k), denoted $(\hat{\delta}_k, \hat{z}_k)$, is not optimal to (P), then $(\hat{\delta}_k, \hat{z}_k)$ must violate some constraints in (2.19) not included in (MP_k), i.e., constraints associated with extreme points $\{y_{k+1}, y_{k+2}, \dots, y_{|I|}\}$. (Remark: Here, the subindex k refers to the iteration counter, and $\hat{\delta}_k$ is the incumbent interdiction vector.)

A natural way to check for one of these extreme points is to identify the vector y_{k+1} satisfying $y_{k+1} \in H$ that violates $\hat{z}_k \leq y_{k+1}(b - B\hat{\delta}_k)$ the most. That identification problem can be stated as the following optimization “subproblem:”

$$\begin{aligned} \text{(SP}_k(\hat{\delta}_k)\text{): } \quad & \min_{y_{k+1}} y_{k+1}(b - B\hat{\delta}_k) \\ \text{s.t. } & y_{k+1}A^v \geq c^v \quad (v_k) \\ & y_{k+1}A^\pi \geq c^\pi \quad (\pi_k) \end{aligned} \quad (2.21)$$

or, in its primal version:

$$\begin{aligned}
(\text{SP}_k(\hat{\delta}_k)): \quad & \max_{v, \pi} \quad c^v v + c^\pi \pi \\
\text{s.t.} \quad & A^v v + A^\pi \pi = b - B\hat{\delta}_k \quad (y_{k+1}) \\
& v \geq 0 \\
& \pi \geq 0
\end{aligned} \tag{2.22}$$

It is interesting to note that model (SP_k) in (2.22) is the same problem as problem (P) in (2.16) when the value of the decision variable δ is fixed as $\delta = \hat{\delta}_k$. (SP_k) is therefore feasible, because problem (P) is feasible for any $\delta = \hat{\delta}_k$. (Recall that the inner problem in (2.16) is equivalent to a DCOPF model, which is always feasible, even if this feasibility entails penalties for unmet load.) In addition, (SP_k) is bounded for any $\delta = \hat{\delta}_k$, because our DCOPF models have non-negative cost coefficients only.

The solution to (SP_k) , denoted $(\hat{v}_k, \hat{\pi}_k)$, along with $\hat{\delta}_k$ from model (MP_k) , form a combined solution $(\hat{\delta}_k, \hat{v}_k, \hat{\pi}_k)$, which is feasible to our original (P). Its objective function value is $c^v \hat{v}_k + c^\pi \hat{\pi}_k$, which represents a lower bound on the optimal solution to problem (P).

Solving the subproblem above yields a new extreme point \hat{y}_{k+1} , whose associated cut $z \leq \hat{y}_{k+1}(b - B\delta)$ will be violated by the incumbent solution $(\hat{z}_k, \hat{\delta}_k)$ unless $(\hat{z}_k, \hat{\delta}_k)$ is already optimal to (P). The newly generated cut is added to (MP_k) , becoming (MP_{k+1}) , and the process is repeated.

E. DECOMPOSITION ALGORITHM

The mathematical derivation described in Section D, leads to the following step-by-step algorithm: (The $\vartheta(\cdot)$ notation refers to the optimal objective function value of the problem in the argument.)

Benders Decomposition Algorithm (BDA):

Input: Initial solution $\hat{\delta}_0 \in \Delta$, matrices A^v , A^π , and B , vector b , and an optimality tolerance $\varepsilon > 0$.

Output: ε -optimal interdiction plan δ^* , and associated power flows, generation phase angles, and load shedding (jointly denoted as y^*).

1. Set the iteration counter $k := 0$, the lower bound $LB := -\infty$, and the upper bound $UB := +\infty$.
2. Solve $SP_k(\hat{\delta}_k)$ for $(\hat{v}_k, \hat{\pi}_k, \hat{y}_{k+1})$. Let $LB_k := \vartheta(SP_k(\hat{\delta}_k))$.
3. If $LB_k \leq LB$, then update the lower bound: $LB := LB_k$, and set $\delta^* := \hat{\delta}_k, y^* := \hat{y}_{k+1}$.
4. If $UB - LB \leq \varepsilon$, STOP; otherwise continue to step 5.
5. Add the newly generated cut: $z \leq \hat{y}_{k+1}(b - B\hat{\delta}_{k+1})$ to (MP_k) .
6. Set $k := k + 1$.
7. Solve (MP_k) for $\hat{\delta}_k$, and $\hat{z}_k = \vartheta(MP_k)$.
8. Update the upper bound: $UB := \hat{z}_k$, and return to step 2.

At each iteration, the solution \hat{y}_{k+1} to $SP(\hat{\delta}_k)$ gives us a new candidate solution $(\hat{\delta}_k, \hat{y}_{k+1})$. Whenever the objective value for this candidate solution is greater than the previous lower bound, we replace the lower bound with this value. This provides a non-decreasing lower bound. The solution to (MP_k) is monotonically decreasing with each cut added, and therefore we automatically update the upper bound at each iteration. This procedure is repeated until the bounds converge, or are sufficiently close, which in the worst case will occur after generating all possible extreme points of the subproblem, i.e., when $k = K$.

To improve the BDA efficiency, we incorporate some enhancements in Chapter VI. Figure 4 depicts the original BDA for ease of comparison with the flow chart for the enhanced BDA.

Benders Decomposition Algorithm (BDA)

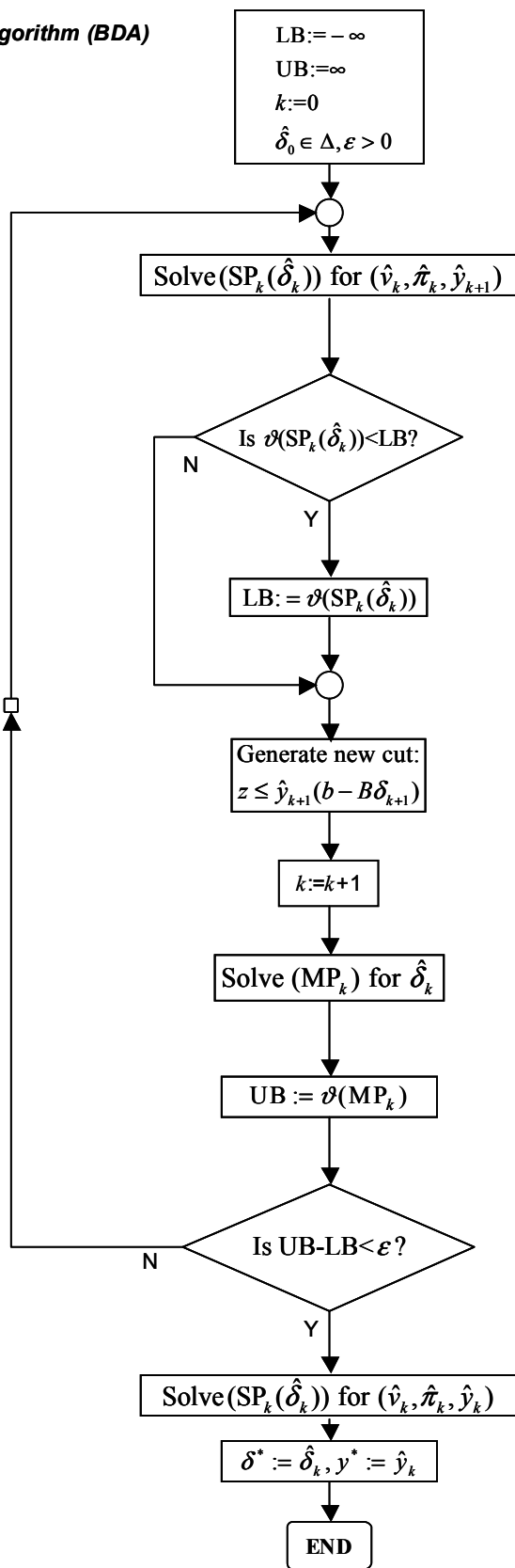


Figure 4. Benders Decomposition Algorithm flowchart.

Using the above template, we implement BDA using the full formulation of the interdiction problem, with and without system restoration, and test it on several benchmark cases.

The decomposition for the model without system restoration is presented in Chapter IV, starting with a simple example to familiarize the reader with the process. Chapter V expands upon this model to take into account system restoration, and presents computational results for that model for BDA.

Before describing details of the decomposition process, we validate the inner power-flow model in the next chapter.

THIS PAGE INTENTIONALLY LEFT BLANK

III. VALIDATING THE DC POWER FLOW MODEL

This chapter validates the DC Power Flow model (DCPF) introduced in Chapter II, whose accuracy must be established to ensure the reasonableness of our interdiction model, I-DCOPF. We do this using non-interdicted and interdicted instances of the IEEE One Area test case (IEEE Reliability Test Data 1999-I).

A. INTRODUCTION

DCPF is a simplification of the full AC Power Flow model (ACPF) (e.g., Wood and Wollenberg 1996). ACPF includes reactive power flows (DCPF disregards these), voltage magnitudes at the buses (DCPF assumes nominal voltages, i.e., 1.00 p.u.), and power losses on the line (DCPF assumes these to be zero), among others.

Overbye et al. (2004) conduct an analysis to validate the use of DCPF in place of ACPF for market analyses; they find it adequate. Wood and Wollenberg (1996) indicate that DCPF is adequate for security analysis of many systems. Although we believe that similar results should hold for interdiction problems, further analysis is desired because these problems have additional complications. In particular, they involve removing critical components of grids and adjusting loads to minimize disruption costs.

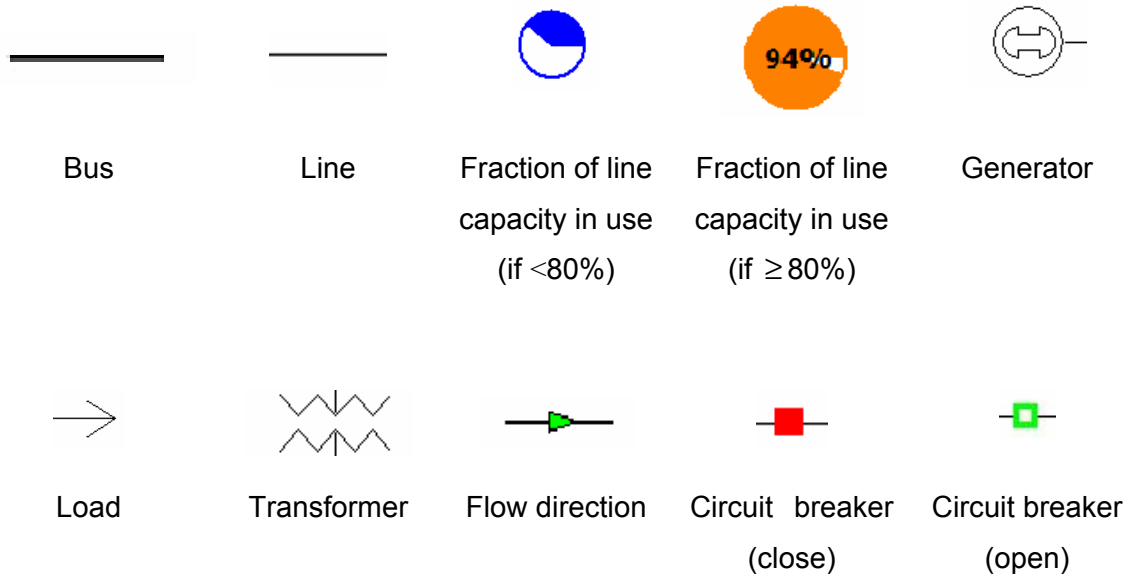
We validate DCPF through comparative analysis with the ACPF provided by software in the PowerWorld Simulator (PWS) (PowerWorld 2003). PWS is standard software, widely used in the electric power industry. Our assessment is carried out by comparing “optimal power flows” (OPFs) obtained using DCOPF with those identified by the ACPF. It is important to note that ACPF does not, per se, attempt to minimize load shedding (or its cost) as DCOPF does. However, for given loads and generation, it provides accurate active and reactive power flows on the lines and bus voltages (magnitude and phase), along with other system values. We want to assess whether power flows and voltage angles,

obtained through DCOPF, are in fact close to those from ACPF when we use our optimized generation and load shedding as input data.

We present the comparison between both approaches assuming no interdiction first, followed by other cases where critical components have been interdicted.

B. DCOPF VS. ACPF IN THE ABSENCE OF INTERDICTION

To enable comparison between the DCOPF and the PWS ACPF, we incorporate the IEEE RTS One Area case into PWS through its one-line diagram building interface. First, we reconstruct the underlying power grid, as shown in Figure 5, using the following symbols to represent the different system components:



For simplicity (and given that generating units are not interdictable in our test cases), we aggregate all generating units at a bus as a single generator at that bus. Next, we associate grid data with the power grid. The reconstructed one-line diagram includes data for bus nominal voltages, line resistances, reactances and thermal limits (line capacities), aggregated generating capacities, etc. Then, we incorporate active power output for each generating unit and active load met at each bus from DCOPF as system data for PWS's ACPF.

Finally, we run ACPF to compute actual power flows, phase angles and adjusted generation at the swing bus. The resulting power flows on the lines are compared to those provided by DCOPF.

The one-line diagram in Figure 5 represents a case without interdiction, which we call “scenario 0,” because it is equivalent to a case with zero interdiction resource. Section C analyzes cases with interdiction.

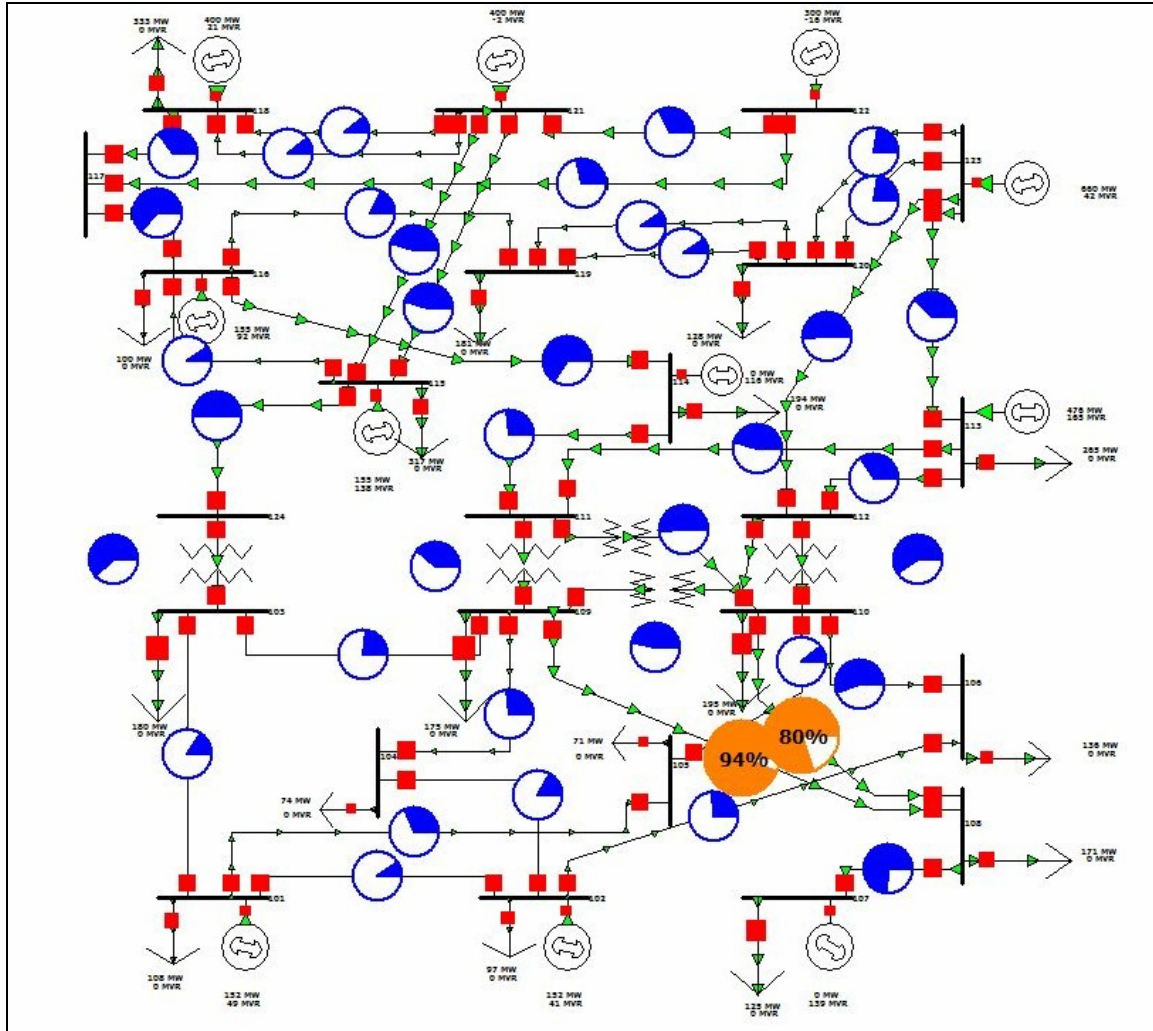


Figure 5. IEEE RTS One Area case one-line diagram without interdiction. This representation is constructed using the PWS software (PowerWorld 2003). It depicts flow directions, fractions of line capacities used, generation outputs and loads.

A side-by-side comparison of the resulting flows is shown in Table 1. We analyze absolute deviations for all lines and transformers. The column headed

“Line” displays the line name. The “From Bus” and “To Bus” columns indicate the two buses connected by the line. The “Transformer” column indicates if we are using a line to represent a transformer. The “PWS flow” and “PWS loss” columns show active power flows and losses, respectively, obtained with PWS, while the “DCOPF flow” column displays active power flows obtained with DCOPF. The last column shows the percentage absolute deviation between the PWS and DCOPF flows. The results show a maximum deviation of 5.29%. Mean deviation is 1.18% with a percentage standard deviation of 0.012 %.

The example above indicates that DCOPF yields a good approximation for the true AC power flow in this RTS case, in the absence of interdiction. In the following section, we analyze what happens when critical elements of the grid are removed through interdiction.

Line	From Bus	To Bus	Transformer	PWS flow (MW)	PWS loss (MW)	DCOPF flow(MW)	Abs. deviation
A1	101	102	No	16.70	0.01	17.00	1.80%
A2	101	103	No	-26.50	0.42	-26.73	0.87%
A3	101	105	No	54.00	0.68	53.73	0.50%
A4	102	104	No	28.60	0.29	28.42	0.63%
A5	102	106	No	44.00	1.01	43.58	0.95%
A6	103	109	No	40.10	0.53	39.85	0.62%
A7	103	124	Yes	-244.30	1.21	-246.58	0.93%
A8	104	109	No	-45.30	0.60	-45.58	0.62%
A9	105	110	No	-17.20	0.07	-17.27	0.41%
A10	106	110	No	-96.80	0.28	-92.42	4.52%
A11	107	108	No	-123.50	2.67	-125.00	1.21%
A12-1	108	109	No	-151.90	11.66	-159.94	5.29%
A13-2	108	110	No	-130.50	8.45	-136.06	4.26%
A14	109	111	Yes	-153.80	0.48	-154.38	0.38%
A15	109	112	Yes	-185.20	0.69	-186.28	0.58%
A16	110	111	Yes	-203.10	0.84	-204.43	0.65%
A17	110	112	Yes	-234.20	1.11	-236.33	0.91%
A18	111	113	No	-223.90	3.11	-226.01	0.94%
A19	111	114	No	-132.20	0.89	-132.81	0.46%
A20	112	113	No	-170.00	1.78	-171.01	0.59%
A21	112	123	No	-245.20	7.68	-251.60	2.61%
A22	113	123	No	-183.20	3.86	-186.01	1.53%
A23	114	116	No	-322.20	5.36	-326.81	1.43%
A24	115	116	No	45.60	0.04	45.90	0.66%
A25-1	115	121	No	-225.00	3.14	-227.24	1.00%

Line	From Bus	To Bus	Transformer	PWS flow (MW)	PWS loss (MW)	DCOPF flow(MW)	Abs. deviation
A26	115	124	No	248.10	4.33	246.50	0.64%
A27	116	117	No	-310.20	2.96	-312.52	0.75%
A28	116	119	No	87.40	0.23	86.81	0.68%
A29	117	118	No	-173.20	0.61	-172.69	0.29%
A30	117	122	No	-137.90	2.78	-139.82	1.39%
A31-1	118	121	No	-52.30	0.08	-52.85	1.05%
A32-1	119	120	No	-47.20	0.11	-47.19	0.02%
A33-1	120	123	No	-111.20	0.38	-111.19	0.01%
A34	121	122	No	-158.70	2.35	-160.18	0.93%

Table 1. ACPF versus DCOPF: IEEE RTS One Area case (no interdiction). For each line and transformer, we show the PWS's ACPF power flow and losses. We compare power flow absolute deviations from those of our DCOPF model. The maximum percentage deviation is 5.29% for the transmission line connecting buses 108 and 109. The average deviation is 1.18%.

C. DCOPF VS. ACPF AFTER INTERDICTION

In order to further validate DCOPF, we also compare flows after interdiction. The main effect of interdiction is, normally, load shedding. We conduct the analysis for a number of possible scenarios; recall that “scenario” corresponds to the amount of interdiction resource available. The flow-comparison procedure is repeated for the RTS One Area case for scenarios $M = 2, 4$, and 6 , in I-DCOPF shown in Appendix A.1.

Although overall results are presented for all cases, we will illustrate the one-line diagram and comparison table for scenario $M = 6$: We open the interdicted lines (found for the optimal interdiction plan which corresponds to this scenario) by opening the circuit breakers, at the ends of the lines, which are represented by green open squares in Figure 6. Then, we run PWS to realize that the flow in a number of lines greatly exceeds the lines' capacities (red circles in Figure 6). While a line can exceed its nominal capacity temporarily, the long-term emergency rating on a line is typically 20% of its nominal rated capacity, and a line can handle this excess flow only for 24 hours (IEEE 1999-I).

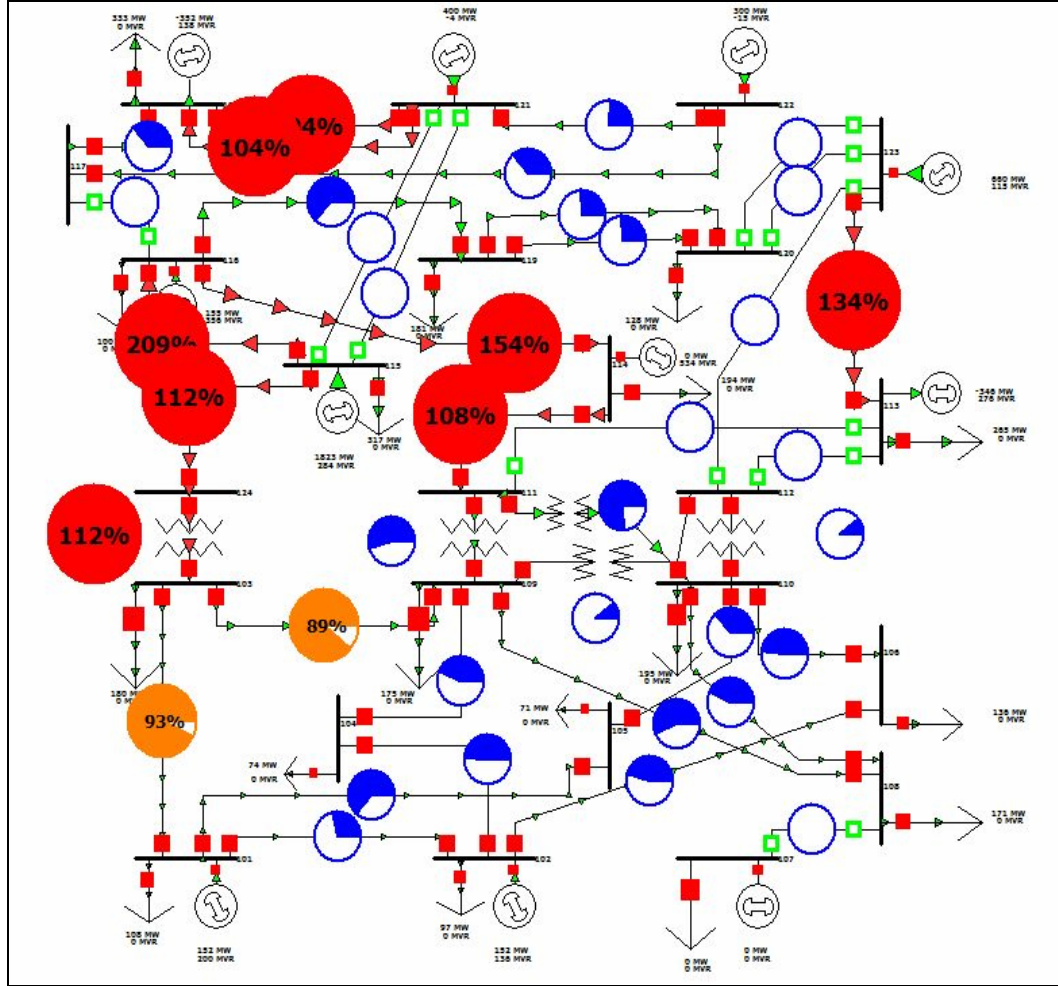


Figure 6. Effects of interdiction to IEEE RTS One Area case. Some lines become overloaded, which is unacceptable but for a few hours and up to certain limits. Note: All loads are kept at their original values to illustrate the infeasibility of the problem after interdiction.

Having determined that ACPF shows the situation to be infeasible after interdiction, we reduce the loads in ACPF to match those provided by DCOPF and run PWS. We then carry out a comparison of the flows across the non-interdicted elements of the grid with those provided by DCOPF; see Table 2.

Note that, again, all the DCOPF flows are relatively close to those produced by ACPF. The average absolute deviation is 3.67% with a standard deviation of 0.0075%.

Line	From Bus	To Bus	Status	Transformer	PWS flow(MW)	PWS loss(MW)	DCOPF flow(MW)	Abs. deviation
A1	101	102	Closed	No	-3.60	0.41	-3.23	10.28%
A2	101	103	Closed	No	68.30	0.02	66.01	3.35%
A3	101	105	Closed	No	136.20	1.18	129.22	5.12%
A4	102	104	Closed	No	104.80	1.93	99.95	4.63%
A5	102	106	Closed	No	92.60	9.82	88.82	4.08%
A6	103	109	Closed	No	76.70	0.00	76.52	0.23%
A7	103	124	Closed	Yes	-10.40	0.00	-10.51	1.05%
A8	104	109	Closed	No	95.70	0.00	99.95	4.25%
A9	105	110	Closed	No	124.90	0.00	129.22	3.34%
A10	106	110	Closed	No	82.80	0.00	88.82	6.78%
A11	107	108	Open	No	0.00	5.00	0	0.00%
A12-1	108	109	Closed	No	-33.70	0.00	-35.42	4.86%
A13-2	108	110	Closed	No	-36.80	0.00	-39.58	7.02%
A14	109	111	Closed	Yes	-27.80	0.00	-29.6	6.08%
A15	109	112	Closed	Yes	-3.90	0.00	-4.35	10.34%
A16	110	111	Closed	Yes	-19.80	0.00	-20.89	5.22%
A17	110	112	Closed	Yes	3.90	0.00	4.35	10.34%
A18	111	113	Open	No	0.00	0.00	0	0.00%
A19	111	114	Closed	No	-56.60	0.00	-50.49	10.80%
A20	112	113	Open	No	0.00	0.00	0	0.00%
A21	112	123	Open	No	0.00	0.00	0	0.00%
A22	113	123	Closed	No	-258.70	7.81	-265	2.38%
A23	114	116	Closed	No	-50.40	1.89	-50.49	0.18%
A24	115	116	Closed	No	204.90	0.00	204.49	0.20%
A25-1	115	121	Open	No	0.00	0.00	0	0.00%
A26	115	124	Closed	No	13.00	0.00	10.51	19.15%
A27	116	117	Open	No	0.00	7.59	0	0.00%
A28	116	119	Closed	No	313.50	1.29	309	1.46%
A29	117	118	Closed	No	122.20	2.29	123.55	1.09%
A30	117	122	Closed	No	-122.20	0.00	-123.55	1.09%
A31-1	118	121	Closed	No	-104.50	0.54	-104.73	0.22%
A32-1	119	120	Closed	No	64.30	0.01	64	0.47%
A33-1	120	123	Open	No	0.00	0.08	0	0.00%
A34	121	122	Closed	No	-174.70	0.00	-176.45	0.99%

Table 2. PWS's ACPF versus DCOPF: IEEE RTS One Area case, scenario $M=6$. All columns are as explained in Table 1 with the exception of the "Status" column which shows which lines are open. Note that the largest percentage deviations occur across lines whose flow is small.

Results for scenarios 2 and 4, summarized in table 3, are similar. Differences in line power flows are negligible either because of their small relative (percentage) values, or because of the low power flowing across lines.

Scenario	Statistics for "Absolute Deviation"					
	Max. (MW)	Max. (%)	Average (MW)	Average (%)	Std. dev. (MW)	Std. dev. (%)
0	8.04	5.29	1.70	1.18	1.96	1.22
2	2.37	13.04	0.44	0.92	0.50	2.28
4	10.37	4.84	1.24	0.83	2.10	0.96
6	6.98	19.15	1.95	3.68	2.21	0.96

Table 3. Overall comparison of power flows provided by DCOPF and PWS. The average deviation across the four scenarios is less than 5%.

Overall, the differences found are probably acceptable in the context of solving interdiction problems. This concurs with the generally accepted notion that DCPF renders acceptable results in the context of contingency analysis (e.g., Wood and Wollenberg 1996). We assume that the differences will remain small in all our analyses.

IV. BENDERS DECOMPOSITION FOR THE PROBLEM WITHOUT SYSTEM RESTORATION

This chapter describes Benders decomposition applied to the MIP interdiction model LDI-DCOPF without system restoration presented in Chapter II, Section B. The chapter begins with the application of the BDA described in Chapter II, Section D to a three-bus test case with interdictable elements limited to lines. The general case is then addressed.

A. SMALL TEST CASE PROBLEM DERIVATION

1. Description

This section illustrates Benders decomposition applied to a small, three-bus test grid. This is intended to familiarize the reader with the mathematical derivation for the general case that will be described later in this chapter. Even for this small example, the mathematical derivation is somewhat tedious. In order to simplify the exposition, we restrict the interdictable components to lines only. Figure 7 gives the one-line diagram for the example grid.

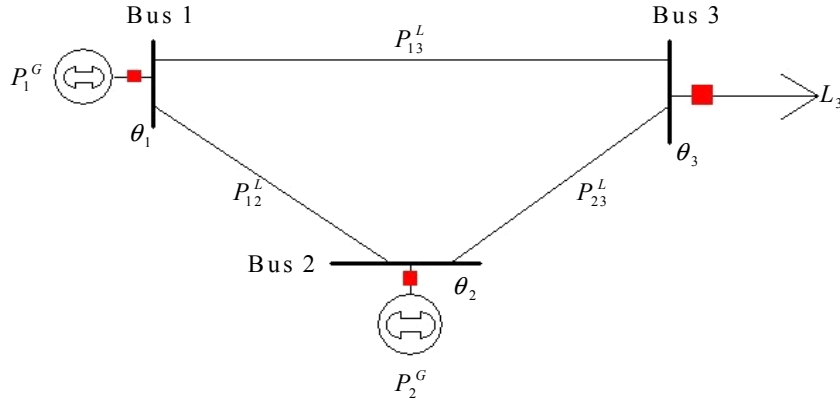


Figure 7. Three-bus (and three-line) example. Buses 1 and 2 are connected to one generator each. Bus 3 is connected to a load of L_3 MW. All the other symbols in the figure represent decision variables: P_1^G, P_2^G are generator outputs; $\theta_1, \theta_2, \theta_3$ are phase angles at the buses; $P_{12}^L, P_{13}^L, P_{23}^L$ are power

flows on the lines.

2. Mathematical Formulation

In this example, generating costs are disregarded, so we seek to minimize the load shed at bus 3. The problem development starting at the DCOPF level follows.

Decision variables(units):

P_i^G ,	Generator output at bus i , for $i = 1, 2$ (MW)
P_{ij}^L ,	Power flow on line (i, j) , for $(i, j) = (1,2), (1,3), (2,3)$ (MW)
S_3 ,	Load shed at bus 3 (MW)
θ_i ,	Phase angle at bus i , for $i = 1, 2, 3$ (radians)

Problem data (units):

L_3 ,	Demand at bus 3 (MW)
r_{ij}, x_{ij} ,	Line resistance and reactance, respectively, for $(i, j) = (1,2), (1,3), (2,3)$ (Ω)
B_{ij} ,	Series susceptance of line (i, j) , $B_{ij} = \frac{x_{ij}}{r_{ij}^2 + x_{ij}^2}$, for $(i, j) = (1,2), (1,3), (2,3)$ ($1/\Omega$)
\bar{P}_i^G ,	Maximum generating capacity at bus i , for $i = 1, 2$ (MW)
\bar{P}_{ij}^L ,	Line (i, j) transmission capacity, for $(i, j) = (1,2), (1,3), (2,3)$ (MW)

(Recall that all our units are converted to p.u. values as described in Chapter II, Section A).

In this small DCOPF example, we seek to minimize load shed at bus 3, that is:

$$\min S_3$$

Subject to:

Power balance constraints:

$$P_1^G - P_{12}^L - P_{13}^L = 0$$

$$P_2^G + P_{12}^L + P_{23}^L = 0$$

$$P_{13}^L + P_{23}^L + S_3 = L_3$$

Admittance constraints:

$$P_{12}^L - B_{12}\theta_1 + B_{12}\theta_2 = 0$$

$$P_{13}^L - B_{13}\theta_1 + B_{13}\theta_3 = 0$$

$$P_{23}^L - B_{23}\theta_2 + B_{23}\theta_3 = 0$$

Power Generation bound constraints:

$$P_1^G \leq \bar{P}_1^G$$

$$P_2^G \leq \bar{P}_2^G$$

Line capacity constraints:

$$P_{12}^L \leq \bar{P}_{12}^L$$

$$P_{12}^L \geq -\bar{P}_{12}^L$$

$$P_{13}^L \leq \bar{P}_{13}^L$$

$$P_{13}^L \geq -\bar{P}_{13}^L$$

$$P_{23}^L \leq \bar{P}_{23}^L$$

$$P_{23}^L \geq -\bar{P}_{23}^L$$

Upper bound on load-shedding constraint:

$$S_3 \leq L_3$$

Variable sign constraints:

$$S_3 \geq 0$$

$$P_1^G, P_2^G \geq 0$$

$$P_{12}^L, P_{13}^L, P_{23}^L \text{ unrestricted}$$

$$\theta_1, \theta_2, \theta_3 \text{ unrestricted}$$

We can now extend this formulation to account for potential interdiction by introducing three variables to represent interdiction of the lines. Note that the interdiction variables must turn off or turn on the power flow on the lines (i.e., open or close the lines, respectively). When $\delta_{ij}^L = 1$, the line (i, j) is interdicted, and when $\delta_{ij}^L = 0$, the line (i, j) is left intact.

Letting $M_{ij} = \bar{P}_{ij}^L + B_{ij}\bar{\theta}_{ij}$, where $\bar{\theta}_{ij}$ bounds the maximum difference between phase angles at buses i and j , the interdiction problem for given interdiction variables $\delta_{12}^L, \delta_{13}^L$, and δ_{23}^L , can be written as follows: (Note: The variables π represent the dual variables of the balance and bound constraints.)

$$(I\text{-DCOPF}): \max_{\delta \in \Delta} \min_{P^G, P^L, \theta, S} S_3$$

s.t.:

$$P_1^G - P_{12}^L - P_{13}^L = 0 \quad (\pi_1^S)$$

$$P_2^G + P_{12}^L + P_{23}^L = 0 \quad (\pi_2^S)$$

$$P_{13}^L + P_{23}^L + S_3 = L_3 \quad (\pi_3^S)$$

$$P_{12}^L - B_{12}\theta_1 + B_{12}\theta_2 \leq M_{12}\delta_{12}^L \quad (\pi_{12}^L)$$

$$P_{12}^L - B_{12}\theta_1 + B_{12}\theta_2 \geq -M_{12}\delta_{12}^L \quad (\pi_{12}^{L+})$$

$$P_{13}^L - B_{13}\theta_1 + B_{13}\theta_3 \leq M_{13}\delta_{13}^L \quad (\pi_{13}^L)$$

$$P_{13}^L - B_{13}\theta_1 + B_{13}\theta_3 \geq -M_{13}\delta_{13}^L \quad (\pi_{13}^{L+})$$

$$P_{23}^L - B_{23}\theta_2 + B_{23}\theta_3 \leq M_{23}\delta_{23}^L \quad (\pi_{23}^L)$$

$$P_{23}^L - B_{23}\theta_2 + B_{23}\theta_3 \geq -M_{23}\delta_{23}^L \quad (\pi_{23}^{L+})$$

$$P_1^G \leq \bar{P}_1^G \quad (\pi_1^G)$$

$$P_2^G \leq \bar{P}_2^G \quad (\pi_2^G)$$

$$P_{12}^L \leq \bar{P}_{12}^L(1 - \delta_{12}^L) \quad (\pi_{12}^{LCap+})$$

$$P_{12}^L \geq -\bar{P}_{12}^L(1 - \delta_{12}^L) \quad (\pi_{12}^{LCap-})$$

$$P_{13}^L \leq \bar{P}_{13}^L(1 - \delta_{13}^L) \quad (\pi_{13}^{LCap+})$$

$$P_{13}^L \geq -\bar{P}_{13}^L(1 - \delta_{13}^L) \quad (\pi_{13}^{LCap-})$$

$$P_{23}^L \leq \bar{P}_{23}^L(1 - \delta_{23}^L) \quad (\pi_{23}^{LCap+})$$

$$P_{23}^L \geq -\bar{P}_{23}^L(1 - \delta_{23}^L) \quad (\pi_{23}^{LCap-})$$

$$S_3 \leq L_3 \quad (\pi_3^{Load})$$

$$S_3 \geq 0$$

$$P_1^G, P_2^G \geq 0$$

$$P_{12}^L, P_{13}^L, P_{23}^L \text{ unrestricted}$$

$$\theta_1, \theta_2, \theta_3 \text{ unrestricted}$$

where:

$$\Delta = \left\{ \delta_{12}^L, \delta_{13}^L, \delta_{23}^L \mid \delta_{12}^L + \delta_{13}^L + \delta_{23}^L \leq 1, \delta_{12}^L, \delta_{13}^L, \delta_{23}^L \in \{0, 1\} \right\}$$

because we assume one unit of interdiction resource is available.

Notice that every admittance equation has been split into two inequalities. This is done in accordance with equation (2.9) (see Chapter II, Section B), to linearize the multivariable product that results from introducing the interdiction variables into the model. When $\delta_{ij}^L = 0$, every pair of inequalities enforces $P_{ij}^L - B_{ij}\theta_i + B_{ij}\theta_j = 0$. When $\delta_{ij}^L = 1$ (line (i, j) is interdicted), these constraints do not bind because M_{ij} is large. However, in this case P_{ij}^L will still be forced to be zero by constraints $P_{ij}^L \leq \bar{P}_{ij}^L(1 - \delta_{ij}^L)$ and $P_{ij}^L \geq -\bar{P}_{ij}^L(1 - \delta_{ij}^L)$.

The optimal interdiction problem consists of maximizing, by choice of interdiction variables δ_{ij}^L , the amount of power that must be shed in the system. As shown in Chapter II, Section B, this max-min problem can be easily reformulated as a max-max problem by taking the dual of the inner problem, I-DCOPF, listed above. This yields:

$$\begin{aligned} \text{(DI-DCOPF): } \max_{\delta} \max_{\pi} \quad & \pi_3^S L_3 + M_{12} \delta_{12}^L (\pi_{12}^L - \pi_{12}^{L+}) + M_{13} \delta_{13}^L (\pi_{13}^L - \pi_{13}^{L+}) \\ & + M_{23} \delta_{23}^L (\pi_{23}^L - \pi_{23}^{L+}) + \bar{P}_1^G (\pi_1^G) + \bar{P}_2^G (\pi_2^G) + \bar{P}_{12}^L (1 - \delta_{12}^L) (\pi_{12}^{LCap-} - \pi_{12}^{LCap+}) \\ & + \bar{P}_{13}^L (1 - \delta_{13}^L) (\pi_{13}^{LCap-} - \pi_{13}^{LCap+}) + \bar{P}_{23}^L (1 - \delta_{23}^L) (\pi_{23}^{LCap-} - \pi_{23}^{LCap+}) + L_3 (\pi_3^{Load}) \\ \text{s.t.} \quad & \pi_1^S + \pi_1^G \leq 0 \quad (P_1^G) \\ & \pi_2^S + \pi_2^G \leq 0 \quad (P_2^G) \\ & \pi_3^S + \pi_3^{Load} \leq 1 \quad (S_3) \\ & -\pi_1^S + \pi_2^S + \pi_{12}^L + \pi_{12}^{L+} + \pi_{12}^{LCap+} + \pi_{12}^{LCap-} = 0 \quad (P_{12}^L) \\ & -\pi_1^S + \pi_3^S + \pi_{13}^L + \pi_{13}^{L+} + \pi_{13}^{LCap+} + \pi_{13}^{LCap-} = 0 \quad (P_{13}^L) \\ & -\pi_2^S + \pi_3^S + \pi_{23}^L + \pi_{23}^{L+} + \pi_{23}^{LCap+} + \pi_{23}^{LCap-} = 0 \quad (P_{23}^L) \end{aligned}$$

$$\begin{aligned}
-B_{12}\pi_{12}^L - B_{12}\pi_{12}^{L^+} - B_{13}\pi_{13}^L - B_{13}\pi_{13}^{L^+} &= 0 & (\theta_1) \\
B_{12}\pi_{12}^L + B_{12}\pi_{12}^{L^+} - B_{23}\pi_{23}^L - B_{23}\pi_{23}^{L^+} &= 0 & (\theta_2) \\
B_{13}\pi_{13}^L + B_{13}\pi_{13}^{L^+} + B_{23}\pi_{23}^L + B_{23}\pi_{23}^{L^+} &= 0 & (\theta_3) \\
\delta_{12}^L + \delta_{13}^L + \delta_{23}^L &\leq 1 \\
\pi^S &\text{unrestricted} \\
\pi^L, \pi^{LCap^-}, \pi^G, \pi_3^{Load} &\leq 0 \\
\pi^{L^+}, \pi^{LCap^+} &\geq 0 \\
\delta_{12}^L, \delta_{13}^L, \delta_{23}^L &\in \{0,1\}
\end{aligned}$$

The resulting model, DI-DCOPF, contains a number of cross-products of the form $\delta\pi$ in the objective function, which we can linearize as described in Chapter II, Section B. This linearization yields the following MIP:

$$\begin{aligned}
(\text{LDI-DCOPF}): \max_{\delta \in \Delta, v, \pi} \quad & \pi_3^S L_3 + M_{12}(v_{12}^L - v_{12}^{L^+}) + M_{13}(v_{13}^L - v_{13}^{L^+}) + M_{23}(v_{23}^L - v_{23}^{L^+}) \\
& + \bar{P}_1^G \pi_1^G + \bar{P}_2^G \pi_2^G + \bar{P}_{12}^L (\pi_{12}^{LCap^-} - \pi_{12}^{LCap^+}) + \bar{P}_{13}^L (\pi_{13}^{LCap^-} - \pi_{13}^{LCap^+}) \\
& + \bar{P}_{23}^L (\pi_{23}^{LCap^-} - \pi_{23}^{LCap^+}) - \bar{P}_{12}^L (v_{12}^{LCap^-} - v_{12}^{LCap^+}) - \bar{P}_{13}^L (v_{13}^{LCap^-} - v_{13}^{LCap^+}) \\
& - \bar{P}_{23}^L (v_{23}^{LCap^-} - v_{23}^{LCap^+}) + L_3 \pi_3^{Load} \\
\text{s.t.} \quad & \\
& \pi_1^S + \pi_1^G \leq 0 & (P_1^G) \\
& \pi_2^S + \pi_2^G \leq 0 & (P_2^G) \\
& \pi_3^S + \pi_3^{Load} \leq 1 & (S_3) \\
& -\pi_1^S + \pi_2^S + \pi_{12}^L + \pi_{12}^{L^+} + \pi_{12}^{LCap^+} + \pi_{12}^{LCap^-} = 0 & (P_{12}^L) \\
& -\pi_1^S + \pi_3^S + \pi_{13}^L + \pi_{13}^{L^+} + \pi_{13}^{LCap^+} + \pi_{13}^{LCap^-} = 0 & (P_{13}^L) \\
& -\pi_2^S + \pi_3^S + \pi_{23}^L + \pi_{23}^{L^+} + \pi_{23}^{LCap^+} + \pi_{23}^{LCap^-} = 0 & (P_{23}^L) \\
& -B_{12}\pi_{12}^L - B_{12}\pi_{12}^{L^+} - B_{13}\pi_{13}^L - B_{13}\pi_{13}^{L^+} = 0 & (\theta_1) \\
& B_{12}\pi_{12}^L + B_{12}\pi_{12}^{L^+} - B_{23}\pi_{23}^L - B_{23}\pi_{23}^{L^+} = 0 & (\theta_2) \\
& B_{13}\pi_{13}^L + B_{13}\pi_{13}^{L^+} + B_{23}\pi_{23}^L + B_{23}\pi_{23}^{L^+} = 0 & (\theta_3) \\
& \delta_{12}^L + \delta_{13}^L + \delta_{23}^L \leq 1 \\
& v \in V(\delta, \pi)
\end{aligned}$$

where:

$$\begin{aligned}
\pi^L, \pi^{LCap^-}, \pi^G, v^L, v^{LCap^-}, \pi_3^{Load} &\leq 0 \\
\pi^{L^+}, \pi^{LCap^+}, v^{L^+}, v^{LCap^+} &\geq 0 \\
\pi^S &\text{unrestricted} \\
\delta_{12}^L, \delta_{13}^L, \delta_{23}^L &\in \{0,1\}
\end{aligned}$$

The linearization of constraints $v \in V(\delta, \pi)$ is specified in detail in Appendix C, but as an example, consider the constraint $v_{ij}^{L^+} = \pi_{ij}^{L^+} \delta_{ij}^L$, where $\pi_{ij}^{L^+} \geq 0$. The linearization uses the following constraints:

$$\begin{aligned}
v_{ij}^{L^+} &\leq \bar{\pi}_{ij}^{L^+} \delta_{ij}^L & (\gamma_{ij1}^{L^+}) \\
v_{ij}^{L^+} &\leq \pi_{ij}^{L^+} & (\gamma_{ij2}^{L^+}) \\
v_{ij}^{L^+} &\geq \pi_{ij}^{L^+} - \bar{\pi}_{ij}^{L^+} (1 - \delta_{ij}^L) & (\gamma_{ij3}^{L^+}) \\
\pi_{ij}^{L^+} &\leq \bar{\pi}_{ij}^{L^+} & (\eta_{ij}^{L^+}) \\
\pi_{ij}^{L^+} &\geq 0
\end{aligned}$$

The procedure delineated above adheres to the formulation developed by Salmeron et al. (2004). This formulation allows us to use any general-purpose MIP solution technique to solve LDI-DCOPF, and therefore, I-DCOPF. The remainder of this section is devoted to demonstrating the application of Benders decomposition to LDI-DCOPF in our three-bus network, following the steps in Chapter II, Section D.

We first construct the subproblem for a given vector of complicating variables $\hat{\delta}_k$ at iteration k :

$$\begin{aligned}
(\text{SP}_k(\hat{\delta}_k)) : \max_{v, \pi} & \pi_3^S L_3 + M_{12}(v_{12}^L - v_{12}^{L^+}) + M_{13}(v_{13}^L - v_{13}^{L^+}) + M_{23}(v_{23}^L - v_{23}^{L^+}) \\
& + \bar{P}_1^G \pi_1^G + \bar{P}_2^G \pi_2^G + \bar{P}_{12}^L (\pi_{12}^{LCap^-} - \pi_{12}^{LCap^+}) + \bar{P}_{13}^L (\pi_{13}^{LCap^-} - \pi_{13}^{LCap^+}) \\
& + \bar{P}_{23}^L (\pi_{23}^{LCap^-} - \pi_{23}^{LCap^+}) - \bar{P}_{12}^L (v_{12}^{LCap^-} - v_{12}^{LCap^+}) - \bar{P}_{13}^L (v_{13}^{LCap^-} - v_{13}^{LCap^+}) \\
& - \bar{P}_{23}^L (v_{23}^{LCap^-} - v_{23}^{LCap^+}) + L_3 \pi_3^{Load}
\end{aligned}$$

s.t.

$$\pi_1^S + \pi_1^G \leq 0 \quad (P_1^G)$$

$$\pi_2^S + \pi_2^G \leq 0 \quad (P_2^G)$$

$$\pi_3^S + \pi_3^{Load} \leq 1 \quad (S_3)$$

$$-\pi_1^S + \pi_2^S + \pi_{12}^L + \pi_{12}^{L^+} + \pi_{12}^{LCap^+} + \pi_{12}^{LCap^-} = 0 \quad (P_{12}^L)$$

$$-\pi_1^S + \pi_3^S + \pi_{13}^L + \pi_{13}^{L^+} + \pi_{13}^{LCap^+} + \pi_{13}^{LCap^-} = 0 \quad (P_{13}^L)$$

$$-\pi_2^S + \pi_3^S + \pi_{23}^L + \pi_{23}^{L^+} + \pi_{23}^{LCap^+} + \pi_{23}^{LCap^-} = 0 \quad (P_{23}^L)$$

$$-B_{12}\pi_{12}^L - B_{12}\pi_{12}^{L^+} - B_{13}\pi_{13}^L - B_{13}\pi_{13}^{L^+} = 0 \quad (\theta_1)$$

$$B_{12}\pi_{12}^L + B_{12}\pi_{12}^{L^+} - B_{23}\pi_{23}^L - B_{23}\pi_{23}^{L^+} = 0 \quad (\theta_2)$$

$$B_{13}\pi_{13}^L + B_{13}\pi_{13}^{L^+} + B_{23}\pi_{23}^L + B_{23}\pi_{23}^{L^+} = 0 \quad (\theta_3)$$

$$v \in V(\hat{\delta}_k, \pi)$$

Constraints $v \in V(\hat{\delta}_k, \pi)$ are linearized as in Appendix C with δ replaced by $\hat{\delta}_k$.

The master problem at iteration k becomes:

$$(MP)_k: \max_{\delta \in \Delta, Z \in \mathbb{R}} z$$

$$\begin{aligned} \text{s.t.} \quad z \leq & \bar{\pi}_{12}^{L^+} \delta_{12} \gamma_{121,k'}^{L^+} - \bar{\pi}_{12}^{L^+} (1 - \delta_{12}) \gamma_{123,k'}^{L^+} + \bar{\pi}_{13}^{L^+} \delta_{13} \gamma_{131,k'}^{L^+} - \bar{\pi}_{13}^{L^+} (1 - \delta_{13}) \gamma_{133,k'}^{L^+} + \bar{\pi}_{23}^{L^+} \delta_{23} \gamma_{231,k'}^{L^+} \\ & - \bar{\pi}_{23}^{L^+} (1 - \delta_{23}) \gamma_{233,k'}^{L^+} - \bar{\pi}_{12}^L \delta_{12} \gamma_{121,k'}^L + \bar{\pi}_{12}^L (1 - \delta_{12}) \gamma_{123,k'}^L - \bar{\pi}_{13}^L \delta_{13} \gamma_{131,k'}^L + \bar{\pi}_{13}^L (1 - \delta_{13}) \gamma_{133,k'}^L \\ & - \bar{\pi}_{23}^L \delta_{23} \gamma_{231,k'}^L + \bar{\pi}_{23}^L (1 - \delta_{23}) \gamma_{233,k'}^L + \bar{\pi}_{12}^{LCap^+} \delta_{12} \gamma_{121,k'}^{LCap^+} - \bar{\pi}_{12}^{LCap^+} (1 - \delta_{12}) \gamma_{123,k'}^{LCap^+} + \bar{\pi}_{13}^{LCap^+} \delta_{13} \gamma_{131,k'}^{LCap^+} \\ & - \bar{\pi}_{13}^{LCap^+} (1 - \delta_{13}) \gamma_{133,k'}^{LCap^+} + \bar{\pi}_{23}^{LCap^+} \delta_{23} \gamma_{231,k'}^{LCap^+} - \bar{\pi}_{23}^{LCap^+} (1 - \delta_{23}) \gamma_{233,k'}^{LCap^+} - \bar{\pi}_{12}^{LCap^-} \delta_{12} \gamma_{121,k'}^{LCap^-} \\ & + \bar{\pi}_{12}^{LCap^-} (1 - \delta_{12}) \gamma_{123,k'}^{LCap^-} - \bar{\pi}_{13}^{LCap^-} \delta_{13} \gamma_{131,k'}^{LCap^-} + \bar{\pi}_{13}^{LCap^-} (1 - \delta_{13}) \gamma_{133,k'}^{LCap^-} - \bar{\pi}_{23}^{LCap^-} \delta_{23} \gamma_{231,k'}^{LCap^-} \\ & + \bar{\pi}_{23}^{LCap^-} (1 - \delta_{23}) \gamma_{233,k'}^{LCap^-} + S_{3,k'} + \bar{\pi}_{12}^{L^+} \eta_{12,k'}^{L^+} + \bar{\pi}_{13}^{L^+} \eta_{13,k'}^{L^+} + \bar{\pi}_{23}^{L^+} \eta_{23,k'}^{L^+} - \bar{\pi}_{12}^L \eta_{12,k'}^L - \bar{\pi}_{13}^L \eta_{13,k'}^L - \bar{\pi}_{23}^L \eta_{23,k'}^L \\ & + \bar{\pi}_{12}^{LCap^+} \eta_{12,k'}^{LCap^+} + \bar{\pi}_{13}^{LCap^+} \eta_{13,k'}^{LCap^+} + \bar{\pi}_{23}^{LCap^+} \eta_{23,k'}^{LCap^+} - \bar{\pi}_{12}^{LCap^-} \eta_{12,k'}^{LCap^-} - \bar{\pi}_{13}^{LCap^-} \eta_{13,k'}^{LCap^-} - \bar{\pi}_{23}^{LCap^-} \eta_{23,k'}^{LCap^-} \end{aligned}$$

$$\forall k' = \{1, 2, \dots, k\}$$

In the above formulation, the subscript k for any variable (e.g., $\gamma_{121,k'}^{L^+}$) refers to the optimal value of the incumbent variable provided by the solution to $(SP_{k'}(\hat{\delta}_{k'}))$ at iteration $k' | k' \leq k$.

Having developed our master problem and subproblem, we implement the BDA in Chapter II, Section D, and test the three-bus case for convergence. We use the following values for the test case:

$$L_3 = 5 \text{ p.u.}$$

$$B_{ij} = 5 \text{ p.u.}$$

$$\bar{P}_1^G, \bar{P}_2^G = 3 \text{ p.u.}$$

$$\bar{P}_{12}^L, \bar{P}_{13}^L, \bar{P}_{23}^L = 4 \text{ p.u.}$$

The algorithm converges successfully to the same optimal interdiction plan: $(\hat{\delta}_{12} = 0, \hat{\delta}_{13} = 1, \hat{\delta}_{23} = 0)$ as that of the MIP formulation in LDI-DCOPF. The following graph illustrates how upper and lower bounds converge after four iterations of the algorithm.

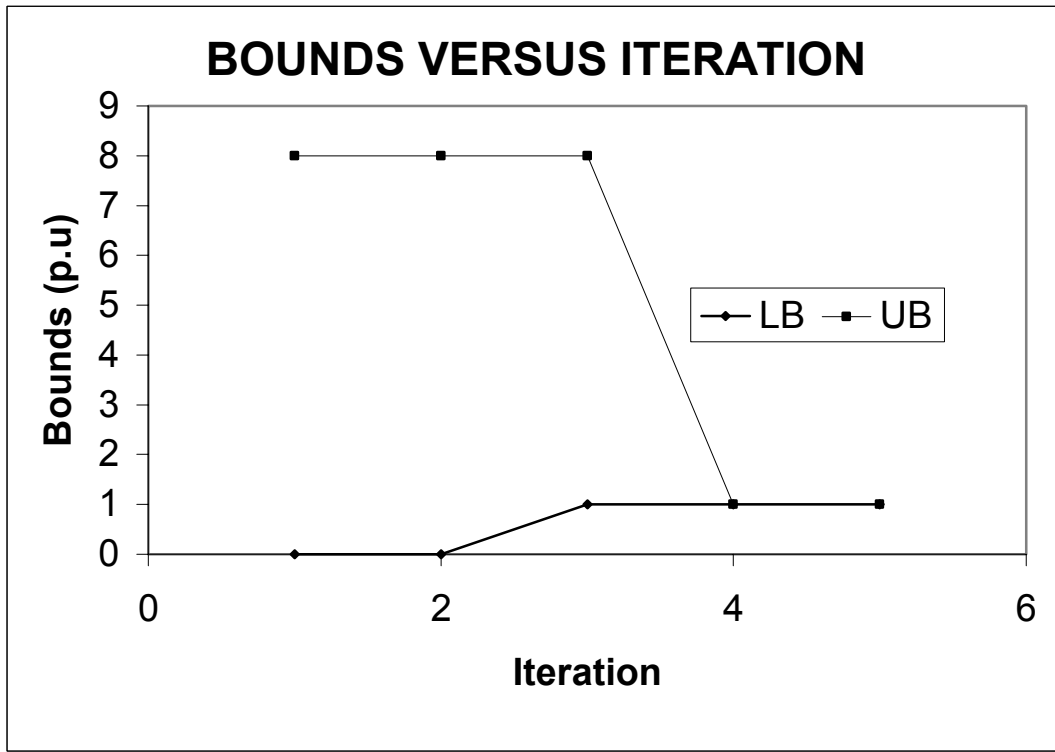


Figure 8. Convergence of Benders decomposition for the three-bus case. The optimal interdiction plan, which consists of interdicting line (1,3) in Figure 7, sheds a load of one p.u..

This section has illustrated Benders decomposition using a small example. This foundation should help the reader understand the generalization of the procedure to any power grid in which buses, generators, substations and lines can be interdicted. The extension to incorporate the effect of system restoration over time will be addressed in Chapter V.

B. BENDERS DECOMPOSITION: GENERAL INTERDICTION PROBLEM WITHOUT SYSTEM RESTORATION

The general interdiction problem should be scalable to let us analyze an arbitrary power system. We will not discuss the derivation of the BDA for I-DCOPF as done in the previous section, however. Appendix A provides a complete derivation of the Benders decomposition procedure for I-DCOPF. The derivation is broken down into these steps:

A.1 shows the interdiction model, I-DCOPF.

A.2 shows the dual of the interdiction model, DI-DCOPF.

A.3. shows the dual of the interdiction model after linearization of $\delta\pi$ products, LDI-DCOPF.

A.4 shows the BDA master problem.

The subproblem at iteration k is LDI-DCOPF with all δ 's replaced by fixed $\hat{\delta}_k$'s (given by the user at iteration $k = 0$ and by (MP_k) at iteration $k > 0$), where $\hat{\delta}_k \in \Delta, \forall k$.

Once the subproblem is solved for a given interdiction plan, we retrieve the dual values for each subproblem constraint and use them as coefficients for the master problem. The master problem at iteration k is displayed in Appendix A.4.

C. RESULTS

The BDA is implemented in GAMS (GAMS 2003) and solved with CPLEX version 8.1 (GAMS-CPLEX 2003) as the underlying solver, and run on a Pentium 4 laptop computer at 3.0 GHz and with 512 Mbytes RAM. We turn off the “presolve” option in CPLEX because it leads us to erroneous duals from the subproblem.

Figure 9 shows the sequence of lower and upper bounds generated by BDA for the IEEE RTS One Area case (1999-I), with interdiction resource $M = 6$

and the assumptions made in Salmeron et al. (2003). The optimal interdiction plan for this case matches the solution obtained by solving the MIP LDI-DCOPF directly.

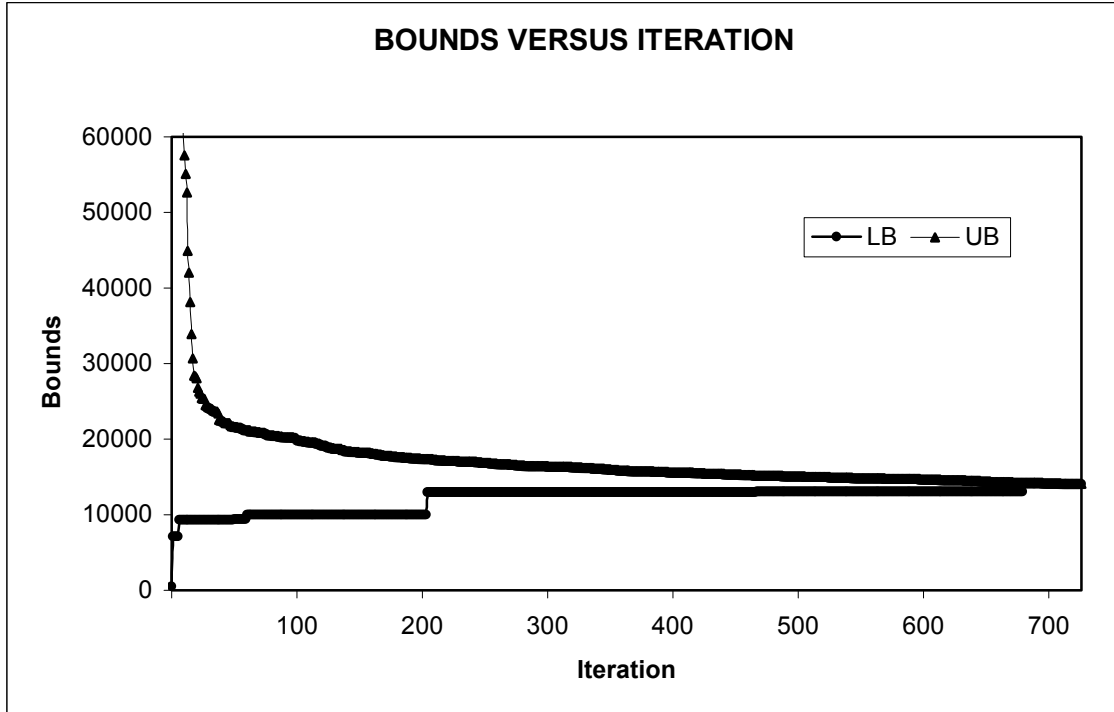


Figure 9. IEEE RTS One Area case without system restoration: Convergence. Note the significant improvement of the lower and upper bound at early iterations. As the number of iterations increases the effectiveness of the cuts (given by the upper bound from the master problem) decreases. Initial upper bound is 140,000, but the vertical axis on the graph is truncated for display purposes.

The results for this problem show that, by iteration 375, the lower bound is already within 7.6% of the optimal solution, while the upper bound is within 12%. (For this comparison we use the optimal solution obtained with LDI-DCOPF.) We achieve these bounds in approximately 10 minutes; however, it takes 1 hour and 20 minutes to reach the optimal solution which is 14,048 \$/hr. This result shows Benders decomposition may obtain sensible bounds in a relatively small number of iterations, and an acceptable time. However, reaching optimality takes considerable effort. This difficulty will be addressed in Chapter VI.

Figure 10 shows how the time required to solve the master problem and subproblem change as the algorithm proceeds. This figure reveals the increasing difficulty of the master problem as more cuts are added with subsequent iterations. While the time to solve each succeeding master problem of the decomposition process significantly increases, the relative efficiency of the new cuts are less significant as shown by Figure 9.

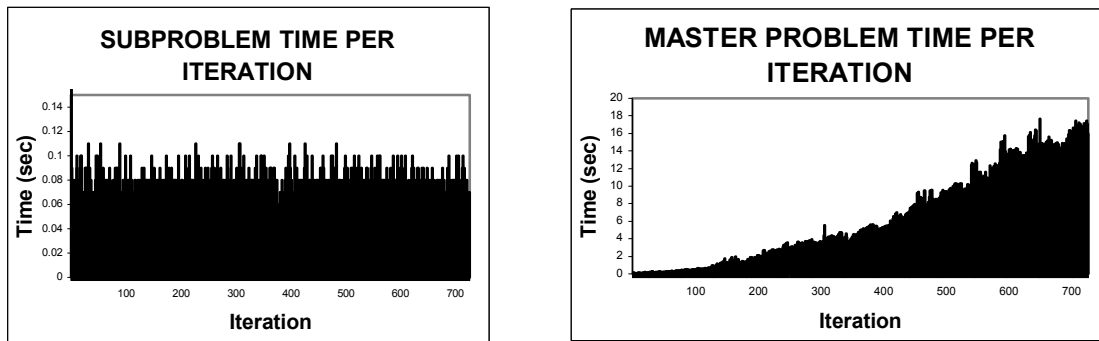


Figure 10. IEEE RTS One Area case without system restoration: Time versus Iteration . The time to solve each master problem in the algorithm significantly increases with subsequent iteration. The maximum time to solve any subproblem is less than 0.2 seconds while master-problem solution times are as high as 18 seconds.

V. BENDERS DECOMPOSITION FOR THE PROBLEM WITH SYSTEM RESTORATION

This chapter extends Benders decomposition to the interdiction problem with system restoration. We describe the models involved in the new decomposition, and show preliminary results. (Chapter VI will show improved results through some refinements in BDA.)

A. FORMULATION

This section illustrates the application of Benders decomposition to the interdiction problem with system restoration, I-DCOPF-R. The derivation of I-DCOPF-R is included in Appendices B.1 and B.2. We will not discuss the complete derivation of the Benders decomposition procedure for the system restoration case, which is included in Appendix B. Specifically:

B.1 shows time-period constructs.

B.2 shows the interdiction model I-DCOPF-R.

B.3 shows DI-DCOPF-R, which is the interdiction model with the inner power flow model replaced by its dual.

B.4 shows DI-DCOPF-R after linearization of cross-products. We denote this model LDI-DCOPF-R.

Finally, B.5 shows the BDA master problem.

We start the description after the linearization of the $\delta\pi$ cross-products. That is, assuming we have LDI-DCOPF-R as the MIP to which we will apply Benders decomposition.

Again, the subproblem at iteration k is the LDI-DCOPF-R with all δ 's replaced by fixed $\hat{\delta}_k$'s (given by the user at iteration $k = 0$ and by the (MP_k) at iteration $k > 0$), where $\hat{\delta}_k \in \Delta, \forall k$, and the dual values for each subproblem constraint are used as coefficients for the master problem.

The BDA master problem is shown in Appendix B.5. At each iteration k , a new cut is added to the master problem. This provides a (monotonically decreasing) upper bound \hat{z}_k , and an interdiction plan that will be used in the subproblem $(SP_k(\hat{\delta}_k))$ to calculate a lower bound.

B. RESULTS

Figure 11 shows the convergence of BDA for the IEEE RTS One Area case with system restoration. Note the significant improvement in the bounds during the early iterations of the decomposition process when compared to the last iterations.

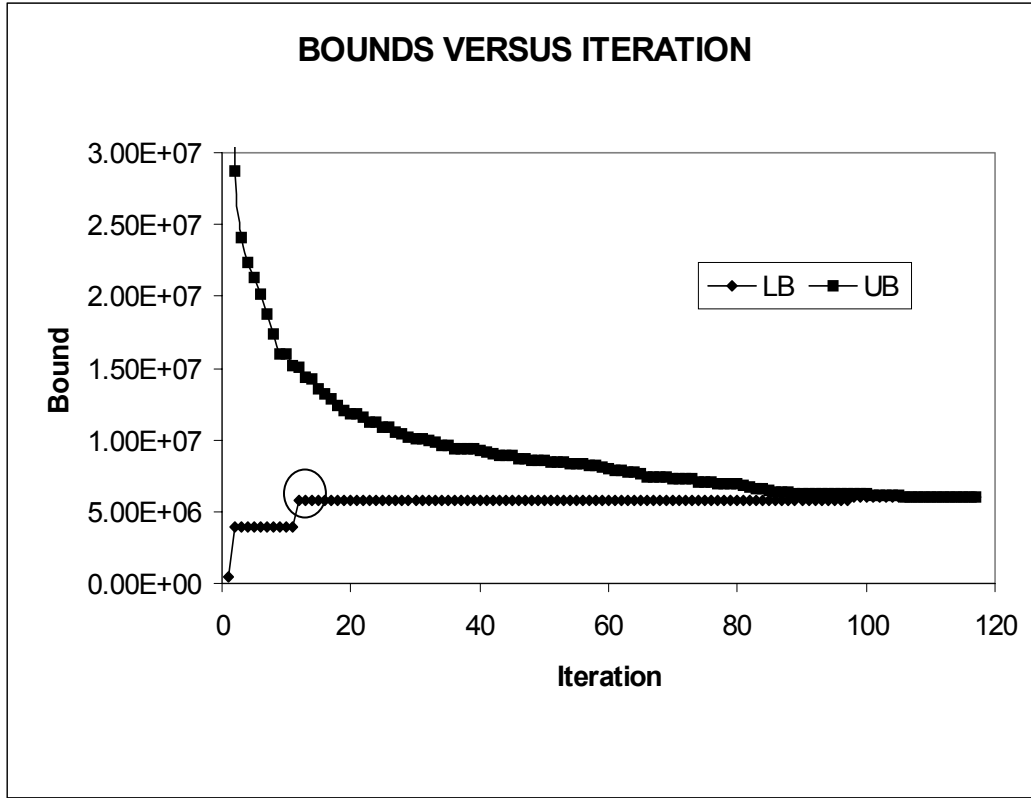


Figure 11. IEEE RTS One Area case with system restoration: Convergence. The upper and lower bounds of this problem converge quickly in early iterations. Convergence is reached in 120 iterations and takes 33 seconds. Also note that the optimal objective value (circled in graph) is reached in early iterations, but it takes the algorithm a relatively long time to prove it has obtained an optimal solution.

Although the case with system restoration is intuitively more difficult to solve than the case without system restoration (because of the number of time periods, and the related number of additional variables), the former actually solves faster in the IEEE RTS One Area case. This could be attributed to the fact that, for the problem with restoration, some candidate components, such as those with the largest repair times, are more obviously attractive than others to become part of the optimal solution. This might allow the BDA to target solutions that include those components at early stages, which in turn provides accurate bounds sooner than in the case without system restoration (in which the attractiveness of all components is more balanced). Our results support this conjecture. While it takes over 700 iterations and 1 hour and 20 minutes to solve the IEEE RTS One Area case without system restoration problem, the problem with system restoration solves in only 120 iterations and 33 seconds. We find similar behavior in the RTS Two Area case.

Figure 12 shows that master problem time by iteration remains almost the same for the IEEE RTS One Area case with system restoration. We will show that this is not the case when we apply the BDA to the IEEE RTS Two Area case.

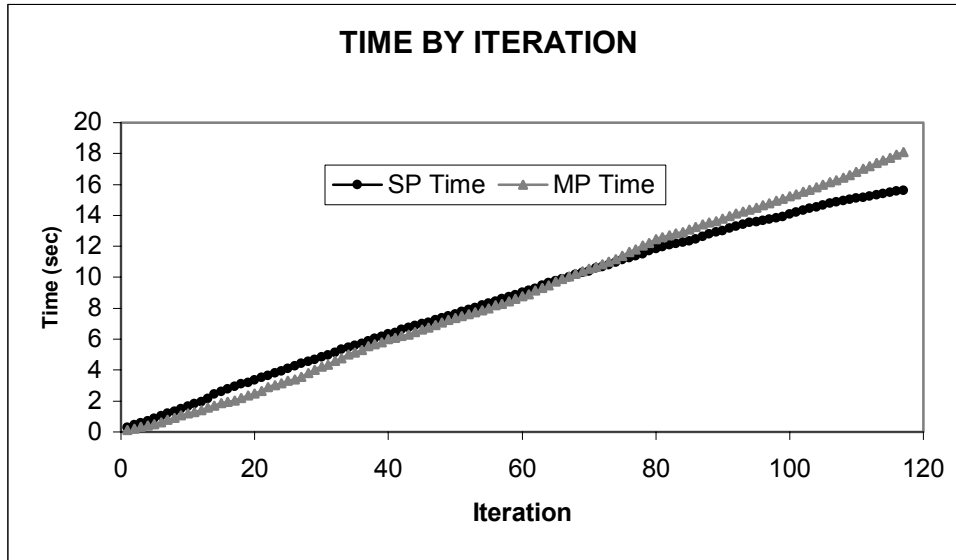


Figure 12. IEEE RTS One Area case with system restoration: Cumulative time. Time is shown for the subproblem and for the master problem separately. Note that the time to solve the master problem appears to remain stable by iteration, despite the increasing number of constraints.

To illustrate the potential difficulty in solving the master problem as the number of iterations increases, we analyze the results for interdiction scenario $M = 12$ for the IEEE RTS Two Area case. Figure 13 shows the results for a 2,000-iteration run of this problem.

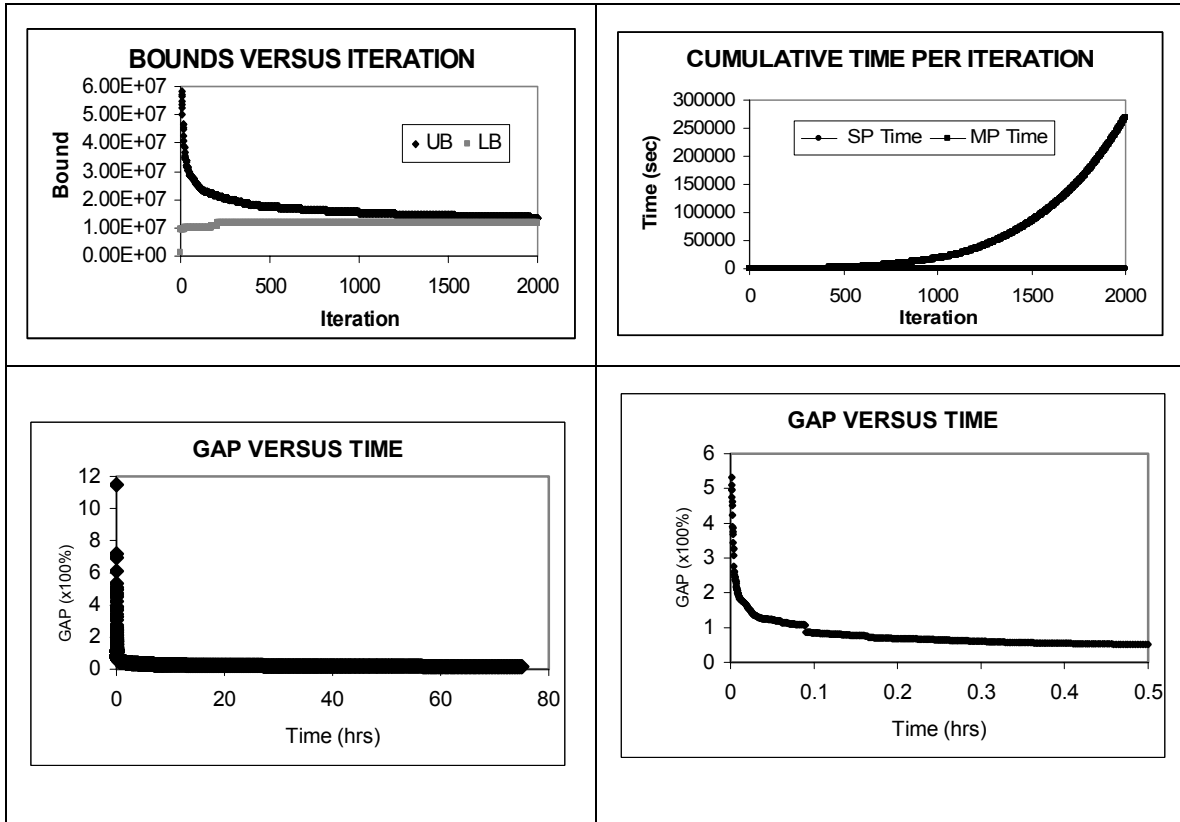


Figure 13. IEEE RTS Two Area case with system restoration: Solution trajectory. In 2,000 iterations, taking 75 hours, a gap of 16% is achieved. The top left graph shows that a near-optimal solution is found at the early stages, but it takes many iterations to prove it. The top right graph shows the cumulative solution time, by iteration, for the master problem and subproblem. Note how the master-problem solution times increase substantially as the algorithm proceeds. The bottom left plot shows how the optimality gap changes with time. Note the large decrease in the gap in the early iterations. The bottom right picture is an expanded view of the first 30 minutes of the “GAP VERSUS TIME” plot. The gap is reduced to 50% in the first 30 minutes. The problem’s lower bound is, in actuality, only 2% from the optimal solution value at this time, although the algorithm cannot prove this within the first 75 hours.

Clearly, BDA is impractically slow for this problem. This suggests the need for strategies to accelerate BDA’s convergence. The next chapter describes and demonstrates techniques we have developed to do this.

VI. ALGORITHM REFINEMENTS AND RESULTS

As seen in Chapter V, long master-problem solution times are a major factor in the overall efficiency (or inefficiency) of BDA. This prompts us to focus on the master problem and reduce its solution times to accelerate overall convergence of BDA.

A. INTRODUCTION

This chapter explores the following techniques to reduced master-problem solution times:

1. Solving a relaxed master problem in some iterations rather than the standard master problem,
2. Dropping certain Benders cuts as iterations proceed, and
3. Not solving the master problem to optimality in all iterations (Sub-optimal integer solutions).

The modified BDA which includes the above strategies 1, 2 and 3 is shown in Figure 14.

The various techniques and associated results are discussed in Sections B through D below. A combined strategy is reviewed in Section E.

**Benders Decomposition Algorithm
with Refinements**

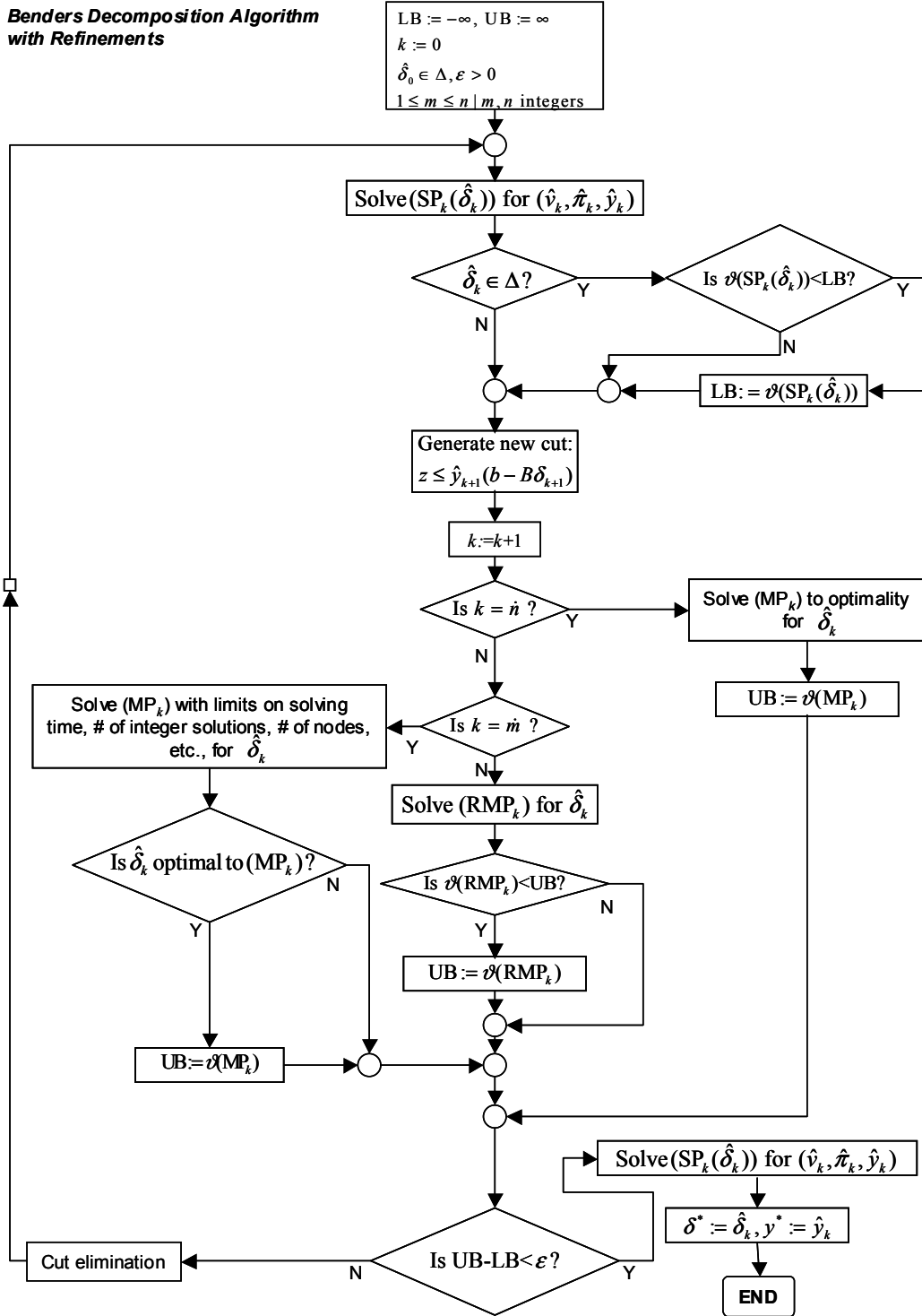


Figure 14. Benders Decomposition Algorithm (with refinements) flowchart. This diagram depicts the steps of our enhanced BDA, incorporating the proposed strategies to speed up convergence. RMP refers to the linear relaxation of the BDA master problem. The flowchart includes the refinement techniques that are explained in Sections B through D of this Chapter.

B. RELAXING THE MASTER PROBLEM

The first technique we try solves a relaxed master problem (RMP_k) in most iterations k , and only solves the true (mixed-integer) master problem periodically. A relaxed master problem should be much faster to solve, and its use may lead to an overall reduction in solution time. We refer to this technique as the “relaxed-MP strategy.”

RMP_k is formed by treating any discrete variables as continuous (while the rest of the problem remains the same). The optimal value of a relaxed maximizing model yields an upper bound on the optimal value of the full model. However, the solution to the relaxed master problem is not a feasible interdiction plan (unless it happens to be an integer solution). For this reason, the relaxed master problem solution cannot be used in the subproblem to obtain a valid lower bound; however, the Benders cut generated by the subproblem at that solution is valid. In order to improve the lower bound, we must solve the actual master problem, and we do this at a specified interval (for example, every ten iterations). Unless specified otherwise, in the test cases that follow, our relaxed-MP strategy consists of solving the true master problem once every ten iterations and otherwise solving RMP_k .

To show the benefits of using the relaxed-MP strategy, we first consider BDA applied to the IEEE RTS One Area case without system restoration. The original algorithm’s solution trajectory for this problem is presented graphically in Chapter IV, Figure 9. Recall that it originally takes about 1 hour and 20 minutes to solve this case. The relaxed-MP strategy solves the problem in only 26 minutes, a 67% improvement over the original algorithm. Figure 15 shows how the problem converges.

The reduction in overall solution time cannot be attributed solely to faster solutions of the master problem, however, since the modified algorithm solves in only 281 iterations compared to the original 768. It appears that cuts generated from non-integer solutions may be more effective than standard cuts generated

at integer solutions. We are unsure why this occurs in this case, and in fact, we will see later that this behavior cannot be generalized to all our cases.

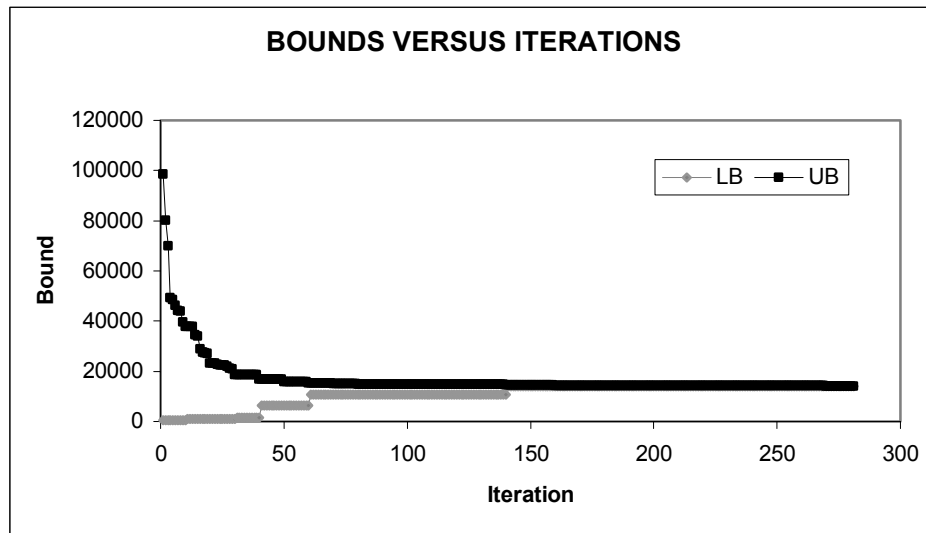
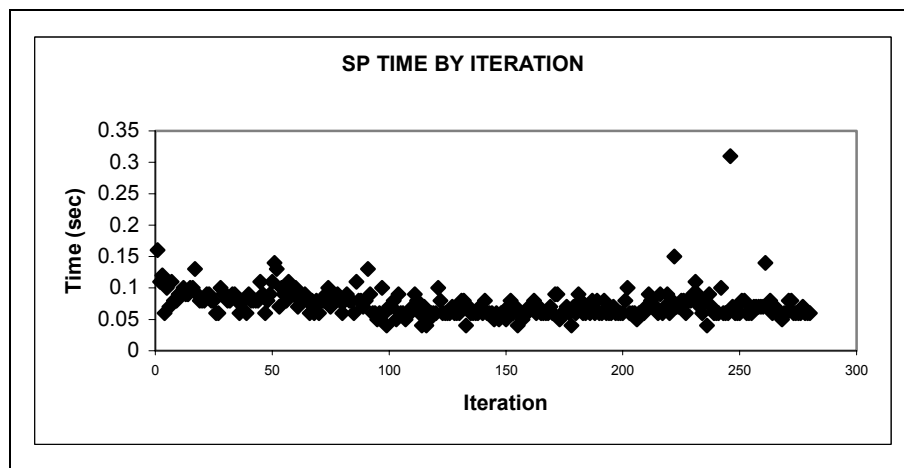


Figure 15. Relaxed master problem strategy: Convergence (I). IEEE RTS One Area case without system restoration. We solve the full master problem every 10th iteration and otherwise solve that problem's continuous relaxation. This problem solves 67% faster using this technique compared to the original BDA which solves the (mixed-integer) master problem in each iteration.

Figure 16 shows the solution times by iteration, for the master problem and for the subproblem.



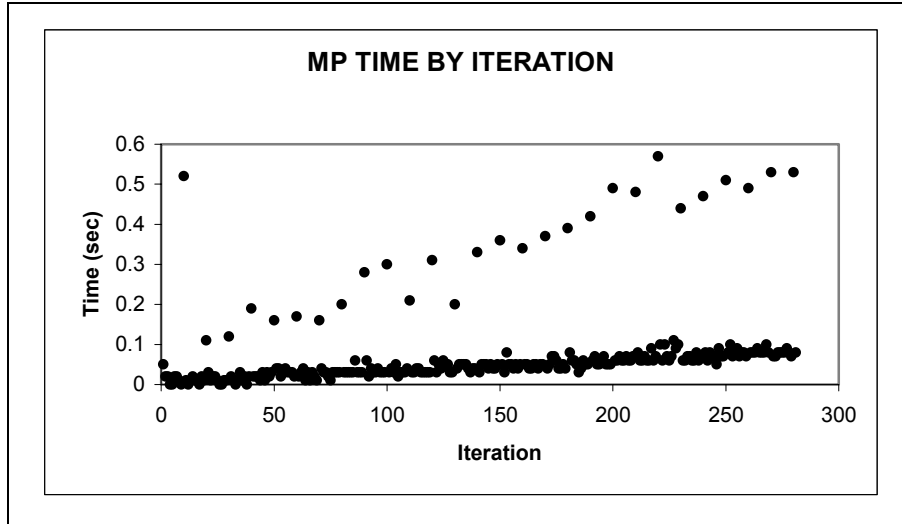


Figure 16. Relaxed master problem strategy: Time versus iteration (I). IEEE RTS One Area case without system restoration. We depict computational times when using the relaxed-MP strategy. The top figure shows the subproblem solution time by iteration (which averages under 0.15 seconds). The full master problem is solved every 10th iteration (these are easily distinguished in the bottom plot due to their longer solution times). The average time required to complete each master problem iteration is reduced to less than one second in contrast to the original BDA whose iteration average is 9.5 seconds.

Figure 16 shows that subproblem solution times are approximately the same as in the original BDA (see Chapter IV, Figure 10), whereas the master problem solution times have been reduced considerably. The apparently exponential increase in master-problem solution times (exhibited by the original BDA as iterations progressed) does not appear now: The new master-problem solution times appear to increase only linearly by iteration. The average time per iteration using the relaxed-MP strategy is 0.15 seconds, much less than the average of 9.5 seconds per iteration for the original BDA.

The results above are for the problem without system restoration. Figure 17 depicts the solution trajectory for the IEEE RTS One Area case with system restoration, using the relaxed-MP strategy.

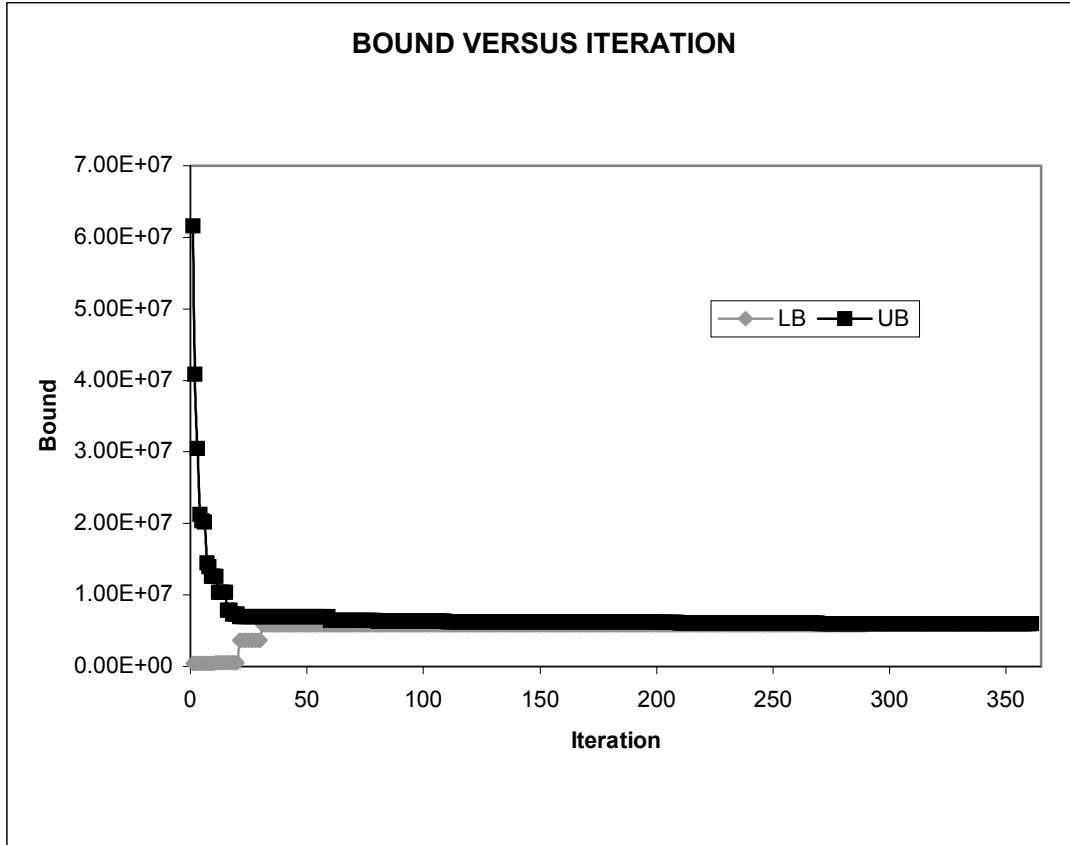


Figure 17. Relaxed master problem strategy: Convergence (II). IEEE RTS One Area case with system restoration. The algorithm closes the gap rapidly in early iterations but takes many iterations to prove optimality. Detailed solving time from the algorithm, not shown, reveals that a 10% gap is reached in 12 seconds, but optimality is not reached until 60 seconds.

Note, however, that this problem takes longer to reach optimality using the relaxed-MP strategy than the original BDA. This fact can be attributed to the number of relaxed master problems (nine in this run) that are solved before we solve the standard master problem in order to update the lower bound. If we reduce the interval for solving the standard master problem, for example, every 3rd iteration, we would be able to solve this problem to optimality in only 23 seconds, a reduction of 8 seconds (25%) over the original BDA.

Figure 18 shows the cumulative solution time for the master problem for both the original BDA and the relaxed-MP strategy. Note the reduced solution time for the master problem when compared to the original BDA.

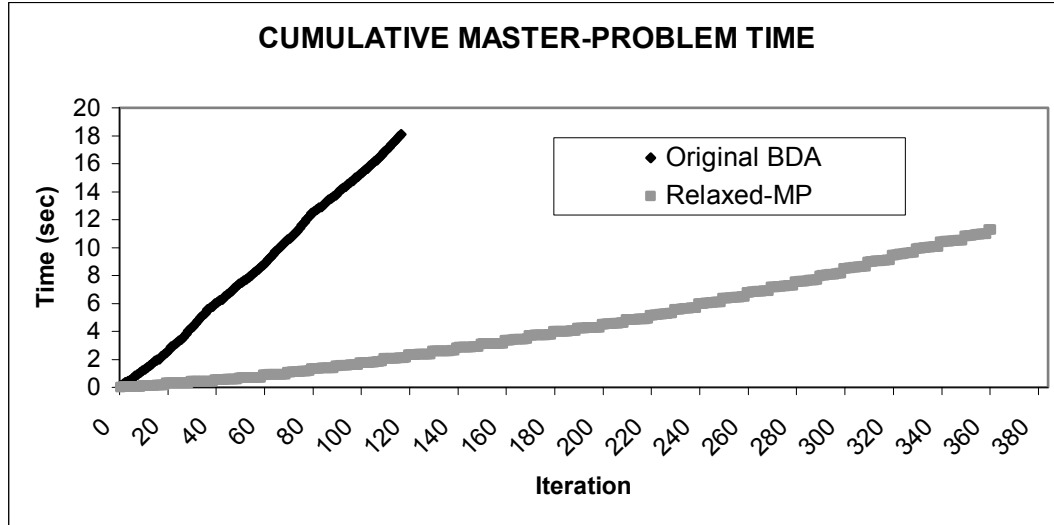


Figure 18. Relaxed master problem strategy: Time versus iteration (II). IEEE RTS One Area case with system restoration. We show cumulative time to solve the master problem. The average time per iteration for the master problem in the relaxed-MP algorithm is 0.03 seconds (including iterations where the master problem is solved exactly), a substantial improvement from the original BDA, which is 0.15 seconds. Cumulative time is reduced accordingly.

The advantages of the relaxed-MP algorithm are more significant as problems become more difficult. This algorithm helps close the optimality gap faster because (1) every relaxed Benders cut is valid and can therefore contribute to the reduction of the upper bound, and (2) the relaxed master problem is so much faster to solve. Figure 19 shows the effect of this algorithmic strategy for the IEEE RTS Two Area case with system restoration.

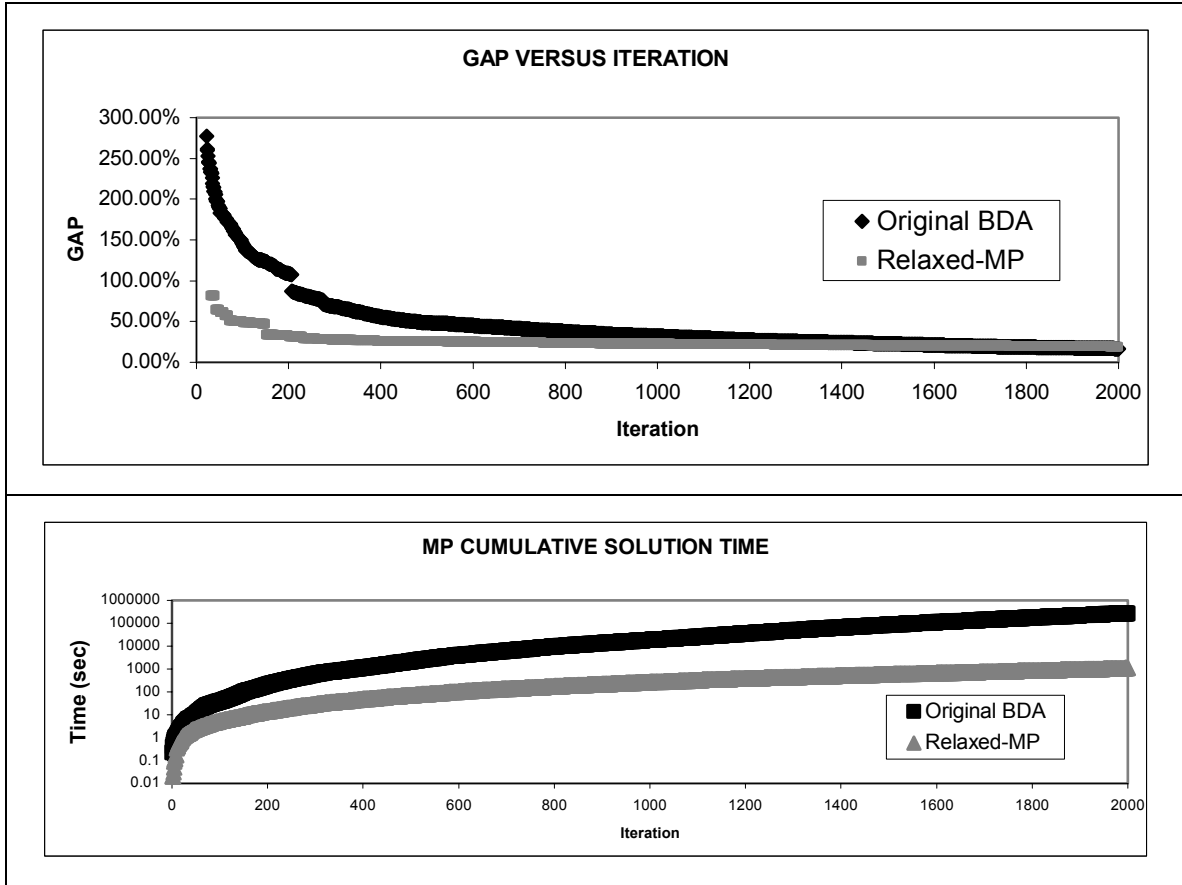


Figure 19. Relaxed master problem strategy: Convergence and Time versus Iteration (III). IEEE RTS Two Area case with system restoration. The top graph illustrates that the relaxed-MP algorithm closes the optimality gap more in earlier iterations. The bottom graph illustrates the master problem's reduced cumulative solution time when we use the relaxed-MP algorithm. Note that a logarithmic scale on the time axis is used for clarity.

In the IEEE RTS Two Area case we can appreciate the impact of the relaxed-MP strategy on overall solution time. The original BDA takes over 75 hours to complete 2,000 iterations, reaching a 16% gap. By solving the relaxed master problem for nine of ten iterations, and solving the standard master problem every 10th iteration, we reduce the total solution time to a mere 26 minutes for 2,000 iterations, and reach a 19% gap. The original algorithm reaches a 20% gap at iteration 1,683 in approximately 37 hours; in contrast, the relaxed-MP algorithm achieves the same gap in 1,762 iterations but only in 20 minutes. The average time per iteration for this test case using the original

algorithm is two minutes and 15 seconds; using the relaxed-MP algorithm, we reduce the average time per iteration to 0.78 seconds. The original BDA, of course, takes much more time to achieve such gap.

C. CUT-DROPPING STRATEGIES

The relaxed-MP algorithm helps solve certain problems, but larger problems need additional techniques like “cut-dropping” if they are to be solved efficiently. The goal of cut-dropping is to limit the number of Benders cuts in the problem so that the master problem remains efficiently solvable. Of course, convergence of BDA may be lost unless care is taken.

We explore the following cut-dropping techniques:

- Drop (delete) all “sufficiently slack cuts,”
- Drop all “non-LP-active cuts,”
- Dropping the first slack cut,
- Keep a minimum number of cuts plus all active cuts, and
- Keep the n -most active cuts.

The following subsections explain and demonstrate each technique in detail.

1. Dropping All Non-active Cuts

This strategy attempts to keep only binding cuts (the cuts that remain “active” between iterations) in the master problem. In a linear problem, an inequality constraint is deemed “active” (or binding) at a given feasible solution if the exact equality holds at that solution. A non-active constraint is said to be slack. The concept of slackness is important here because though basic sensitivity analysis one can show that, at the optimal solution to a linear problem, slack constraints can be dropped without changing the optimal solution to the problem. Moreover, it is well known that, for linear problems solved through Benders decomposition, one may eliminate non-active cuts in the master problem at a given iteration without losing convergence to an optimal solution.

For a mixed-integer master problem, the above property is also true, but checking for active cuts is a more complicated task because a cut might be (in fact, will be in most cases) slack at the optimal integer solution, yet removing it could cause a (strict) relaxation of the master problem. Checking for active cuts in a MIP requires removing the cut and solving the new MIP (in order to assess if the optimal objective function value has changed). Doing this for every cut is not likely to yield an efficient algorithm, of course. Instead, our approach consists of dropping cuts that are “estimated” to be non-active. We accomplish this by removing all cuts at any iteration that have a slack greater than a percentage of the optimal value of the current MP. The slack for a cut of the form $z \leq c^t \cdot \delta$ (where $z \in \mathbb{R}$, $c, \delta \in \mathbb{R}^n$) at a given feasible solution $(\hat{z}, \hat{\delta})$ is given by $s = c^t \cdot \hat{\delta} - \hat{z} \geq 0$. Then, s is compared with the master-problem objective function value \hat{z} . Ideally, we would use $(\hat{z}, \hat{\delta}) = (z^*, \delta^*)$ (optimal solution to the master problem) to evaluate the (relative) cut slackness. However, sometimes we must rely on relaxed-MP solutions (see Section B) or even on sub-optimal solutions (see Section D) to carry out this comparison.

We use the RTS One Area case for basic tests and perform several runs with various “slackness criteria.” In particular, we eliminate any cut whose slack s is greater than 0.1%, 1%, 5%, 10% and 20%, respectively of the current \hat{z} . The results for all these cases are similar and unsatisfactory: It appears that this technique eliminates some cuts that are necessary for the convergence of the problem. For example, if we use $s \geq 0.20\hat{z}$ (20%), the master problem bound does not improve after the 85th iteration, impeding this variant of BDA from converging (see Figure 20).

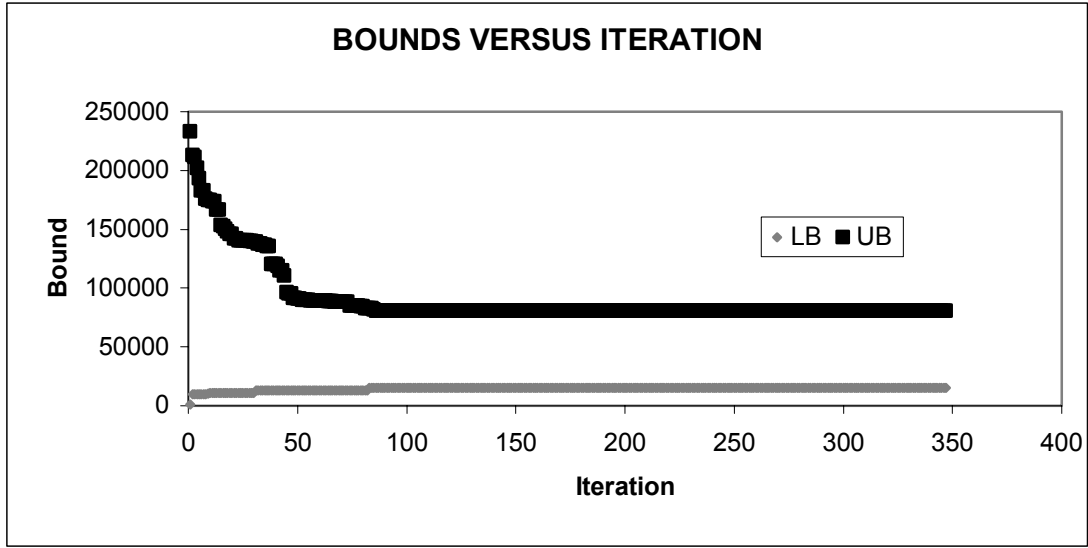


Figure 20. Dropping non-active cuts: Convergence. IEEE RTS Two Area case without system restoration. Lower and Upper Bounds versus number of iterations. We only use estimated active cuts in the master problem. These cuts cannot close the optimality gap.

2. Dropping Non-LP Active Cuts

This strategy estimates the active cuts in the master problem by using the active cuts in the relaxed master problem. We keep only LP-active cuts in the master problem. We consider a cut to be LP-active if it is active in the relaxed master problem. This technique showed no significant improvement over the previous cut dropping technique because it also appears to remove too many cuts from the master problem. For example, in the IEEE RTS One Area case with system restoration, only four LP-active cuts remain in iteration 566, yielding a weak upper bound.

3. Dropping the First Slack Cut

We check all incumbent cuts at any given iteration until we find one whose slack exceeds a pre-specified threshold, for example, being 20% above the master problem objective function value. If none of the cuts satisfies this criterion, none is dropped. In addition, a cut that is removed is no longer considered in the master problem.

This strategy still removes cuts that are needed for convergence. In the IEEE RTS One Area case with system restoration and a slackness threshold of 20%, only nine cuts remain in the master problem by iteration 300 and the optimality gap is 597%. When we increase the criterion to 80%, 52 cuts remain at iteration 300, but the optimality gap is still unacceptable at 180%.

A variant of this strategy consists of selecting the first cut whose dual variable (at the optimal branch-and-bound node for the master problem solution) is zero for elimination. Again, this alternative does not provide us with the necessary set of cuts to close the optimality gap.

4. Keeping the n -Most Active Cuts

The results in the previous subsections show that we must sustain an elevated number of cuts in order to avoid destroying convergence. Additionally, we can see from those strategies that if we eliminate cuts based on a pre-set slackness criterion we may be eliminating cuts needed for convergence.

Here we try a new strategy where we limit the number of cuts to a pre-specified value, n . We assume the master problem with n cuts is solvable in a reasonable amount of time. At every iteration, we replace the cut with largest slack by the cut generated at the incumbent iteration. This strategy guarantees that the “best” $n-1$ cuts are always used, keeping the problem to a manageable size that will solve relatively quickly.

Testing indicates that being too restrictive in the value given to n can prevent the algorithm from converging. For example, Figure 21 shows that for the IEEE RTS One Area case with system restoration, restricting the number of cuts to $n = 30$ is not efficient, whereas the algorithm converges successfully for $n = 110$.

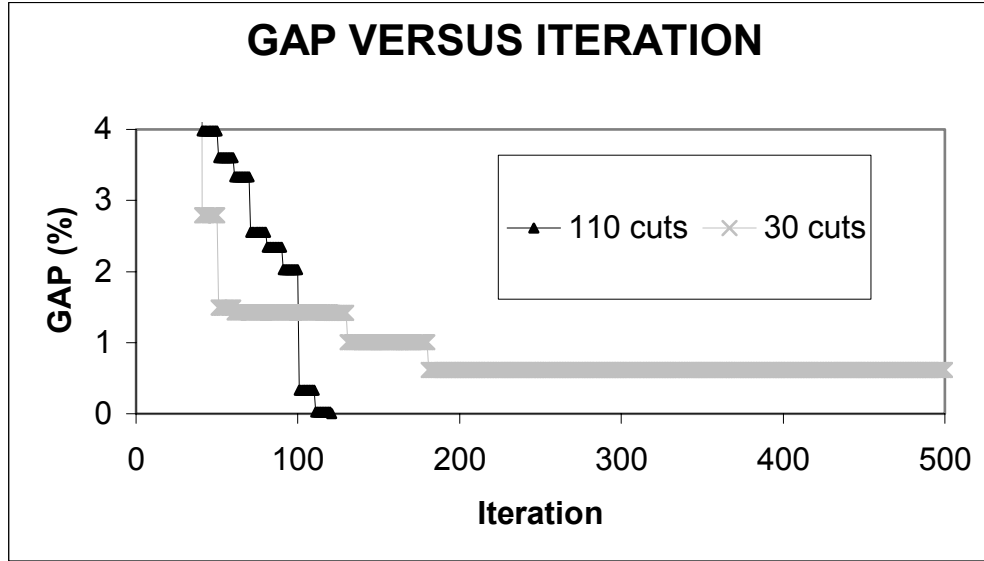


Figure 21. Keeping the n most active cuts: Convergence. IEEE RTS One Area case with system restoration. Gap versus iteration plot. Limiting the number of cuts makes the problem simpler to solve. However, as illustrated in this figure, too few cuts will prevent the problem from closing the optimality gap.

Specifically for $n = 30$ cuts, we can only close the gap to 60% after 180 iterations (in 45 seconds), and cannot improve after then. For $n = 60$ cuts, we can achieve a 34% gap in 62 iterations (19 seconds). For $n = 90$ cuts, a gap of 4% is achieved in 99 iterations (30 seconds). Finally, for any $n = 110$ cuts or more, the problem solves to optimality in 117 iterations (35 seconds).

D. SUB-OPTIMAL INTEGER SOLUTIONS

In this section we consider a strategy that is similar to the master-problem relaxation described in Section B. This extension involves establishing a termination criterion for the (full, mixed-integer) master problem before it is solved to optimality. Typical termination criteria are based on limiting any of the following: the number of integer solutions found during the branch-and-bound process, the number of nodes explored in the branch-and-bound tree, the computational time spent, or combinations of the above, such as: “Stop after a maximum number of seconds, if at least one integer solution has been found.”

If the integer solution found is not integer-optimal (due to the early termination according to pre-specified criteria) then the upper bound cannot be updated. However, it is still a candidate solution for improving the lower bound, which will be obtained after solving the subproblem for that candidate solution.

To ensure that the upper bound eventually improves, at least every m iterations (e.g., $m = 50$) the full master problem needs to be solved to optimality. (Recall that the upper bound can also be updated whenever we solve a relaxed master problem). Figure 22, shows the bound trajectory graph for the RTS Two Area case where (a) the master problem is solved to optimality every 50th iteration, (b) the master problem is solved to a sub-optimal integer solution every 10th iteration that is not a 50th iteration, and where (c) RMP _{k} is solved otherwise.

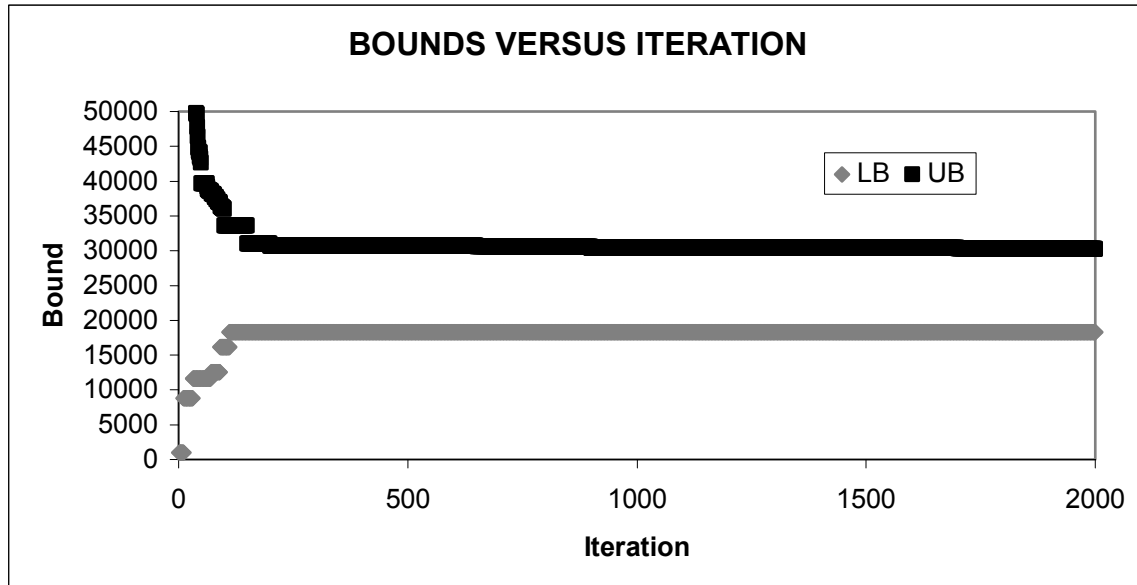


Figure 22. Master problem sub-optimal solution strategy: Convergence. RTS Two Area case without system restoration. This strategy uses relaxed-MP nine of every ten iterations, sub-optimal integer solutions to the master problem at every 10th iteration except every 50th iteration when the full master problem is solved to optimality. After 2,000 iterations, we achieve a 65% gap in 26 minutes. In comparison, the relaxed-MP algorithm alone (where master problems are solved to optimality every 10th iteration) achieves a 62% gap in 1 hour and 42 minutes in the same number of iterations.

This strategy performs better than the original BDA at early iterations (gap and time per iteration are reduced). However, it reaches a point where the convergence stalls.

E. COMBINED STRATEGY

Here, we present the relaxed-MP strategy combined with the cut dropping strategy that keeps the n most-active cuts. This combined strategy proves to be the best among all possible combinations. We show this combined strategy applied to the RTS Two Area case with system restoration.

Table 4 compares results for 2,000 iterations using the different strategies. We take $n = 500$ most active cuts, and then combine it with the relaxed-MP strategy where the full MP_k is solved at every 10^{th} iteration only.

Technique	Original BDA	Relaxed MP	Best 500 cuts	Combined
Final GAP	16.8%	19.1%	48.6%	8.3%
CPU time	75h 12 m	26m	1h 45m	16m

Table 4. Combined strategies: n -most active cuts with relaxed-MP. RTS Two Area case with system restoration. This table shows the Gap and Time comparisons for the most effective strategies. The results show over 99% improvement in time and a 50% improvement in the gap achieved when using the combined strategy in lieu of the original BDA.

In fact, we can even obtain better solutions for this case by increasing the number of cuts allowed in the solution strategy. For example, if we increase the number of most active cuts to keep to 700, at the end of 2,000 iterations, a gap of only 4% remains, but the time to complete this process increases to 20 minutes. We can also increase the number of iterations to decrease the gap. Figure 23 illustrates results for the combined strategy with $n = 700$ when applied to the RTS Two Area case.

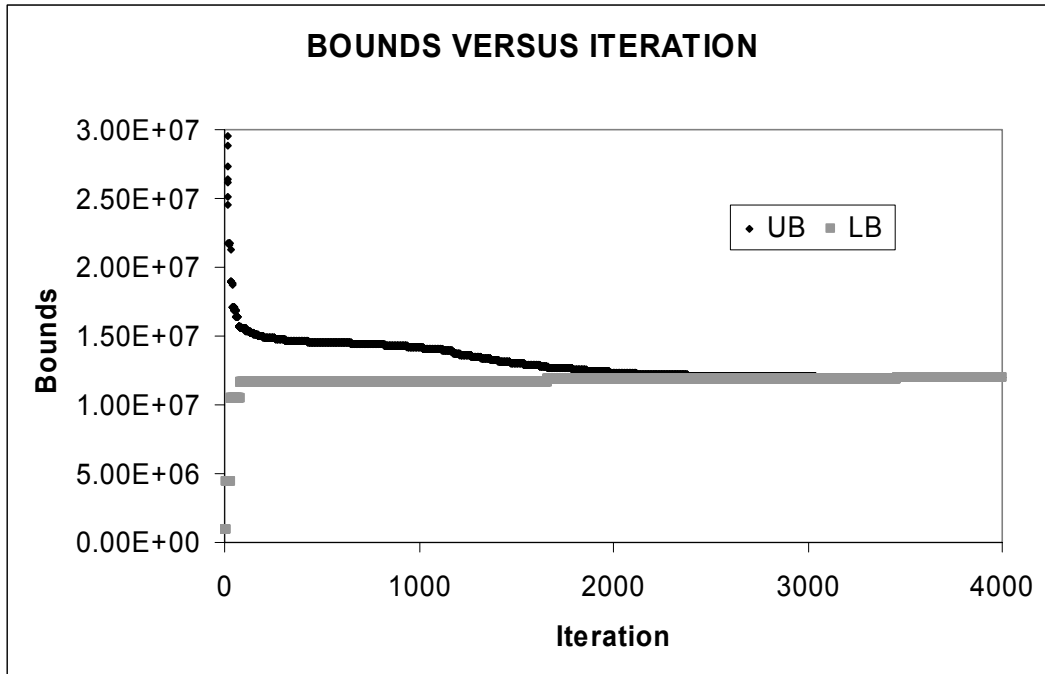


Figure 23. Combined strategy, n-most active cuts with relaxed-MP. IEEE RTS Two Area case without system restoration. 700-most active cuts are used, and the full MP is solved every 10th iteration. The problem reaches a 5% gap within 20 minutes and proves optimality in 45 minutes.

The solution obtained through this combined strategy represents a 99.12% improvement over the time required by the original BDA. (Comparison is made for a 16% gap, which is the gap achieved by the original BDA.) Additionally, this combined technique allowed us to prove optimality through complete convergence.

VII. CONCLUSIONS AND RECOMMENDATIONS FOR FURTHER RESEARCH

This chapter summarizes the most important findings of the thesis, and proposes areas for future research.

A. CONCLUSIONS

This thesis has expanded upon the models and solution methods of Salmeron et al. (2003, 2004) for optimal interdiction (by terrorists) of electric power grids, using limited offensive resources.

Our first task was to validate the DC power-flow model that forms the core of our interdiction models. We compare power flows computed through the full AC power-flow model provided by the PowerWorld Simulator (PowerWorld 2003) to those computed by our own DC model, DCOPF. The IEEE One Area Reliability Test Case (IEEE 1999-I), with several versions representing different interdiction scenarios, make up the set of test problems. The average deviation in power flows across all scenarios is less than 5%, and all lines showing deviations over 10% carry a negligible fraction of the system's total power. These results indicate that the DC power-flow model is acceptable for interdiction analysis.

After consolidating the mixed-integer formulations of the interdiction models (with and without system restoration) developed by Salmeron et al., we have demonstrated that Benders decomposition—this involves iterating between a mixed-integer master problem and a linear-programming subproblem—is a viable technique for solving these problems. We use interdiction decisions as “complicating variables” and develop the decomposition methodology through a small example first. We then extend the procedure to a generic power grid, apply it to larger test problems, and find that convergence is too slow for practical use. For example, an instance of the IEEE Two Area Reliability Test Case (IEEE 1999-I), which has 48 buses, requires two-thousand iterations to close the gap to 16%; and that takes 75 hours on a 3.0 GHz personal computer.

Not only is the number of iterations large, but each one requires us to solve a mixed-integer master problem that becomes more difficult to solve as the iterations proceed, i.e., as more Benders cuts are added to it. For example, in the problem mentioned above, initial master problems solve in less than one second, but by iteration 1,900 they are taking up to up to 600 seconds to solve. (Subproblem solution times remains stable and short throughout for this problem and all others tested.)

In order to improve the efficiency of the original decomposition algorithm, we propose some refinements to the way the master problem is solved. Among the techniques investigated, this combination works best: (a) Solve the full master problem only periodically, say, every 10th iteration, and otherwise solve the master-problem's linear-programming relaxation, and (b) drop certain "unimportant" Benders cuts to limit the size of the master problem (we keep at most n cuts, those that are estimated in some way to be "the most important.") Computational times drop dramatically with this strategy. For example, a 4.7% gap is reached in 2,000 iterations for the previously mentioned problem, but this is accomplished in a mere 20 minutes. Thus, our improved techniques represent important steps toward solving large-scale, real-world interdiction problems.

B. RECOMMENDATIONS FOR FURTHER RESEARCH

We identify the following areas of research from which the existing work could greatly benefit:

1. Further reductions of the computational burden imposed by the master problem. Further research is required in the areas of valid inequalities and cut-dropping techniques, among others.
2. Enhancements to speed solutions of the Benders subproblems. The current implementation does not take advantage of the decomposable structure of these problems, which arises when the goal of the interdicator is to maximize total unmet demand for energy (unmet demand for power, integrated over the time) and

when repair times for interdicted components can vary. This enhancement is not important for small test problems, but it should not be disregarded for larger, real-world problems.

3. Testing on real-world problems.
4. Embedding of our bi-level model into a tri-level “system-protection model.” The ultimate goal of the study of electric-grid interdiction is to help analysts develop plans that minimize the potential for system disruption. Formulation of a tri-level system-protection model, and provision of solutions through exact and heuristic methods are thus required. The system-defense model introduced by Israeli (1999) can serve as the foundation for such work.

THIS PAGE INTENTIONALLY LEFT BLANK

LIST OF REFERENCES

- Allen, W. (January 2003). "Power-Grid Independence Means Better Homeland Security," Energy Pulse,
http://www.energypulse.net/centers/article/article_display.cfm?a_id=152
(accessed March 2004).
- Benders, J. F. (1962). "Partitioning Procedures for Solving Mixed Integer Variables Programming Problems," *Numerische Mathematik*, **4**, pp. 238-252.
- Brown, G. and McBride, R. (1984). "Solving Generalized Networks," *Management Science* **30** (12) 1497-1523.
- Cormican, K. J. (1995). "Computational Methods for Deterministic and Stochastic Network Interdiction Problems," Masters Thesis, Operations Research Department, Naval Post-Graduate School, Monterey, California.
- EIA (Energy Information Administration) (2003).
<http://www.eia.doe.gov/cneaf/electricity/page/glossary.html> (accessed December 2003).
- Elec-Saver (2003). <http://www.elec-saver.com/e-defs.htm#a> (accessed December 2003).
- Frauendorfer, K., Glavitsch, H., Bacher, R. (1993). *Optimization in Planning and Opreation of Electric Power Systems*, Springer-Verlag, New York.
- GAMS (2003). Software available from www.gams.com (accessed January 2003).
- GAMS-CPLEX (2003). <http://www.gams.com/solvers/solvers.htm#CPLEX> (accessed January 2003).
- Geoffrion, A. M. and Graves, G. W. (1974). "Multicommodity Distribution System Design by Benders Decomposition," *Management Science* **20** (5) 822-844
- Germain, J. M. (2003). "Network Vulnerability and the Electrical Grid," Linux Insider (October). <http://www.linuxinsider.com/perl/story/31987.html> (accessed January 2004).
- ICF Consulting (2003). "The Economic Cost of the Blackout,"
http://www.icfconsulting.com/Markets/Energy/doc_files/blackout-economic-costs.pdf (accessed January 2004).
- IEEE Reliability Test Data (1999-I). "The IEEE Reliability Test System – 1996," *IEEE Transactions on Power Systems*, **14**, pp. 1010-1020.
- IEEE Reliability Test Data (1999-II). Data from
www.ee.washington.edu/research/pstca/.

- Israeli, E. (1999). "System Interdiction and Defense," PhD Dissertation, Operations Research Department, Naval Postgraduate School, Monterey, California.
- Israeli, E. and Wood, R. K. (2002). "System Interdiction and Defense," working paper, Operations Research Department, Naval Postgraduate School, Monterey, California.
- NSTAC (National Security Telecommunication Advisory Committee) (1997). Information Assurance Task Force, Electric Power Risk Assessment. March 1997. http://www.ncs.gov/n5_hp/Reports/EPRA/electric.html (accessed January 2004).
- Overbye, T. J., Cheng, X., Sun, Y. (2004). "A Comparison of the AC and DC Power Flow Models for Lmaster problem Calculations," Department of Electrical and Computer Engineering, University of Illinois at Urbana-Champaign.
- PowerWorld (2003). <http://www.powerworld.com> (accessed July 2003).
- Salmeron, J., Wood, K., and Baldick, R. (2003). "Analysis of Electric Grid Security Under Terrorist Threat," *IEEE Transactions on Power Systems*, to appear. http://www.nps.navy.mil/orfacpag/resumePages/Wood-pubs/SalmeronWoodBaldick_Part_I.pdf.
- Salmeron, J., Wood, K. and Baldick, R. (2004). "Optimizing Electric Grid Design Under Asymmetric Threat," Technical Report NPS-OR-03-002, Naval Postgraduate School, Monterey, California.
- SIEMENS (2004). Basics of Electricity introductory course from <http://www.sea.siemens.com/step/templates/lesson.mason?electricity:6:3:1> (accessed February 2004).
- Wolsey, L. (1998). *Integer Programming*. John Wiley & Sons, New York.
- Wood, A. J. and Wollenberg, B. F. (1996). *Power Generation, Operation and Control*, 2nd Edition, John Wiley & Sons, New York.

APPENDICES

APPENDIX A: MIP MODEL WITHOUT SYSTEM RESTORATION

A.1 The Interdiction Model (I-DCOPF)

This interdiction model, I-DCOPF, attempts to maximize the interdiction cost (that is, the sum of generating costs plus load-shedding penalties provided by DCOPF) by choosing an optimal set of components to be interdicted. The following notation is required in addition to that specified for DCOPF:

Additional sets:

L^{**} : Interdictable lines (directly or indirectly)

G^{**} : Interdictable generators (directly or indirectly)

Additional model data:

$$\lambda_l^L = \begin{cases} 1 & \text{if } l \in L^* \\ 0 & \text{otherwise} \end{cases}$$

$$\lambda_g^G = \begin{cases} 1 & \text{if } g \in G^* \\ 0 & \text{otherwise} \end{cases}$$

$$\lambda_l^{L_0} = \begin{cases} 1 & \text{if } l \in L^{**} \\ 0 & \text{otherwise} \end{cases}$$

$$\lambda_g^{G_0} = \begin{cases} 1 & \text{if } g \in G^{**} \\ 0 & \text{otherwise} \end{cases}$$

$i(g)$ = Bus for generator g

$$s(i) = \begin{cases} \text{Substation for bus } i, & \text{if any} \\ 0, & \text{otherwise} \end{cases}$$

Remark: $s(i(g)) = \begin{cases} \text{substation for bus } i \text{ that generator } g \text{ is connected to,} & \text{if any} \\ 0, & \text{otherwise} \end{cases}$

I-DCOPF:

$$\max_{\delta \in \Delta} \min_{P^{Gen}, P^{Line}, S, \theta} \sum_i \sum_{g \in G_i} h(P_{i,g}^{Gen}) + \sum_i \sum_c f(S_{ic})$$

s.t.

Admittance constraints, prior to linearization:

$$P_l^{Line} - B_l(\theta_{o(l)} - \theta_{d(l)})(1 - \lambda_l^{Line} \delta_l^{Line}) \prod_{i \in I^* | l \in L_i^{Bus}} (1 - \delta_i^{Bus}) \prod_{s \in S^* | l \in L_s^{Sub}} (1 - \delta_s^{Sub}) \prod_{ll \in L^* | ll \in L_l^{Par}} (1 - \delta_{ll}^{Line}) \quad \forall l$$

which are re-written below after linearization of the $\delta\theta$ products:

$$P_l^{Line} - B_l(\theta_{o(l)} - \theta_{d(l)}) \leq M_l(\lambda_l^{Line} \delta_l^{Line} + \sum_{i \in I^* | l \in L_i^{Bus}} \delta_i^{Bus} + \sum_{s \in S^* | l \in L_s^{Sub}} \delta_s^{Sub} + \sum_{ll \in L^* | ll \in L_l^{Par}} \delta_{ll}^{Line}) \quad \forall l \quad (\pi_l^A)$$

$$P_l^{Line} - B_l(\theta_{o(l)} - \theta_{d(l)}) \geq -M_l(\lambda_l^{Line} \delta_l^{Line} + \sum_{i \in I^* | l \in L_i^{Bus}} \delta_i^{Bus} + \sum_{s \in S^* | l \in L_s^{Sub}} \delta_s^{Sub} + \sum_{ll \in L^* | ll \in L_l^{Par}} \delta_{ll}^{Line}) \quad \forall l \quad (\pi_l^A)$$

Power balance constraints:

$$\sum_{g \in G_i} P_g^{Gen} - \sum_{l | o(l)=i} P_l^{Line} + \sum_{l | d(l)=i} P_l^{Line} + \sum_c S_{ic} = \sum_c d_{ic} \quad \forall i \quad (\pi_i^{Bal})$$

Line capacity constraints:

$$\begin{aligned} P_l^{Line} &\leq \bar{P}_l^{Line} & \forall l \notin L^{**} & (\pi_l^{L_0^-}) \\ P_l^{Line} &\leq \bar{P}_l^{Line} (1 - \delta_l^{Line}) & \forall l \in L^* & (\pi_l^{LCap^-}) \\ P_l^{Line} &\leq \bar{P}_l^{Line} (1 - \delta_i^{Bus}) & \forall l, i | i \in I^*, l \in L_i^{Bus} & (\pi_{l,i}^{LB^-}) \\ P_l^{Line} &\leq \bar{P}_l^{Line} (1 - \delta_s^{Sub}) & \forall l, s | s \in S^*, l \in L_s^{Sub} & (\pi_{l,s}^{LS^-}) \\ P_l^{Line} &\leq \bar{P}_l^{Line} (1 - \delta_{ll}^{Line}) & \forall l, ll | ll \in L^*, ll \in L_l^{Par} & (\pi_{l,ll}^{LL^-}) \\ P_l^{Line} &\geq -\bar{P}_l^{Line} & \forall l \notin L^{**} & (\pi_l^{L_0^+}) \\ P_l^{Line} &\geq -\bar{P}_l^{Line} (1 - \delta_l^{Line}) & \forall l \in L^* & (\pi_l^{LCap^+}) \\ P_l^{Line} &\geq -\bar{P}_l^{Line} (1 - \delta_i^{Bus}) & \forall l, i | i \in I^*, l \in L_i^{Bus} & (\pi_{l,i}^{LB^+}) \\ P_l^{Line} &\geq -\bar{P}_l^{Line} (1 - \delta_s^{Sub}) & \forall l, s | s \in S^*, l \in L_s^{Sub} & (\pi_{l,s}^{LS^+}) \\ P_l^{Line} &\geq -\bar{P}_l^{Line} (1 - \delta_{ll}^{Line}) & \forall l, ll | ll \in L^*, ll \in L_l^{Par} & (\pi_{l,ll}^{LL^+}) \end{aligned}$$

Power generation constraints:

$$\begin{aligned}
P_g^{Gen} &\leq \bar{P}_g^{Gen} & \forall g \notin G^{**} & (\pi_g^{G_0}) \\
P_g^{Gen} &\leq \bar{P}_g^{Gen} (1 - \delta_g^{Gen}) & \forall g \in G^* & (\pi_g^G) \\
P_g^{Gen} &\leq \bar{P}_g^{Gen} (1 - \delta_{i(g)}^{Bus}) & \forall g \mid i(g) \in I^* & (\pi_g^{GB}) \\
P_g^{Gen} &\leq \bar{P}_g^{Gen} (1 - \delta_{s(i(g))}^{Sub}) & \forall g \mid s(i(g)) \neq 0, s(i(g)) \in S^* & (\pi_g^{GS})
\end{aligned}$$

Upper bounds on the load shedding:

$$S_{ic} \leq d_{ic} \quad \forall i, c \quad (\pi_{i,c}^{Load})$$

Variable sign constraints:

$$\begin{aligned}
P_g^{Gen} &\geq 0 & \forall i, g \mid g \in G_i \\
P_l^{Line} &URS & \forall l \\
S_{ic} &\geq 0 & \forall i, c \\
\theta_i &URS & \forall i
\end{aligned}$$

where

$$\Delta = \left\{ \begin{aligned} & \delta_l^{Line}, \delta_i^{Bus}, \delta_s^{Sub}, \delta_g^{Gen} \in \{0, 1\} \mid \\ & \sum_{i \in I} \sum_{g \in G_i^*} M_{i,g}^{Gen} \delta_{i,g}^{Gen,t} + \sum_{l \in L^*} M_l^{Line,t} \delta_l^{Line,t} + \sum_{i \in I^*} M_i^{Bus,t} \delta_i^{Bus,t} + \sum_{s \in S^*} M_s^{Sub,t} \delta_s^{Sub,t} \leq M \end{aligned} \right\}$$

A.2 The Dual Interdiction Model, DI-DCOPF

Taking the dual of the inner model presented in section A.1 yields the dual interdiction model shown below.

DI-DCOPF:

$$\begin{aligned}
& \max_{\pi} \sum_l M_l \left\{ \lambda_l^L \delta_l^{Line} (\pi_l^{A^-} - \pi_l^{A^+}) + \sum_{l,i \in I^*, l \in L_i^{Bus}} \delta_i^{Bus} (\pi_l^{A^-} - \pi_l^{A^+}) \right. \\
& \quad \left. + \sum_{l,s \in S^*, l \in L_s^{Sub}} \delta_s^{Sub} (\pi_l^{A^-} - \pi_l^{A^+}) + \sum_{l,ll \in L^*, ll \in L_l^{Par}} \delta_{ll}^{Line} (\pi_l^{A^-} - \pi_l^{A^+}) \right\} \\
& + \sum_i \pi_i^{Bal} \cdot (\sum_c d_{ic}) + \sum_{g \notin G^{**}} \bar{P}_g^G \pi_g^{G_0} + \sum_{g \in G^*} \bar{P}_g^G (1 - \delta_g^{Gen}) \pi_g^G + \sum_{g|i(g) \in I^*} \bar{P}_g^G (1 - \delta_{i(g)}^{Bus}) \pi_g^{GB} \\
& + \sum_{g|s(i(g)) \in S^*} \bar{P}_g^G (1 - \delta_{s(i(g))}^{Sub}) \pi_g^{GS} + \sum_{l \notin L^{**}} \bar{P}_l^{Line} (\pi_l^{L_0^-} - \pi_l^{L_0^+}) + \sum_{l \in L^*} \bar{P}_l^{Line} (1 - \delta_l^{Line}) (\pi_l^{L^-} - \pi_l^{L^+}) \\
& + \sum_{l,i \in I^*, l \in L_i^{Bus}} \bar{P}_l^{Line} (1 - \delta_i^{Bus}) (\pi_{l,i}^{LB^-} - \pi_{l,i}^{LB^+}) + \sum_{l,s \in S^*, l \in L_s^{Sub}} \bar{P}_l^{Line} (1 - \delta_{s(i(g))}^{Sub}) (\pi_{l,s}^{LS^-} - \pi_{l,s}^{LS^+}) \\
& + \sum_{l,ll \in L^*, ll \in L_l^{Par}} \bar{P}_l^{Line} (1 - \delta_{ll}^{Line}) (\pi_{l,ll}^{LL^-} - \pi_{l,ll}^{LL^+}) + \sum_{i,c} d_{ic} \pi_{ic}^{Load}
\end{aligned}$$

s.t.

Power-generation dual constraints:

$$\pi_{i(g)}^{Bal} + (1 - \lambda_g^{G_0}) \pi_g^{G_0} + \lambda_g^G \pi_g^G + \lambda_{i(g)}^I \pi_g^{GB} + \lambda_{s(i(g))}^S \pi_g^{GS} \leq h_g \quad \forall g$$

Line-flow dual constraints:

$$\begin{aligned}
& \pi_l^{A^-} + \pi_l^{A^+} + (1 - \lambda_l^{L_0}) (\pi_l^{L_0^-} + \pi_l^{L_0^+}) + \lambda_l^L \pi_l^{L^-} + \lambda_l^L \pi_l^{L^+} + \sum_{l,i \in I^*, l \in L_i} (\pi_{l,i}^{LB^-} + \pi_{l,i}^{LB^+}) \\
& + \sum_{l,s \in S^*, l \in L_s} (\pi_{l,s}^{LS^-} + \pi_{l,s}^{LS^+}) + \sum_{l,ll \in L^*, ll \in L_l^{Par}} (\pi_{l,ll}^{LL^-} + \pi_{l,ll}^{LL^+}) - \pi_{o(l)}^{Bal} + \pi_{d(l)}^{Bal} = 0 \quad \forall l
\end{aligned}$$

Power-shedding dual constraints:

$$\pi_i^{Bal} + \pi_{i,c}^{Load} \leq f_{ic} \quad \forall i, c$$

Phase-angle dual constraints:

$$- \sum_{l|i=o(l)} B_l (\pi_l^{A^-} + \pi_l^{A^+}) + \sum_{l|i=d(l)} B_l (\pi_l^{A^-} + \pi_l^{A^+}) = 0 \quad \forall i$$

Signs on dual variables:

π^{Bal} unrestricted

$$\pi^{A^-}, \pi_l^{L_0^-}, \pi^{L^-}, \pi^{LB^-}, \pi^{LS^-}, \pi^{LL^-} \leq 0$$

$$\pi^{A^+}, \pi_l^{L_0^+}, \pi^{L^+}, \pi^{LB^+}, \pi^{LS^+}, \pi^{LL^+} \geq 0$$

$$\pi^G, \pi^{G_0}, \pi^{GB}, \pi^{GS} \leq 0$$

$$\pi^{Load} \leq 0$$

Bounds on the dual variables:

$$\pi^{G_0}, \pi^G, \pi^{GB}, \pi^{GS} : -\bar{\pi}^G = -\text{Max. shedding cost} - \text{Max. Generating cost}$$

$$\pi^{L_0^-}, \pi^{L^-}, \pi^{LB^-}, \pi^{LS^-}, \pi^{LL^-} : -\bar{\pi}^L = -\text{Max. shedding cost} - \text{Max. Generating cost}$$

$$\pi^{L_0^+}, \pi^{L^+}, \pi^{LB^+}, \pi^{LS^+}, \pi^{LL^+} : \bar{\pi}^L = \text{Max. shedding cost} + \text{Max. Generating cost}$$

$$\pi^{A^-} : -\bar{\pi}^A = -\bar{P}_l^{Line} - B_l \bar{\theta}$$

$$\pi^{A^+} : \bar{\pi}^A = \bar{P}_l^{Line} + B_l \bar{\theta}$$

where we take $\bar{\theta} = 1$ radian.

A.3 Linearization of DI-DCOPF

Linearizing the $\delta\pi$ products in DI-DCOPF yields:

LDI-DCOPF:

$$\begin{aligned} \max_{\pi, v} \sum_l M_l & \left\{ \lambda_l^L (v_l^{A^-} - v_l^{A^+}) + \sum_{l, i | i \in I^*, l \in L_i^{Bus}} (v_l^{BA^-} - v_l^{BA^+}) + \sum_{l, s | s \in S^*, l \in L_s^{Sub}} (v_{l,s}^{SA^-} - v_{l,s}^{SA^+}) + \sum_{l, ll | ll \in L^*, ll \in L_l^{Par}} (v_{l,ll}^{LA^-} - v_{l,ll}^{LA^+}) \right\} \\ & + \sum_{g \notin G^*} \bar{P}_g^G \pi_g^{G_0} + \sum_{g \in G^*} \bar{P}_g^G (\pi_g^G - v_g^G) + \sum_{i | i(g) \in I^*} \bar{P}_g^G (\pi_g^{GB} - v_g^{GB}) + \sum_{s | s(i(g)) \in S^*} \bar{P}_g^G (\pi_g^{GS} - v_g^{GS}) \\ & + \sum_{l \notin L^*} \bar{P}_l^{Line} (\pi_l^{L_0^-} - \pi_l^{L_0^+}) + \sum_{l \in L^*} \bar{P}_l^{Line} [(\pi_l^L - \pi_l^{L^+}) - (v_l^L - v_l^{L^+})] \\ & + \sum_{l, i | i \in I^*, l \in L_i^{Bus}} \bar{P}_l^{Line} [(\pi_{l,i}^{LB^-} - \pi_{l,i}^{LB^+}) - (v_{l,i}^{LB^-} - v_{l,i}^{LB^+})] + \sum_{l, s | s \in S^*, l \in L_s^{Sub}} \bar{P}_l^{Line} [(\pi_{l,s}^{LS^-} - \pi_{l,s}^{LS^+}) - (v_{l,s}^{LS^-} - v_{l,s}^{LS^+})] \\ & + \sum_{l, ll | ll \in L^*, ll \in L_l^{Par}} \bar{P}_l^{Line} [(\pi_{l,ll}^{LL^-} - \pi_{l,ll}^{LL^+}) - (v_{l,ll}^{LL^-} - v_{l,ll}^{LL^+})] + \sum_i (\sum_c d_{ic}) \cdot \pi_i^{Bal} + \sum_i \sum_c d_{ic} \pi_{ic}^{Load} \end{aligned}$$

s.t.

$$\pi_{i(g)}^{Bal} + (1 - \lambda_{g_0}^G) \pi_g^{G_0} + \lambda_g^G \pi_g^G + \lambda_{i(g)}^I \pi_g^{GB} + \lambda_{s(i(g))}^S \pi_g^{GS} \leq h_g \quad \forall g \quad (P_g^G)$$

$$\begin{aligned}
& \pi_l^{A^-} + \pi_l^{A^+} + (1 - \lambda_l^{L_0})(\pi_l^{L_0^-} + \pi_l^{L_0^+}) + \lambda_l^L \pi_l^L + \lambda_l^L \pi_l^{L^+} + \sum_{l,i \mid i \in I^*, l \in L_i} (\pi_{l,i}^{LB^-} + \pi_{l,i}^{LB^+}) \\
& + \sum_{l,s \mid s \in S^*, l \in L_s} (\pi_{l,s}^{LS^-} + \pi_{l,s}^{LS^+}) + \sum_{l,ll \mid ll \in L^*, ll \in L_l^{Par}} (\pi_{l,ll}^{LL^-} + \pi_{l,ll}^{LL^+}) - \pi_{o(l)}^{Bal} + \pi_{d(l)}^{Bal} = 0 \quad \forall l \quad (P_l^L) \\
& \pi_i^{Bal} + \pi_{i,c}^{Load} \leq f_{ic} \quad \forall i, c \quad (S_{i,c}) \\
& - \sum_{l \mid i=o(l)} B_l (\pi_l^{A^-} + \pi_l^{A^+}) + \sum_{l \mid i=d(l)} B_l (\pi_l^{A^-} + \pi_l^{A^+}) = 0 \quad \forall i \quad (\theta_i)
\end{aligned}$$

Linearizing constraints are:

$$\begin{aligned}
v_l^{A^+} &\leq \bar{\pi}_l^A \delta_l^{Line} & \forall l \in L^* & (\gamma_l^{A^+}) \\
v_l^{A^+} - \pi_l^{A^+} &\leq 0 & \forall l \in L^* & (\gamma_l^{A^+}) \\
v_l^{A^+} - \pi_l^{A^+} &\geq -\bar{\pi}_l^A (1 - \delta_l^{Line}) & \forall l \in L^* & (\gamma_l^{A^+}) \\
\\
v_{l,i}^{BA^+} &\leq \bar{\pi}_l^A \delta_i^{Bus} & \forall i, l \mid i \in I^*, l \in L_i^{Bus} & (\gamma_{(l,i)_1}^{BA^+}) \\
v_{l,i}^{BA^+} - \pi_l^{A^+} &\leq 0 & \forall i, l \mid i \in I^*, l \in L_i^{Bus} & (\gamma_{(l,i)_2}^{BA^+}) \\
v_{l,i}^{BA^+} - \pi_l^{A^+} &\geq -\bar{\pi}_l^A (1 - \delta_i^{Bus}) & \forall i, l \mid i \in I^*, l \in L_i^{Bus} & (\gamma_{(l,i)_3}^{BA^+}) \\
\\
v_{l,s}^{SA^+} &\leq \bar{\pi}_l^A \delta_s^{Sub} & \forall s, l \mid s \in S^*, l \in L_s^{Sub} & (\gamma_{(l,s)_1}^{SA^+}) \\
v_{l,s}^{SA^+} - \pi_l^{A^+} &\leq 0 & \forall s, l \mid s \in S^*, l \in L_s^{Sub} & (\gamma_{(l,s)_2}^{SA^+}) \\
v_{l,s}^{SA^+} - \pi_l^{A^+} &\geq -\bar{\pi}_l^A (1 - \delta_s^{Sub}) & \forall s, l \mid s \in S^*, l \in L_s^{Sub} & (\gamma_{(l,s)_3}^{SA^+}) \\
\\
v_{l,ll}^{LA^+} &\leq \bar{\pi}_l^A \delta_{ll}^{Line} & \forall l, ll \mid ll \in L^*, ll \in L_l^{Par} & (\gamma_{(l,ll)_1}^{LA^+}) \\
v_{l,ll}^{LA^+} - \pi_l^{A^+} &\leq 0 & \forall l, ll \mid ll \in L^*, ll \in L_l^{Par} & (\gamma_{(l,ll)_2}^{LA^+}) \\
v_{l,ll}^{LA^+} - \pi_l^{A^+} &\geq -\bar{\pi}_l^A (1 - \delta_{ll}^{Line}) & \forall l, ll \mid ll \in L^*, ll \in L_l^{Par} & (\gamma_{(l,ll)_3}^{LA^+}) \\
\\
v_l^{L^+} &\leq \bar{\pi}_l^L \delta_l^{Line} & \forall l \in L^* & (\gamma_l^{L^+}) \\
v_l^{L^+} - \pi_l^{L^+} &\leq 0 & \forall l \in L^* & (\gamma_l^{L^+}) \\
v_l^{L^+} - \pi_l^{L^+} &\geq -\bar{\pi}_l^L (1 - \delta_l^{Line}) & \forall l \in L^* & (\gamma_l^{L^+})
\end{aligned}$$

$v_{l,i}^{LB^+} \leq \bar{\pi}_l^L \delta_i^{Bus}$	$\forall l, i \mid i \in I^*, l \in L_i^{Bus}$	$(\gamma_{(l,i)_1}^{LB^+})$
$v_{l,i}^{LB^+} - \pi_{l,i}^{LB^+} \leq 0$	$\forall l, i \mid i \in I^*, l \in L_i^{Bus}$	$(\gamma_{(l,i)_2}^{LB^+})$
$v_{l,i}^{LB^+} - \pi_{l,i}^{LB^+} \geq -\bar{\pi}_l^L (1 - \delta_i^{Bus})$	$\forall l, i \mid i \in I^*, l \in L_i^{Bus}$	$(\gamma_{(l,i)_3}^{LB^+})$
$v_{l,s}^{LS^+} \leq \bar{\pi}_l^L \delta_s^{Sub}$	$\forall s, l \mid s \in S^*, l \in L_s^{Sub}$	$(\gamma_{(l,s)_1}^{LS^+})$
$v_{l,s}^{LS^+} - \pi_{l,s}^{LS^+} \leq 0$	$\forall s, l \mid s \in S^*, l \in L_s^{Sub}$	$(\gamma_{(l,s)_2}^{LS^+})$
$v_{l,s}^{LS^+} - \pi_{l,s}^{LS^+} \geq -\bar{\pi}_l^L (1 - \delta_s^{Sub})$	$\forall s, l \mid s \in S^*, l \in L_s^{Sub}$	$(\gamma_{(l,s)_3}^{LS^+})$
$v_{l,ll}^{LL^+} \leq \bar{\pi}_l^L \delta_{ll}^{Line}$	$\forall l, ll \mid ll \in L^*, ll \in L_l^{Par}$	$(\gamma_{(l,ll)_1}^{LL^+})$
$v_{l,ll}^{LL^+} - \pi_{l,ll}^{LL^+} \leq 0$	$\forall l, ll \mid ll \in L^*, ll \in L_l^{Par}$	$(\gamma_{(l,ll)_2}^{LL^+})$
$v_{l,ll}^{LL^+} - \pi_{l,ll}^{LL^+} \geq -\bar{\pi}_l^L (1 - \delta_{ll}^{Line})$	$\forall l, ll \mid ll \in L^*, ll \in L_l^{Par}$	$(\gamma_{(l,ll)_3}^{LL^+})$
$v_l^{A^-} \geq -\bar{\pi}_l^A \delta_l^{Line}$	$\forall l \in L^*$	$(\gamma_l^{A^-})$
$v_l^{A^-} - \pi_l^{A^-} \geq 0$	$\forall l \in L^*$	$(\gamma_{l_2}^{A^-})$
$v_l^{A^-} - \pi_l^{A^-} \leq \bar{\pi}_l^A (1 - \delta_l^{Line})$	$\forall l \in L^*$	$(\gamma_{l_3}^{A^-})$
$v_{l,i}^{BA^-} \geq -\bar{\pi}_l^A \delta_i^{Bus}$	$\forall i, l \mid i \in I^*, l \in L_i^{Bus}$	$(\gamma_{(l,i)_1}^{BA^-})$
$v_{l,i}^{BA^-} - \pi_{l,i}^{BA^-} \geq 0$	$\forall i, l \mid i \in I^*, l \in L_i^{Bus}$	$(\gamma_{(l,i)_2}^{BA^-})$
$v_{l,i}^{BA^-} - \pi_{l,i}^{BA^-} \leq \bar{\pi}_l^A (1 - \delta_i^{Bus})$	$\forall i, l \mid i \in I^*, l \in L_i^{Bus}$	$(\gamma_{(l,i)_3}^{BA^-})$
$v_{l,s}^{SA^-} \geq -\bar{\pi}_l^A \delta_s^{Sub}$	$\forall s, l \mid s \in S^*, l \in L_s^{Sub}$	$(\gamma_{(l,s)_1}^{SA^-})$
$v_{l,s}^{SA^-} - \pi_{l,s}^{SA^-} \geq 0$	$\forall s, l \mid s \in S^*, l \in L_s^{Sub}$	$(\gamma_{(l,s)_2}^{SA^-})$
$v_{l,s}^{SA^-} - \pi_{l,s}^{SA^-} \leq \bar{\pi}_l^A (1 - \delta_s^{Sub})$	$\forall s, l \mid s \in S^*, l \in L_s^{Sub}$	$(\gamma_{(l,s)_3}^{SA^-})$
$v_{l,ll}^{LA^-} \geq -\bar{\pi}_l^A \delta_{ll}^{Line}$	$\forall l, ll \mid ll \in L^*, ll \in L_l^{Par}$	$(\gamma_{(l,ll)_1}^{LA^-})$
$v_{l,ll}^{LA^-} - \pi_{l,ll}^{LA^-} \geq 0$	$\forall l, ll \mid ll \in L^*, ll \in L_l^{Par}$	$(\gamma_{(l,ll)_2}^{LA^-})$
$v_{l,ll}^{LA^-} - \pi_{l,ll}^{LA^-} \leq \bar{\pi}_l^A (1 - \delta_{ll}^{Line})$	$\forall l, ll \mid ll \in L^*, ll \in L_l^{Par}$	$(\gamma_{(l,ll)_3}^{LA^-})$

$v_l^L \geq -\bar{\pi}_l^L \delta_l^{Line}$	$\forall l \in L^*$	(γ_l^L)
$v_l^L - \pi_l^L \geq 0$	$\forall l \in L^*$	(γ_l^L)
$v_l^L - \pi_l^L \leq \bar{\pi}_l^L (1 - \delta_l^{Line})$	$\forall l \in L^*$	(γ_l^L)
$v_{l,i}^{LB^-} \geq -\bar{\pi}_l^L \delta_i^{Bus}$	$\forall i, l \mid i \in I^*, l \in L_i^{Bus}$	$(\gamma_{(l,i)_1}^{LB^-})$
$v_{l,i}^{LB^-} - \pi_{l,i}^{LB^-} \geq 0$	$\forall i, l \mid i \in I^*, l \in L_i^{Bus}$	$(\gamma_{(l,i)_2}^{LB^-})$
$v_{l,i}^{LB^-} - \pi_{l,i}^{LB^-} \leq \bar{\pi}_l^L (1 - \delta_i^{Bus})$	$\forall i, l \mid i \in I^*, l \in L_i^{Bus}$	$(\gamma_{(l,i)_3}^{LB^-})$
$v_{l,s}^{LS^-} \geq -\bar{\pi}_l^L \delta_s^{Sub}$	$\forall s, l \mid s \in S^*, l \in L_s^{Sub}$	$(\gamma_{(l,s)_1}^{LS^-})$
$v_{l,s}^{LS^-} - \pi_{l,s}^{LS^-} \geq 0$	$\forall s, l \mid s \in S^*, l \in L_s^{Sub}$	$(\gamma_{(l,s)_2}^{LS^-})$
$v_{l,s}^{LS^-} - \pi_{l,s}^{LS^-} \leq \bar{\pi}_l^L (1 - \delta_s^{Sub})$	$\forall s, l \mid s \in S^*, l \in L_s^{Sub}$	$(\gamma_{(l,s)_3}^{LS^-})$
$v_{l,ll}^{LL^-} \geq -\bar{\pi}_l^L \delta_{ll}^{Line}$	$\forall l, ll \mid ll \in L^*, ll \in L_l^{Par}$	$(\gamma_{(l,ll)_1}^{LL^-})$
$v_{l,ll}^{LL^-} - \pi_{l,ll}^{LL^-} \geq 0$	$\forall l, ll \mid ll \in L^*, ll \in L_l^{Par}$	$(\gamma_{(l,ll)_2}^{LL^-})$
$v_{l,ll}^{LL^-} - \pi_{l,ll}^{LL^-} \leq \bar{\pi}_l^L (1 - \delta_{ll})$	$\forall l, ll \mid ll \in L^*, ll \in L_l^{Par}$	$(\gamma_{(l,ll)_3}^{LL^-})$
$v_g^G \geq -\bar{\pi}_g^G \delta_g^G$	$\forall g \in G^*$	$(\gamma_{g_1}^G)$
$v_g^G - \pi_g^G \geq 0$	$\forall g \in G^*$	$(\gamma_{g_2}^G)$
$v_g^G - \pi_g^G \leq \bar{\pi}_g^G (1 - \delta_g^G)$	$\forall g \in G^*$	$(\gamma_{g_3}^G)$
$v_g^{GB} \geq -\bar{\pi}_g^G \delta_{i(g)}^{Bus}$	$\forall g \mid i(g) \in I^*$	$(\gamma_{g_1}^{GB})$
$v_g^{GB} - \pi_g^{GB} \geq 0$	$\forall g \mid i(g) \in I^*$	$(\gamma_{g_2}^{GB})$
$v_g^{GB} - \pi_g^{GB} \leq \bar{\pi}_g^G (1 - \delta_{i(g)}^{Bus})$	$\forall g \mid i(g) \in I^*$	$(\gamma_{g_3}^{GB})$
$v_g^{GS} \geq -\bar{\pi}_g^G \delta_{s(i(g))}^{Sub}$	$\forall g \mid s(i(g)) \in S^*$	$(\gamma_{g_1}^{GS})$
$v_g^{GS} - \pi_g^{GS} \geq 0$	$\forall g \mid s(i(g)) \in S^*$	$(\gamma_{g_2}^{GS})$
$v_g^{GS} - \pi_g^{GS} \leq \bar{\pi}_g^G (1 - \delta_{s(i(g))}^{Sub})$	$\forall g \mid s(i(g)) \in S^*$	$(\gamma_{g_3}^{GS})$
$\pi_l^{A^+} \leq \bar{\pi}_l^A$	$\forall l$	$(\eta_l^{A^+})$
$\pi_l^{L^+} \leq \bar{\pi}_l^L$	$\forall l$	$(\eta_l^{L^+})$

$$\begin{array}{lll}
\pi_{l,i}^{LB+} \leq \bar{\pi}_l^L & \forall l, i \mid i \in I^*, l \in L_i^{Bus} & (\eta_{l,i}^{LB+}) \\
\pi_{l,s}^{LS+} \leq \bar{\pi}_l^L & \forall l, s \mid s \in S^*, l \in L_s^{Sub} & (\eta_{l,s}^{LS+}) \\
\pi_{l,ll}^{LL+} \leq \bar{\pi}_l^L & \forall l, ll \mid ll \in L^*, ll \in L_l^{Par} & (\eta_{l,ll}^{LL+}) \\
\\
\pi_l^{A-} \geq -\bar{\pi}_l^A & \forall l \in L^* & (\eta_l^{A-}) \\
\pi_l^L \geq -\bar{\pi}_l^L & \forall l \in L^* & (\eta_l^L) \\
\pi_{l,i}^{LB-} \geq -\bar{\pi}_l^L & \forall l, i \mid i \in I^*, l \in L_i^{Bus} & (\eta_{l,i}^{LB-}) \\
\pi_{l,s}^{LS-} \geq -\bar{\pi}_l^L & \forall l, s \mid s \in S^*, l \in L_s^{Sub} & (\eta_{l,s}^{LS-}) \\
\pi_{l,ll}^{LL-} \geq -\bar{\pi}_l^L & \forall l, ll \mid ll \in L^*, ll \in L_l^{Par} & (\eta_{l,ll}^{LL-}) \\
\\
\pi_g^G \geq -\bar{\pi}_g^G & \forall g \in G^* & (\eta_g^G) \\
\pi_g^{GB} \geq -\bar{\pi}_g^G & \forall g \mid i(g) \in I^* & (\eta_g^{GB}) \\
\pi_g^{GS} \geq -\bar{\pi}_g^G & \forall g \mid s(i(g)) \in S^* & (\eta_g^{GS})
\end{array}$$

π^{Bal} unrestricted

$$\begin{array}{l}
\pi^{A+}, \pi^{L_0+}, \pi^{L+}, \pi^{LB+}, \pi^{LS+}, \pi^{LL+} \geq 0 \\
v^{A+}, v^{L+}, v^{LB+}, v^{LS+}, v^{LL+} \geq 0 \\
\pi^{A-}, \pi^{L_0-}, \pi^{L-}, \pi^{LB-}, \pi^{LS-}, \pi^{LL-} \leq 0 \\
v^{A-}, v^{L-}, v^{LB-}, v^{LS-}, v^{LL-}, v^G, v^{GB}, v^{GS} \leq 0 \\
\pi^G, \pi^{G_0}, \pi^{GB}, \pi^{GS} \leq 0 \\
\pi^{Load} \leq 0
\end{array}$$

A.4 The Master Problem

The master problem for Benders decomposition derives from the dual of LDI-DCOPF. At iteration k , the master problem has the form:

$$(MP_k): \max_{\delta \in \Delta, z \in \mathbb{R}} z$$

s.t.

$$\begin{aligned}
z \leq & \sum_{l \in L^*} \delta_l^{Line} (\bar{\pi}_l^A \gamma_{l_1, k'}^{A^+} + \bar{\pi}_l^A \gamma_{l_3, k'}^{A^+} - \bar{\pi}_l^A \gamma_{l_1, k'}^{A^-} - \bar{\pi}_l^A \gamma_{l_3, k'}^{A^-}) \\
& + \sum_{l, i | i \in I^*, l \in L_i^{Bus}} \delta_i^{Bus} (\bar{\pi}_l^A \gamma_{(l, i)_1, k'}^{BA^+} + \bar{\pi}_l^A \gamma_{(l, i)_3, k'}^{BA^+} - \bar{\pi}_l^A \gamma_{(l, i)_1, k'}^{BA^-} - \bar{\pi}_l^A \gamma_{(l, i)_3, k'}^{BA^-}) \\
& + \sum_{l, s | s \in S^*, l \in L_s^{Sub}} \delta_s^{Sub} (\bar{\pi}_l^A \gamma_{(l, s)_1, k'}^{SA^+} + \bar{\pi}_l^A \gamma_{(l, s)_3, k'}^{SA^+} - \bar{\pi}_l^A \gamma_{(l, s)_1, k'}^{SA^-} - \bar{\pi}_l^A \gamma_{(l, s)_3, k'}^{SA^-}) \\
& + \sum_{l, ll | ll \in L^*, ll \in L_l^{Par}} \delta_{ll}^{Line} (\bar{\pi}_l^A \gamma_{(l, ll)_1, k'}^{LA^+} + \bar{\pi}_l^A \gamma_{(l, ll)_3, k'}^{LA^+} - \bar{\pi}_l^A \gamma_{(l, ll)_1, k'}^{LA^-} - \bar{\pi}_l^A \gamma_{(l, ll)_3, k'}^{LA^-}) \\
& + \sum_{l \in L^*} \delta_l^{Line} (\bar{\pi}_l^L \gamma_{l_1, k'}^{L^+} + \bar{\pi}_l^L \gamma_{l_3, k'}^{L^+} - \bar{\pi}_l^L \gamma_{l_1, k'}^{L^-} - \bar{\pi}_l^L \gamma_{l_3, k'}^{L^-}) \\
& + \sum_{l, i | i \in I^*, l \in L_i^{Bus}} \delta_i^{Bus} (\bar{\pi}_l^L \gamma_{(l, i)_1, k'}^{LB^+} + \bar{\pi}_l^L \gamma_{(l, i)_3, k'}^{LB^+} - \bar{\pi}_l^L \gamma_{(l, i)_1, k'}^{LB^-} - \bar{\pi}_l^L \gamma_{(l, i)_3, k'}^{LB^-}) \\
& + \sum_{l, s | s \in S^*, l \in L_s^{Sub}} \delta_s^{Sub} (\bar{\pi}_l^L \gamma_{(l, s)_1, k'}^{LS^+} + \bar{\pi}_l^L \gamma_{(l, s)_3, k'}^{LS^+} - \bar{\pi}_l^L \gamma_{(l, s)_1, k'}^{LS^-} - \bar{\pi}_l^L \gamma_{(l, s)_3, k'}^{LS^-}) \\
& + \sum_{l, ll | ll \in L^*, ll \in L_l^{Par}} \delta_{ll}^{Line} (\bar{\pi}_l^L \gamma_{(l, ll)_1, k'}^{LL^+} + \bar{\pi}_l^L \gamma_{(l, ll)_3, k'}^{LL^+} - \bar{\pi}_l^L \gamma_{(l, ll)_1, k'}^{LL^-} - \bar{\pi}_l^L \gamma_{(l, ll)_3, k'}^{LL^-}) \\
& + \sum_{g | g \in G^*} \delta_g^{Gen} (-\bar{\pi}_g^G \gamma_{g_1, k'}^G - \bar{\pi}_g^G \gamma_{g_3, k'}^G) + \sum_{g | g \in G^*} \bar{\pi}_g^G \gamma_{g_3, k'}^G \\
& + \sum_{g | i(g) \in I^*} \delta_{i(g)}^{Bus} (-\bar{\pi}_g^G \gamma_{g_1, k'}^{GB} - \bar{\pi}_g^G \gamma_{g_3, k'}^{GB}) + \sum_{g | i(g) \in I^*} \bar{\pi}_g^G \gamma_{g_3, k'}^{GB} \\
& + \sum_{g | s(i(g)) \in S^*} \delta_s^{Sub} (-\bar{\pi}_g^G \gamma_{g_1, k'}^{GS} - \bar{\pi}_g^G \gamma_{g_3, k'}^{GS}) + \sum_{g | s(i(g)) \in S^*} \bar{\pi}_g^G \gamma_{g_3, k'}^{GS} \\
& + \sum_{l | l \in L^*} \bar{\pi}_l^A (\gamma_{l_3, k'}^{A^-} - \gamma_{l_3, k'}^{A^+}) + \sum_{l, i | i \in I^*, l \in L_i^{Bus}} \bar{\pi}_l^A (\gamma_{(l, i)_3, k'}^{BA^-} - \gamma_{(l, i)_3, k'}^{BA^+}) + \sum_{l, s | s \in S^*, l \in L_s^{Sub}} \bar{\pi}_l^A (\gamma_{(l, s)_3, k'}^{SA^-} - \gamma_{(l, s)_3, k'}^{SA^+}) \\
& + \sum_{l, ll | ll \in L^*, ll \in L_l^{Par}} \bar{\pi}_l^A (\gamma_{(l, ll)_3, k'}^{LA^-} - \gamma_{(l, ll)_3, k'}^{LA^+}) + \sum_{l | l \in L^*} \bar{\pi}_l^L (\gamma_{l_3, k'}^{L^-} - \gamma_{l_3, k'}^{L^+}) + \sum_{l, i | i \in I^*, l \in L_i^{Bus}} \bar{\pi}_l^L (\gamma_{(l, i)_3, k'}^{LB^-} - \gamma_{(l, i)_3, k'}^{LB^+}) \\
& + \sum_{l, s | s \in S^*, l \in L_s^{Sub}} \bar{\pi}_l^L (\gamma_{(l, s)_3, k'}^{LS^-} - \gamma_{(l, s)_3, k'}^{LS^+}) + \sum_{l, ll | ll \in L^*, ll \in L_l^{Par}} \bar{\pi}_l^L (\gamma_{(l, ll)_3, k'}^{LL^-} - \gamma_{(l, ll)_3, k'}^{LL^+}) \\
& + \sum_l \left[\left(\bar{\pi}_l^A (\eta_{l, k'}^{A^+} - \eta_{l, k'}^{A^-}) \right) + \left(\bar{\pi}_l^L (\eta_{l, k'}^{L^+} - \eta_{l, k'}^{L^-}) \right) \right] + \sum_{l, i | i \in I^*, l \in L_i^{Bus}} \left[\left(\bar{\pi}_l^L (\eta_{(l, i), k'}^{LB^+} - \eta_{(l, i), k'}^{LB^-}) \right) \right] \\
& + \sum_{l, s | s \in S^*, l \in L_s^{Sub}} \left[\left(\bar{\pi}_l^L (\eta_{(l, s), k'}^{LS^+} - \eta_{(l, s), k'}^{LS^-}) \right) \right] + \sum_{l, ll | ll \in L^*, ll \in L_l^{Par}} \left[\left(\bar{\pi}_l^L (\eta_{(l, ll), k'}^{LL^+} - \eta_{(l, ll), k'}^{LL^-}) \right) \right] \\
& + \sum_{g \in G^*} (-\bar{\pi}_g^G \eta_{g, k'}^G) + \sum_{i(g) \in I^*} (-\bar{\pi}_g^G \eta_{g, k'}^{GB}) + \sum_{s(i(g)) \in S^*} (-\bar{\pi}_g^G \eta_{g, k'}^{GS}) + \sum_g h_g P_{g, k'}^G + \sum_{i, c} f_{i, c} S_{(i, c), k'}
\end{aligned}$$

$$\forall k' = 1, 2, \dots, k$$

APPENDIX B: MIP MODEL WITH SYSTEM RESTORATION

B.1 Constructing Time Periods, and Additional Notation

The notation below and time period construct algorithm are extracted from Salmeron et al. (2004).

Required notation:

T = set of periods, for $t \in T$

$\xi = L^* \cup G^* \cup B^* \cup S^*$, set of all (directly) interdictable elements

$Dur(e)$ = Duration (hours) of outage for element $e \in \xi$, if attacked

D_t = Duration (hours) of time period t , for $t \in T$

$$\beta_{t,e} = \begin{cases} 1, & \text{if component } e \text{ remains unrepaired in time period } t \text{ after being attacked} \\ 0, & \text{if component } e \text{ is repaired before time period } t \text{ after being attacked} \end{cases},$$

for $t \in T$, $e \in \xi$.

Remark: In the above notation $\beta_{t,l}^{\text{Line}}$, $\beta_{t,i}^{\text{Bus}}$, $\beta_{t,g}^{\text{Gen}}$, and $\beta_{t,s}^{\text{Sub}}$ denote $\beta_{t,e}$ when $e=l$ is a line, or $e=i$ is a bus, or $e=g$ is a generator, or $e=s$ is a substation, respectively.

The following algorithm constructs the set of time periods, T , based on the different outage durations for all interdictable elements. In the course of the algorithm, D_t and $\eta_{t,e}$ are also constructed:

Algorithm “Construct Time Periods”:

Initialization: $\tilde{\xi} \leftarrow \xi$, $T \leftarrow \emptyset$, $t \leftarrow 0$, $m_0 \leftarrow 0$;

While $\tilde{\xi} \neq \emptyset$:

$t \leftarrow t + 1$

$T \leftarrow T \cup \{t\}$

$\beta_{t,e} \leftarrow \begin{cases} 1, & \text{if } e \in \tilde{\xi} \\ 0, & \text{otherwise} \end{cases}$

$m_t \leftarrow \min\{Dur(e) \mid e \in \tilde{\xi}\}$

$\xi_t \leftarrow \{e \mid e \in \tilde{\xi} \wedge Dur(e) = m_t\}$

$D_t \leftarrow m_t - m_{t-1}$

$\tilde{\xi} \leftarrow \tilde{\xi} \setminus \xi_t$

End While

Additional notation for interdiction model:

L_t^{**} = Set of lines l that can be directly or indirectly interdicted in period t .

Note :

$l \in L_t^{**}$ if either:

$\beta_{t,l}^{\text{Line}} = 1$, or

$\beta_{t,i}^{\text{Bus}} = 1$ for some $i \mid l \in L_i^{\text{Bus}}$, or

$\beta_{t,s}^{\text{Sub}} = 1$ for some $s \mid l \in L_s^{\text{Sub}}$, or

$\beta_{t,ll}^{\text{Line}} = 1$ for some $ll \mid ll \in L_l^{\text{Par}}$

$$\lambda_l^L = \begin{cases} 1 & \text{if } l \in L^* \\ 0 & \text{otherwise} \end{cases}$$

$$\lambda_{t,l}^L = \begin{cases} 1 & \text{if } l \in L_t^{**} \\ 0 & \text{otherwise} \end{cases}$$

$$\lambda_g^G = \begin{cases} 1 & \text{if } g \in G^* \\ 0 & \text{otherwise} \end{cases}$$

$$\lambda_{t,g}^G = \begin{cases} 1 & \text{if } g \in G_t^{**} \\ 0 & \text{otherwise} \end{cases}$$

$$\lambda_i^I = \begin{cases} 1 & \text{if } i \in I^* \\ 0 & \text{otherwise} \end{cases}$$

$$\lambda_s^S = \begin{cases} 1 & \text{if } s \in S^* \\ 0 & \text{otherwise} \end{cases}$$

B.2 The Interdiction Model, I-DCOPF-R

I-DCOPF-R:

$$\max_{\delta} \min_{(P^{Gen}, P^{Line}, S_t, \theta_t)} \sum_{t=1}^{\zeta} D(t) \cdot \left\{ \sum_g h_g P_{t,g}^{Gen} + \sum_i \sum_c f_{i,c} S_{t,i,c} \right\}$$

s.t.

$$P_{t,l}^{Line} - B_l(\theta_{t,o(l)} - \theta_{t,d(l)}) \leq M_l(\lambda_l^{Line} \beta_{t,l}^{Line} \delta_l^{Line} + \sum_{i \in I^* | l \in L_i^{Bus}} \beta_{t,i}^{Bus} \delta_i^{Bus} + \sum_{s \in S^* | l \in L_s^{Sub}} \beta_{t,s}^{Sub} \delta_s^{Sub} + \sum_{ll \in L^* | ll \in L_l^{Line}} \beta_{t,ll}^{Line} \delta_{ll}^{Line}) \quad \forall l, \forall t \quad (\pi_{t,l}^A)$$

$$P_{t,l}^{Line} - B_l(\theta_{t,o(l)} - \theta_{t,d(l)}) \geq -M_l(\lambda_l^{Line} \beta_{t,l}^{Line} \delta_l^{Line} + \sum_{i \in I^* | l \in L_i^{Bus}} \beta_{t,i}^{Bus} \delta_i^{Bus} + \sum_{s \in S^* | l \in L_s^{Sub}} \beta_{t,s}^{Sub} \delta_s^{Sub} + \sum_{ll \in L^* | ll \in L_l^{Line}} \beta_{t,ll}^{Line} \delta_{ll}^{Line}) \quad \forall l, \forall t \quad (\pi_{t,l}^+)$$

$$\sum_{g \in G_i} P_{t,g}^{Gen} - \sum_{l | o(l)=i} P_{t,l}^{Line} + \sum_{l | d(l)=i} P_{t,l}^{Line} + \sum_c S_{t,i,c} = \sum_c d_{i,c} \quad \forall i, t \quad (\pi_{t,i}^{Bal})$$

$$P_{t,l}^{Line} \leq \bar{P}_l^{Line} \quad \forall t, l \notin L_i^{**} \quad (\pi_{t,l}^{L_0^-})$$

$$P_{t,l}^{Line} \leq \bar{P}_l^{Line} (1 - \delta_l^{Line}) \quad \forall t, l \in L^*, \beta_{t,l}^{Line} = 1 \quad (\pi_{t,l}^L)$$

$$P_{t,l}^{Line} \leq \bar{P}_l^{Line} (1 - \delta_i^{Bus}) \quad \forall t, l, i \mid i \in I^*, l \in L_i^{Bus}, \beta_{t,i}^{Bus} = 1 \quad (\pi_{t,l,i}^{LB^+})$$

$$P_{t,l}^{Line} \leq \bar{P}_l^{Line} (1 - \delta_s^{Sub}) \quad \forall t, l, s \mid s \in S^*, l \in L_s, \beta_{t,s}^{Sub} = 1 \quad (\pi_{t,l,s}^{LS^+})$$

$$P_{t,l}^{Line} \leq \bar{P}_l^{Line} (1 - \delta_{ll}^{Line}) \quad \forall t, l, ll \mid ll \in L^*, ll \in L_l^{Par}, \beta_{t,ll}^{Line} = 1 \quad (\pi_{t,l,ll}^{LL})$$

$$P_{t,l}^{Line} \geq -\bar{P}_l^{Line} \quad \forall t, l \notin L_i^{**} \quad (\pi_{t,l}^{L_0^+})$$

$$P_{t,l}^{Line} \geq -\bar{P}_l^{Line} (1 - \delta_l^{Line}) \quad \forall t, l \in L^*, \beta_{t,l}^{Line} = 1 \quad (\pi_{t,l}^{L^+})$$

$$P_{t,l}^{Line} \geq -\bar{P}_l^{Line} (1 - \delta_i^{Bus}) \quad \forall t, l, i \mid i \in I^*, l \in L_i^{Bus}, \beta_{t,i}^{Bus} = 1 \quad (\pi_{t,l,i}^{LB^+})$$

$$P_{t,l}^{Line} \geq -\bar{P}_l^{Line} (1 - \delta_s^{Sub}) \quad \forall t, l, s \mid s \in S^*, l \in L_s, \beta_{t,s}^{Sub} = 1 \quad (\pi_{t,l,s}^{LS^+})$$

$$P_{t,l}^{Line} \geq -\bar{P}_l^{Line} (1 - \delta_{ll}^{Line}) \quad \forall t, l, ll \mid ll \in L^*, ll \in L_l^{Par}, \beta_{t,ll}^{Line} = 1 \quad (\pi_{t,l,ll}^{LL^+})$$

$$P_{t,g}^{Gen} \leq \bar{P}_g^{Gen} \quad \forall t, g \notin G_i^{**} \quad (\pi_{t,g}^{G_0})$$

$$P_{t,g}^{Gen} \leq \bar{P}_g^{Gen} (1 - \delta_g^{Gen}) \quad \forall t, g \mid g \in G^*, \beta_{t,g}^{Gen} = 1 \quad (\pi_{t,g}^G)$$

$$P_{t,g}^{Gen} \leq \bar{P}_g^{Gen} (1 - \delta_{i(g)}^{Bus}) \quad \forall t, g \mid i(g) \in I^*, \beta_{t,i(g)}^{Bus} = 1 \quad (\pi_{t,g}^{GB})$$

$$P_{t,g}^{Gen} \leq \bar{P}_g^{Gen} (1 - \delta_{s(i(g))}^{Sub}) \quad \forall t, g \mid s(i(g)) \in S^*, \beta_{t,s(i(g))}^{Sub} = 1 \quad (\pi_{t,g}^{GS})$$

$$S_{t,i,c} \leq d_{i,c} \quad \forall i, c \quad (\pi_{t,i,c}^{Load})$$

$$P_{t,g}^{Gen} \geq 0 \quad \forall t, g$$

$$P_{t,l}^{Line} \quad URS \quad \forall t, l$$

$$S_{t,i,c} \geq 0 \quad \forall t, i, c$$

$$\theta_{t,i} \quad URS \quad \forall t, i$$

Bounds on :

$$\pi^{G_0}, \pi^G, \pi^{GB}, \pi^{GS} : -\bar{\pi}^G = -\text{Max. shedding cost} - \text{Max. Generating cost}$$

$$\pi^{L_0^-}, \pi^L, \pi^{LB^-}, \pi^{LS^-}, \pi^{LL^-} : -\bar{\pi}^L = -\text{Max. shedding cost} - \text{Max. Generating cost}$$

$$\pi^{L_0^+}, \pi^{L^+}, \pi^{LB^+}, \pi^{LS^+}, \pi^{LL^+} : \bar{\pi}^L = \text{Max. shedding cost} + \text{Max. Generating cost}$$

$$\pi^{A^-} : -\bar{\pi}^A = -\bar{P}_l^{Line} - B_l \bar{\theta}$$

$$\pi^{A^+} : \bar{\pi}^A = \bar{P}_l^{Line} + B_l \bar{\theta}$$

where we take $\bar{\theta} = 1$ radian.

B.3 The Dual Interdiction Model, DI-DCOPF-R

Taking the dual of the above primal problem yields:

DI-DCOPF-R:

$$\begin{aligned}
\max_{\delta} \max_{\pi} \sum_l M_l \sum_t \left\{ \lambda_l^L \beta_{t,l}^L \delta_l^{Line} (\pi_{t,l}^{A^-} - \pi_{t,l}^{A^+}) + \sum_{i \in I^* | l \in L_i^{Bus}} \beta_{t,i}^B \delta_i^{Bus} (\pi_{t,l}^{A^-} - \pi_{t,l}^{A^+}) \right. \\
+ \sum_{s \in S^* | l \in L_s^{Sub}} \beta_{t,s}^{Sub} \delta_s^{Sub} (\pi_{t,l}^{A^-} - \pi_{t,l}^{A^+}) + \sum_{ll \in L^* | ll \in L_{ll}^{Line}} \beta_{t,ll}^L \delta_{ll}^{Line} (\pi_{t,l}^{A^-} - \pi_{t,l}^{A^+}) \left. \right\} \\
+ \sum_{i,t} (\sum_c d_{ic}) \cdot \pi_{t,i}^{Bal} + \sum_t \sum_{g \notin G^{**}} \bar{P}_g^G \pi_{t,g}^{G_0} + \sum_{g \in G^*} \sum_{t | \beta_{t,g}^{Gen} = 1} \bar{P}_g^G (1 - \delta_g^{Gen}) \pi_{t,g}^G \\
+ \sum_{g | i(g) \in I^*} \sum_{t | \beta_{t,i(g)}^{Bus} = 1} \bar{P}_g^G (1 - \delta_{i(g)}^{Bus}) \pi_{t,g}^{GB} + \sum_{g | s(i(g)) \in S^*} \sum_{t | \beta_{t,s(i(g))}^{Sub} = 1} \bar{P}_g^G (1 - \delta_{s(i(g))}^{Sub}) \pi_{t,g}^{GS} \\
+ \sum_t \sum_{l \notin L^{**}} \bar{P}_l^L (\pi_{t,l}^{L_0^-} - \pi_{t,l}^{L_0^+}) + \sum_{ll \in L^*} \sum_{t | \beta_{t,ll}^{Line} = 1} \bar{P}_l^L (1 - \delta_{ll}^{Line}) (\pi_{t,l}^{L^-} - \pi_{t,l}^{L^+}) \\
+ \sum_{i \in I^* | l \in L_i^{Bus}} \sum_{t | \beta_{t,i}^{Bus} = 1} \bar{P}_l^L (1 - \delta_i^{Bus}) (\pi_{t,l,i}^{LB^-} - \pi_{t,l,i}^{LB^+}) + \sum_{s \in S^* | l \in L_s^{Sub}} \sum_{t | \beta_{t,s}^{Sub} = 1} \bar{P}_l^L (1 - \delta_s^{Sub}) (\pi_{t,l,s}^{LS^-} - \pi_{t,l,s}^{LS^+}) \\
+ \sum_{ll \in L^* | ll \in L_{ll}^{Line}} \sum_{t | \beta_{t,ll}^{Line} = 1} \bar{P}_l^L (1 - \delta_{ll}^{Line}) (\pi_{t,l,ll}^{LL^-} - \pi_{t,l,ll}^{LL^+}) + \sum_{i,c,t} d_{i,c} \pi_{t,i,c}^{Load}
\end{aligned}$$

s.t.

$$\pi_{t,i(g)}^{Bal} + (1 - \lambda_{t,g}^{G_0}) \pi_{t,g}^{G_0} + \lambda_g^G \pi_{t,g}^G + \lambda_{l(g)}^L \beta_{t,i(g)}^{Bus} \pi_{t,g}^{GB} + \lambda_{s(i(g))}^S \beta_{t,s(i(g))}^{Bus} \pi_{t,g}^{GS} \leq D(t) h_g \quad \forall t, g \quad (P_{t,g}^G)$$

$$\begin{aligned}
\pi_{t,l}^{A^-} + \pi_{t,l}^{A^+} + (1 - \lambda_{t,l}^{L_0}) (\pi_{t,l}^{L_0^-} + \pi_{t,l}^{L_0^+}) + \lambda_l^L \beta_{t,l}^{Line} \pi_{t,l}^{LCap^-} + \lambda_l^L \beta_{t,l}^{Line} \pi_{t,l}^{LCap^+} + \sum_{i \in I^* | l \in L_i^{Bus}, \beta_{t,i}^{Bus} = 1} (\pi_{t,l,i}^{LB^-} + \pi_{t,l,i}^{LB^+}) \\
+ \sum_{s \in S^* | l \in L_s^{Sub}, \beta_{t,s}^{Sub} = 1} (\pi_{t,l,s}^{LS^-} + \pi_{t,l,s}^{LS^+}) + \sum_{ll \in L^* | ll \in L_{ll}^{Line}, \beta_{t,ll}^{Line} = 1} (\pi_{t,l,ll}^{LL^-} + \pi_{t,l,ll}^{LL^+}) - \pi_{t,o(l)}^{Bal} + \pi_{t,d(l)}^{Bal} = 0 \quad \forall t, l \quad (P_{t,l}^L)
\end{aligned}$$

$$\pi_{t,i}^{Bal} + \pi_{t,i,c}^{Load} \leq D(t) \cdot f_{ic} \quad \forall t, i, c \quad (S_{t,i,c})$$

$$-\sum_{l|o(l)=i} B_l(\pi_{t,l}^{A^-} + \pi_{t,l}^{A^+}) + \sum_{l|d(l)=i} B_l(\pi_{t,l}^{A^-} + \pi_{t,l}^{A^+}) = 0 \quad \forall t, i \quad (\theta_{t,i})$$

$$\begin{aligned} & \pi^{Bal} \text{ unrestricted} \\ & \pi^{A^+}, \pi^{L_0^+}, \pi^{L^+}, \pi^{LB^+}, \pi^{LS^+}, \pi^{LL^+} \geq 0 \\ & \pi^{A^-}, \pi^{L_0^-}, \pi^{L^-}, \pi^{LB^-}, \pi^{LS^-}, \pi^{LL^-} \leq 0 \\ & \pi^{G_0}, \pi^G, \pi^{GB}, \pi^{GS} \leq 0 \\ & \pi^{Load} \leq 0 \end{aligned}$$

B.4 Linearization of DI-DCOPF-R

Linearizing the products $\delta\pi$ yields:

LDI-DCOPF-R:

$$\begin{aligned} \max_{\delta, \pi, v} \sum_l M_l \sum_t & \left\{ \lambda_l^L \beta_{t,l}^{Line} (v_{t,l}^{A^-} - v_{t,l}^{A^+}) + \sum_{i \in I^*} \beta_{t,i}^{Bus} (v_{t,i}^{BA^-} - v_{t,i}^{BA^+}) \right. \\ & \left. + \sum_{s \in S^*} \beta_{t,s}^{Sub} (v_{t,l,s}^{SA^-} - v_{t,l,s}^{SA^+}) + \sum_{ll \in L^*} \beta_{t,ll}^{Line} (v_{t,l,ll}^{LA^-} - v_{t,l,ll}^{LA^+}) \right\} \\ & + \sum_{i,t} (\sum_c d_{ic}) \cdot \pi_{t,i}^{Bal} + \sum_t \sum_{g \notin G^*} \bar{P}_g^G \pi_{t,g}^{G_0} + \sum_{g \in G^*} \sum_{t|\beta_{t,g}^{Gen}=1} \bar{P}_g^G (\pi_{t,g}^G - v_{t,g}^G) \\ & + \sum_{g|i(g) \in I^*} \sum_{t|\beta_{t,i(g)}^{Bus}=1} \bar{P}_g^G (\pi_{t,g}^{GB} - v_{t,g}^{GB}) + \sum_{g|s(i(g)) \in S^*} \sum_{t|\beta_{t,s(i(g))}^{Sub}=1} \bar{P}_g^G (\pi_{t,g}^{GS} - v_{t,g}^{GS}) \\ & + \sum_t \sum_{l \notin L^*} \bar{P}_l^L (\pi_{t,l}^{L_0^-} - \pi_{t,l}^{L_0^+}) + \sum_{l \in L^*} \sum_{t|\beta_{t,l}^{Line}=1} \bar{P}_l^L ((\pi_{t,l}^L - \pi_{t,l}^{L^+}) - (v_{t,l}^L - v_{t,l}^{L^+})) \\ & + \sum_{i \in I^*} \sum_{l \in L_i^{Bus}} \sum_{t|\beta_{t,i}^{Bus}=1} \bar{P}_l^L ((\pi_{t,l,i}^{LB^-} - \pi_{t,l,i}^{LB^+}) - (v_{t,l,i}^{LB^-} - v_{t,l,i}^{LB^+})) \\ & + \sum_{s \in S^*} \sum_{l \in L_s^{Sub}} \sum_{t|\beta_{t,s}^{Sub}=1} \bar{P}_l^L ((\pi_{t,l,s}^{LS^-} - \pi_{t,l,s}^{LS^+}) - (v_{t,l,s}^{LS^-} - v_{t,l,s}^{LS^+})) \\ & + \sum_{ll \in L^*} \sum_{l \in L_{ll}^{Line}} \sum_{t|\beta_{t,ll}^{Line}=1} \bar{P}_l^L ((\pi_{t,l,ll}^{LL^-} - \pi_{t,l,ll}^{LL^+}) - (v_{t,l,ll}^{LL^-} - v_{t,l,ll}^{LL^+})) + \sum_i \sum_c \sum_t d_{ic} \pi_{t,i,c}^{Load} \end{aligned}$$

With balance constraints:

$$\pi_{t,i(g)}^{Bal} + (1 - \lambda_{t,g}^{G_0}) \pi_{t,g}^{G_0} + \lambda_g^G \pi_{t,g}^G + \lambda_{i(g)}^L \beta_{t,i(g)}^{Bus} \pi_{t,g}^{GB} + \lambda_{s(i(g))}^S \beta_{t,s(i(g))}^{Bus} \pi_{t,g}^{GS} \leq D(t) h_g \quad \forall t, g \quad (P_{t,g}^G)$$

$$\begin{aligned}
& \pi_{t,l}^A + \pi_{t,l}^{A^+} + (1 - \lambda_{t,l}^{L_0})(\pi_{t,l}^{L_0^-} + \pi_{t,l}^{L_0^+}) + \lambda_l^L \beta_{t,l}^{Line} \pi_{t,l}^L + \lambda_l^L \beta_{t,l}^{Line} \pi_{t,l}^{L^+} + \sum_{i \in I^* | l \in L_i^{Bus}, \beta_{t,i}^{Bus} = 1} (\pi_{t,l,i}^{LB^*} + \pi_{t,l,i}^{LB^+}) \\
& + \sum_{s \in S^* | l \in L_s^{Sub}, \beta_{t,s}^{Sub} = 1} (\pi_{t,l,s}^{LS^-} + \pi_{t,l,s}^{LS^+}) + \sum_{ll \in L^* | ll \in L_l^{Par}, \beta_{t,ll}^{Line} = 1} (\pi_{t,l,ll}^{LL} + \pi_{t,l,ll}^{LL^+}) - \pi_{t,o(l)}^{Bal} + \pi_{t,d(l)}^{Bal} = 0 \quad \forall t, l \quad (P_{t,l}^L) \\
& \pi_{t,i}^{Bal} + \pi_{t,i,c}^{Load} \leq D(t) \cdot f_{ic} \quad \forall t, i, c \quad (S_{t,i,c}) \\
& - \sum_{l|o(l)} B_l (\pi_{t,l}^A + \pi_{t,l}^{A^+}) + \sum_{l|d(l)} B_l (\pi_{t,l}^A + \pi_{t,l}^{A^+}) = 0 \quad \forall t, i \quad (\theta_{t,i})
\end{aligned}$$

Linearizing constraints:

$$\begin{aligned}
v_{t,l}^{A^+} &\leq \bar{\pi}_{t,l}^A \delta_l^{Line} & \forall t, l | l \in L^*, t \in T, \beta_{t,l}^{Line} = 1 & (\mathcal{V}_{(t,l)_1}^{A^+}) \\
v_{t,l}^{A^+} - \pi_{t,l}^{A^+} &\leq 0 & \forall t, l | l \in L^*, t \in T, \beta_{t,l}^{Line} = 1 & (\mathcal{V}_{(t,l)_2}^{A^+}) \\
v_{t,l}^{A^+} - \pi_{t,l}^{A^+} &\geq -\bar{\pi}_{t,l}^A (1 - \delta_l^{Line}) & \forall t, l | l \in L^*, t \in T, \beta_{t,l}^{Line} = 1 & (\mathcal{V}_{(t,l)_3}^{A^+}) \\
\\
v_{t,l,i}^{BA^+} &\leq \bar{\pi}_{t,l,i}^A \delta_i^{Bus} & \forall t, i, l | i \in I^*, l \in L_i^{Bus}, t \in T, \beta_{t,i}^{Bus} = 1 & (\mathcal{V}_{(t,l,i)_1}^{BA^+}) \\
v_{t,l,i}^{BA^+} - \pi_{t,l,i}^{A^+} &\leq 0 & \forall t, i, l | i \in I^*, l \in L_i^{Bus}, t \in T, \beta_{t,i}^{Bus} = 1 & (\mathcal{V}_{(t,l,i)_2}^{BA^+}) \\
v_{t,l,i}^{BA^+} - \pi_{t,l,i}^{A^+} &\geq -\bar{\pi}_{t,l,i}^A (1 - \delta_i^{Bus}) & \forall t, i, l | i \in I^*, l \in L_i^{Bus}, t \in T, \beta_{t,i}^{Bus} = 1 & (\mathcal{V}_{(t,l,i)_3}^{BA^+}) \\
\\
v_{t,l,s}^{SA^+} &\leq \bar{\pi}_{t,l,s}^A \delta_s^{Sub} & \forall t, s, l | s \in S^*, l \in L_s^{Sub}, t \in T, \beta_{t,s}^{Sub} = 1 & (\mathcal{V}_{(t,l,s)_1}^{SA^+}) \\
v_{t,l,s}^{SA^+} - \pi_{t,l,s}^{A^+} &\leq 0 & \forall t, s, l | s \in S^*, l \in L_s^{Sub}, t \in T, \beta_{t,s}^{Sub} = 1 & (\mathcal{V}_{(t,l,s)_2}^{SA^+}) \\
v_{t,l,s}^{SA^+} - \pi_{t,l,s}^{A^+} &\geq -\bar{\pi}_{t,l,s}^A (1 - \delta_s^{Sub}) & \forall t, s, l | s \in S^*, l \in L_s^{Sub}, t \in T, \beta_{t,s}^{Sub} = 1 & (\mathcal{V}_{(t,l,s)_3}^{SA^+}) \\
\\
v_{t,l,ll}^{LA^+} &\leq \bar{\pi}_{t,l,ll}^A \delta_{ll}^{Line} & \forall t, l, ll | ll \in L^*, ll \in L_l^{Par}, t \in T, \beta_{t,ll}^{Line} = 1 & (\mathcal{V}_{(t,l,ll)_1}^{LA^+}) \\
v_{t,l,ll}^{LA^+} - \pi_{t,l,ll}^{A^+} &\leq 0 & \forall t, l, ll | ll \in L^*, ll \in L_l^{Par}, t \in T, \beta_{t,ll}^{Line} = 1 & (\mathcal{V}_{(t,l,ll)_2}^{LA^+}) \\
v_{t,l,ll}^{LA^+} - \pi_{t,l,ll}^{A^+} &\geq -\bar{\pi}_{t,l,ll}^A (1 - \delta_{ll}^{Line}) & \forall t, l, ll | ll \in L^*, ll \in L_l^{Par}, t \in T, \beta_{t,ll}^{Line} = 1 & (\mathcal{V}_{(t,l,ll)_3}^{LA^+}) \\
\\
v_{t,l}^{L^+} &\leq \bar{\pi}_{t,l}^L \delta_l^{Line} & \forall t, l \in L^*, t \in T, \beta_{t,l}^{Line} = 1 & (\mathcal{V}_{(t,l)_1}^{L^+}) \\
v_{t,l}^{L^+} - \pi_{t,l}^{L^+} &\leq 0 & \forall t, l \in L^*, t \in T, \beta_{t,l}^{Line} = 1 & (\mathcal{V}_{(t,l)_2}^{L^+}) \\
v_{t,l}^{L^+} - \pi_{t,l}^{L^+} &\geq -\bar{\pi}_{t,l}^L (1 - \delta_l^{Line}) & \forall t, l \in L^*, t \in T, \beta_{t,l}^{Line} = 1 & (\mathcal{V}_{(t,l)_3}^{L^+})
\end{aligned}$$

$v_{t,l,i}^{LB^+} \leq \bar{\pi}_{t,l}^L \delta_i^{Bus}$	$\forall t, l, i \mid i \in I^*, l \in L_i^{Bus}, t \in T, \beta_{t,i}^{Bus} = 1$	$(\gamma_{(t,l,i)_1}^{LB^+})$
$v_{t,l,i}^{LB^+} - \pi_{t,l,i}^{LB^+} \leq 0$	$\forall t, l, i \mid i \in I^*, l \in L_i^{Bus}, t \in T, \beta_{t,i}^{Bus} = 1$	$(\gamma_{(t,l,i)_2}^{LB^+})$
$v_{t,l,i}^{LB^+} - \pi_{t,l,i}^{LB^+} \geq -\bar{\pi}_{t,l}^L (1 - \delta_i^{Bus})$	$\forall t, l, i \mid i \in I^*, l \in L_i^{Bus}, t \in T, \beta_{t,i}^{Bus} = 1$	$(\gamma_{(t,l,i)_3}^{LB^+})$
$v_{t,l,s}^{LS^+} \leq \bar{\pi}_{t,l}^L \delta_s^{Sub}$	$\forall t, s, l \mid s \in S^*, l \in L_s^{Sub}, t \in T, \beta_{t,s}^{Sub} = 1$	$(\gamma_{(t,l,s)_1}^{LS^+})$
$v_{t,l,s}^{LS^+} - \pi_{t,l,s}^{LS^+} \leq 0$	$\forall t, s, l \mid s \in S^*, l \in L_s^{Sub}, t \in T, \beta_{t,s}^{Sub} = 1$	$(\gamma_{(t,l,s)_2}^{LS^+})$
$v_{t,l,s}^{LS^+} - \pi_{t,l,s}^{LS^+} \geq -\bar{\pi}_{t,l}^L (1 - \delta_s^{Sub})$	$\forall t, s, l \mid s \in S^*, l \in L_s^{Sub}, t \in T, \beta_{t,s}^{Sub} = 1$	$(\gamma_{(t,l,s)_3}^{LS^+})$
$v_{t,l,ll}^{LL^+} \leq \bar{\pi}_{t,l}^L \delta_{ll}^{Line}$	$\forall t, l, ll \mid ll \in L^*, ll \in L_l^{Par}, t \in T, \beta_{t,ll}^{Line} = 1$	$(\gamma_{(t,l,ll)_1}^{LL^+})$
$v_{t,l,ll}^{LL^+} - \pi_{t,l,ll}^{LL^+} \leq 0$	$\forall t, l, ll \mid ll \in L^*, ll \in L_l^{Par}, t \in T, \beta_{t,ll}^{Line} = 1$	$(\gamma_{(t,l,ll)_2}^{LL^+})$
$v_{t,l,ll}^{LL^+} - \pi_{t,l,ll}^{LL^+} \geq -\bar{\pi}_{t,l}^L (1 - \delta_{ll}^{Line})$	$\forall t, l, ll \mid ll \in L^*, ll \in L_l^{Par}, t \in T, \beta_{t,ll}^{Line} = 1$	$(\gamma_{(t,l,ll)_3}^{LL^+})$
$v_{t,l}^A \geq -\bar{\pi}_{t,l}^A \delta_l^{Line}$	$\forall t, l \mid l \in L^*, t \in T, \beta_{t,l}^{Line} = 1$	$(\gamma_{(t,l)_1}^A)$
$v_{t,l}^A - \pi_{t,l}^A \geq 0$	$\forall t, l \mid l \in L^*, t \in T, \beta_{t,l}^{Line} = 1$	$(\gamma_{(t,l)_2}^A)$
$v_{t,l}^A - \pi_{t,l}^A \leq \bar{\pi}_{t,l}^A (1 - \delta_l^{Line})$	$\forall t, l \mid l \in L^*, t \in T, \beta_{t,l}^{Line} = 1$	$(\gamma_{(t,l)_3}^A)$
$v_{t,l,i}^{BA^-} \geq -\bar{\pi}_{t,l}^A \delta_i^{Bus}$	$\forall t, i, l \mid i \in I^*, l \in L_i^{Bus}, t \in T, \beta_{t,i}^{Bus} = 1$	$(\gamma_{(t,l,i)_1}^{BA^-})$
$v_{t,l,i}^{BA^-} - \pi_{t,l,i}^{BA^-} \geq 0$	$\forall t, i, l \mid i \in I^*, l \in L_i^{Bus}, t \in T, \beta_{t,i}^{Bus} = 1$	$(\gamma_{(t,l,i)_2}^{BA^-})$
$v_{t,l,i}^{BA^-} - \pi_{t,l,i}^{BA^-} \leq \bar{\pi}_{t,l}^A (1 - \delta_i^{Bus})$	$\forall t, i, l \mid i \in I^*, l \in L_i^{Bus}, t \in T, \beta_{t,i}^{Bus} = 1$	$(\gamma_{(t,l,i)_3}^{BA^-})$
$v_{t,l,s}^{SA^-} \geq -\bar{\pi}_{t,l}^A \delta_s^{Sub}$	$\forall t, s, l \mid s \in S^*, l \in L_s^{Sub}, t \in T, \beta_{t,s}^{Sub} = 1$	$(\gamma_{(t,l,s)_1}^{SA^-})$
$v_{t,l,s}^{SA^-} - \pi_{t,l,s}^{SA^-} \geq 0$	$\forall t, s, l \mid s \in S^*, l \in L_s^{Sub}, t \in T, \beta_{t,s}^{Sub} = 1$	$(\gamma_{(t,l,s)_2}^{SA^-})$
$v_{t,l,s}^{SA^-} - \pi_{t,l,s}^{SA^-} \leq \bar{\pi}_{t,l}^A (1 - \delta_s^{Sub})$	$\forall t, s, l \mid s \in S^*, l \in L_s^{Sub}, t \in T, \beta_{t,s}^{Sub} = 1$	$(\gamma_{(t,l,s)_3}^{SA^-})$
$v_{t,l,ll}^{LA^-} \geq -\bar{\pi}_{t,l}^A \delta_{ll}^{Line}$	$\forall t, l, ll \mid ll \in L^*, ll \in L_l^{Par}, t \in T, \beta_{t,ll}^{Line} = 1$	$(\gamma_{(t,l,ll)_1}^{LA^-})$
$v_{t,l,ll}^{LA^-} - \pi_{t,l,ll}^{LA^-} \geq 0$	$\forall t, l, ll \mid ll \in L^*, ll \in L_l^{Par}, t \in T, \beta_{t,ll}^{Line} = 1$	$(\gamma_{(t,l,ll)_2}^{LA^-})$
$v_{t,l,ll}^{LA^-} - \pi_{t,l,ll}^{LA^-} \leq \bar{\pi}_{t,l}^A (1 - \delta_{ll}^{Line})$	$\forall t, l, ll \mid ll \in L^*, ll \in L_l^{Par}, t \in T, \beta_{t,ll}^{Line} = 1$	$(\gamma_{(t,l,ll)_3}^{LA^-})$
$v_{t,l}^L \geq -\bar{\pi}_{t,l}^L \delta_l^{Line}$	$\forall t, l \mid l \in L^*, t \in T, \beta_{t,l}^{Line} = 1$	$(\gamma_{(t,l)_1}^L)$
$v_{t,l}^L - \pi_{t,l}^L \geq 0$	$\forall t, l \mid l \in L^*, t \in T, \beta_{t,l}^{Line} = 1$	$(\gamma_{(t,l)_2}^L)$
$v_{t,l}^L - \pi_{t,l}^L \leq \bar{\pi}_{t,l}^L (1 - \delta_l^{Line})$	$\forall t, l \mid l \in L^*, t \in T, \beta_{t,l}^{Line} = 1$	$(\gamma_{(t,l)_3}^L)$

$$\begin{aligned}
v_{t,l,i}^{LB^-} &\geq -\bar{\pi}_{t,l}^L \delta_i^{Bus} & \forall t, i, l \mid i \in I^*, l \in L_i^{Bus}, t \in T, \beta_{t,i}^{Bus} = 1 & (\gamma_{(t,l,i)_1}^{LB^-}) \\
v_{t,l,i}^{LB^-} - \pi_{t,l,i}^{LB^-} &\geq 0 & \forall t, i, l \mid i \in I^*, l \in L_i^{Bus}, t \in T, \beta_{t,i}^{Bus} = 1 & (\gamma_{(t,l,i)_2}^{LB^-}) \\
v_{t,l,i}^{LB^-} - \pi_{t,l,i}^{LB^-} &\leq \bar{\pi}_{t,l}^L (1 - \delta_i^{Bus}) & \forall t, i, l \mid i \in I^*, l \in L_i^{Bus}, t \in T, \beta_{t,i}^{Bus} = 1 & (\gamma_{(t,l,i)_3}^{LB^-}) \\
\\
v_{t,l,s}^{LS^-} &\geq -\bar{\pi}_{t,l}^L \delta_s^{Sub} & \forall t, s, l \mid s \in S^*, l \in L_s^{Sub}, t \in T, \beta_{t,s}^{Sub} = 1 & (\gamma_{(t,l,s)_1}^{LS^-}) \\
v_{t,l,s}^{LS^-} - \pi_{t,l,s}^{LS^-} &\geq 0 & \forall t, s, l \mid s \in S^*, l \in L_s^{Sub}, t \in T, \beta_{t,s}^{Sub} = 1 & (\gamma_{(t,l,s)_2}^{LS^-}) \\
v_{t,l,s}^{LS^-} - \pi_{t,l,s}^{LS^-} &\leq \bar{\pi}_{t,l}^L (1 - \delta_s^{Sub}) & \forall t, s, l \mid s \in S^*, l \in L_s^{Sub}, t \in T, \beta_{t,s}^{Sub} = 1 & (\gamma_{(t,l,s)_3}^{LS^-}) \\
\\
v_{t,l,ll}^{LL^-} &\geq -\bar{\pi}_{t,l}^L \delta_{ll}^{Line} & \forall t, l, ll \mid ll \in L^*, ll \in L_l^{Par}, t \in T, \beta_{t,ll}^{Line} = 1 & (\gamma_{(t,l,ll)_1}^{LL^-}) \\
v_{t,l,ll}^{LL^-} - \pi_{t,l,ll}^{LL^-} &\geq 0 & \forall t, l, ll \mid ll \in L^*, ll \in L_l^{Par}, t \in T, \beta_{t,ll}^{Line} = 1 & (\gamma_{(t,l,ll)_2}^{LL^-}) \\
v_{t,l,ll}^{LL^-} - \pi_{t,l,ll}^{LL^-} &\leq \bar{\pi}_{t,l}^L (1 - \delta_{ll}) & \forall t, l, ll \mid ll \in L^*, ll \in L_l^{Par}, t \in T, \beta_{t,ll}^{Line} = 1 & (\gamma_{(t,l,ll)_3}^{LL^-}) \\
\\
v_{t,g}^G &\geq -\bar{\pi}_{t,g}^G \delta_g^G & \forall t, g \mid g \in G^*, t \in T, \beta_{t,g}^{Gen} = 1 & (\gamma_{(t,g)_1}^G) \\
v_{t,g}^G - \pi_{t,g}^G &\geq 0 & \forall t, g \mid g \in G^*, t \in T, \beta_{t,g}^{Gen} = 1 & (\gamma_{(t,g)_2}^G) \\
v_{t,g}^G - \pi_{t,g}^G &\leq \bar{\pi}_{t,g}^G (1 - \delta_g^G) & \forall t, g \mid g \in G^*, t \in T, \beta_{t,g}^{Gen} = 1 & (\gamma_{(t,g)_3}^G) \\
\\
v_{t,g}^{GB} &\geq -\bar{\pi}_{t,g}^G \delta_{i(g)}^{Bus} & \forall t, g \mid i(g) \in I^*, t \in T, \beta_{t,i(g)}^{Bus} = 1 & (\gamma_{(t,g)_1}^{GB}) \\
v_{t,g}^{GB} - \pi_{t,g}^{GB} &\geq 0 & \forall t, g \mid i(g) \in I^*, t \in T, \beta_{t,i(g)}^{Bus} = 1 & (\gamma_{(t,g)_2}^{GB}) \\
v_{t,g}^{GB} - \pi_{t,g}^{GB} &\leq \bar{\pi}_{t,g}^G (1 - \delta_{i(g)}^{Bus}) & \forall t, g \mid i(g) \in I^*, t \in T, \beta_{t,i(g)}^{Bus} = 1 & (\gamma_{(t,g)_3}^{GB}) \\
\\
v_{t,g}^{GS} &\geq -\bar{\pi}_{t,g}^G \delta_{s(i(g))}^{Sub} & \forall t, g \mid s(i(g)) \in S^*, t \in T, \beta_{t,s(i(g))}^{Sub} = 1 & (\gamma_{(t,g)_1}^{GS}) \\
v_{t,g}^{GS} - \pi_{t,g}^{GS} &\geq 0 & \forall t, g \mid s(i(g)) \in S^*, t \in T, \beta_{t,s(i(g))}^{Sub} = 1 & (\gamma_{(t,g)_2}^{GS}) \\
v_{t,g}^{GS} - \pi_{t,g}^{GS} &\leq \bar{\pi}_{t,g}^G (1 - \delta_{s(i(g))}^{Sub}) & \forall t, g \mid s(i(g)) \in S^*, t \in T, \beta_{t,s(i(g))}^{Sub} = 1 & (\gamma_{(t,g)_3}^{GS}) \\
\\
\pi_{t,l}^{A^+} &\leq \bar{\pi}_{t,l}^A & \forall t, l \mid l \in L^*, t \in T & (\eta_{t,l}^{A^+}) \\
\pi_{t,l}^{L^+} &\leq \bar{\pi}_{t,l}^L & \forall t, l \mid l \in L^*, t \in T, \beta_{t,l}^{Line} = 1 & (\eta_{t,l}^{L^+}) \\
\\
\pi_{t,l,i}^{LB^+} &\leq \bar{\pi}_{t,l}^L & \forall t, l, i \mid i \in I^*, l \in L_i^{Bus}, t \in T, \beta_{t,i}^{Bus} = 1 & (\eta_{t,l,i}^{LB^+}) \\
\pi_{t,l,s}^{LS^+} &\leq \bar{\pi}_{t,l}^L & \forall t, l, s \mid s \in S^*, l \in L_s^{Sub}, t \in T, \beta_{t,s}^{Sub} = 1 & (\eta_{t,l,s}^{LS^+}) \\
\pi_{t,l,ll}^{LL^+} &\leq \bar{\pi}_{t,l}^L & \forall t, l, ll \mid ll \in L^*, ll \in L_l^{Par}, t \in T, \beta_{t,ll}^{Line} = 1 & (\eta_{t,l,ll}^{LL^+})
\end{aligned}$$

$$\pi_{t,l}^{A^-} \geq -\bar{\pi}_{t,l}^A \quad \forall t, l \mid l \in L^*, t \in T \quad (\eta_{t,l}^{A^-})$$

$$\pi_{t,l}^{L^-} \geq -\bar{\pi}_{t,l}^L \quad \forall t, l \mid l \in L^*, t \in T, \beta_{t,l}^{Line} = 1 \quad (\eta_{t,l}^{L^-})$$

$$\pi_{t,l,i}^{LB^-} \geq -\bar{\pi}_{t,l}^L \quad \forall t, l, i \mid i \in I^*, l \in L_i^{Bus}, t \in T, \beta_{t,i}^{Bus} = 1 \quad (\eta_{t,l,i}^{LB^-})$$

$$\pi_{t,l,s}^{LS^-} \geq -\bar{\pi}_{t,l}^L \quad \forall t, l, s \mid s \in S^*, l \in L_s^{Sub}, t \in T, \beta_{t,s}^{Sub} = 1 \quad (\eta_{t,l,s}^{LS^-})$$

$$\pi_{t,l,ll}^{LL^-} \geq -\bar{\pi}_{t,l}^L \quad \forall t, l, ll \mid ll \in L^*, ll \in L_l^{Par}, t \in T, \beta_{t,ll}^{line} = 1 \quad (\eta_{t,l,ll}^{LL^-})$$

$$\pi_{t,g}^G \geq -\bar{\pi}_{t,g}^G \quad \forall t, g \mid g \in G^*, t \in T, \beta_{t,g}^{Gen} = 1 \quad (\eta_{t,g}^G)$$

$$\pi_{t,g}^{GB} \geq -\bar{\pi}_{t,g}^G \quad \forall t, g \mid i(g) \in I^*, t \in T, \beta_{t,i(g)}^{Gen} = 1 \quad (\eta_{t,g}^{GB})$$

$$\pi_{t,g}^{GS} \geq -\bar{\pi}_{t,g}^G \quad \forall t, g \mid s(i(g)) \in S^*, t \in T, \beta_{t,s(i(g))}^{Gen} = 1 \quad (\eta_{t,g}^{GS})$$

$$\pi^{Bal} \text{ unrestricted}$$

$$\pi^{A^+}, \pi^{L_0^+}, \pi^{LCap^+}, \pi^{LB^+}, \pi^{LS^+}, \pi^{LL^+} \geq 0$$

$$v^{A^+}, v^{LCap^+}, v^{LB^+}, v^{LS^+}, v^{LL^+} \geq 0$$

$$\pi^{A^-}, \pi^{L_0^-}, \pi^{LCap^-}, \pi^{LB^-}, \pi^{LS^-}, \pi^{LL^-} \leq 0$$

$$v^{A^-}, v^{LCap^-}, v^{LB^-}, v^{LS^-}, v^{LL^-}, v^G, v^{GB}, v^{GS} \leq 0$$

$$\pi^G, \pi^{G_0}, \pi^{GB}, \pi^{GS} \leq 0$$

$$\pi^{Load} \leq 0$$

B.5 The Master Problem

The master problem of the Benders decomposition results from the dual of LDI-DCOPF-R. At iteration k , the master problem has the form:

$$(MP_k): \max_{\delta \in \Delta, z \in \mathbb{R}} z$$

s.t.

$$\begin{aligned}
z \leq & \sum_{t|\beta_{t,j}^{Line}=1} \sum_{l \in L^*} \delta_l^{Line} (\bar{\pi}_{t,l}^A \gamma_{(t,l)_1}^{A^+} + \bar{\pi}_{t,l}^A \gamma_{(t,l)_3}^{A^+} - \bar{\pi}_{t,l}^A \gamma_{(t,l)_1}^{A^-} - \bar{\pi}_{t,l}^A \gamma_{(t,l)_3}^{A^-}) \\
& + \sum_{t|\beta_{t,i}^{Bus}=1} \sum_{l,i \in I^*, l \in L_i^{Bus}} \delta_i^{Bus} (\bar{\pi}_{t,l}^A \gamma_{(t,l)_1}^{BA^+} + \bar{\pi}_{t,l}^A \gamma_{(t,l)_3}^{BA^+} - \bar{\pi}_{t,l}^A \gamma_{(t,l)_1}^{BA^-} - \bar{\pi}_{t,l}^A \gamma_{(t,l)_3}^{BA^-}) \\
& + \sum_{t|\beta_{t,s}^{Sub}=1} \sum_{l,s \in S^*, l \in L_s^{Sub}} \delta_s^{Sub} (\bar{\pi}_{t,l}^A \gamma_{(t,l)_1}^{SA^+} + \bar{\pi}_{t,l}^A \gamma_{(t,l)_3}^{SA^+} - \bar{\pi}_{t,l}^A \gamma_{(t,l)_1}^{SA^-} - \bar{\pi}_{t,l}^A \gamma_{(t,l)_3}^{SA^-}) \\
& + \sum_{t|\beta_{t,ll}^{Line}=1} \sum_{l,ll \in L^*, ll \in L_l^{Par}} \delta_{ll}^{Line} (\bar{\pi}_{t,l}^A \gamma_{(t,l)_1}^{LA^+} + \bar{\pi}_{t,l}^A \gamma_{(t,l)_3}^{LA^+} - \bar{\pi}_{t,l}^A \gamma_{(t,l)_1}^{LA^-} - \bar{\pi}_{t,l}^A \gamma_{(t,l)_3}^{LA^-}) \\
& + \sum_{t|\beta_{t,j}^{Line}=1} \sum_{l \in L^*} \delta_l^{Line} (\bar{\pi}_{t,l}^L \gamma_{(t,l)_1}^{L^+} + \bar{\pi}_{t,l}^L \gamma_{(t,l)_3}^{L^+} - \bar{\pi}_{t,l}^L \gamma_{(t,l)_1}^{L^-} - \bar{\pi}_{t,l}^L \gamma_{(t,l)_3}^{L^-}) \\
& + \sum_{t|\beta_{t,i}^{Bus}=1} \sum_{l,i \in I^*, l \in L_i^{Bus}} \delta_i^{Bus} (\bar{\pi}_{t,l}^L \gamma_{(t,l)_1}^{LB^+} + \bar{\pi}_{t,l}^L \gamma_{(t,l)_3}^{LB^+} - \bar{\pi}_{t,l}^L \gamma_{(t,l)_1}^{LB^-} - \bar{\pi}_{t,l}^L \gamma_{(t,l)_3}^{LB^-}) \\
& + \sum_{t|\beta_{t,s}^{Sub}=1} \sum_{l,s \in S^*, l \in L_s^{Sub}} \delta_s^{Sub} (\bar{\pi}_{t,l}^L \gamma_{(t,l)_1}^{LS^+} + \bar{\pi}_{t,l}^L \gamma_{(t,l)_3}^{LS^+} - \bar{\pi}_{t,l}^L \gamma_{(t,l)_1}^{LS^-} - \bar{\pi}_{t,l}^L \gamma_{(t,l)_3}^{LS^-}) \\
& + \sum_{t|\beta_{t,ll}^{Line}=1} \sum_{l,ll \in L^*, ll \in L_l^{Par}} \delta_{ll}^{Line} (\bar{\pi}_{t,l}^L \gamma_{(t,l)_1}^{LL^+} + \bar{\pi}_{t,l}^L \gamma_{(t,l)_3}^{LL^+} - \bar{\pi}_{t,l}^L \gamma_{(t,l)_1}^{LL^-} - \bar{\pi}_{t,l}^L \gamma_{(t,l)_3}^{LL^-}) \\
& + \sum_{t|\beta_{t,g}^{Gen}=1} \sum_{g \in G^*} \delta_g^{Gen} (-\bar{\pi}_{t,g}^G \gamma_{(t,g)_1}^G - \bar{\pi}_{t,g}^G \gamma_{(t,g)_3}^G) + \sum_{t|\beta_{t,g}^{Gen}=1} \sum_{g \in G^*} \bar{\pi}_{t,g}^G \gamma_{(t,g)_3}^G \\
& + \sum_{t|\beta_{t,i(g)}^{Bus}=1} \sum_{g|i(g) \in I^*} \delta_{i(g)}^{Bus} (-\bar{\pi}_{t,g}^G \gamma_{(t,g)_1}^{GB} - \bar{\pi}_{t,g}^G \gamma_{(t,g)_3}^{GB}) + \sum_{t|\beta_{t,i(g)}^{Bus}=1} \sum_{g|i(g) \in I^*} \bar{\pi}_{t,g}^G \gamma_{(t,g)_3}^{GB} \\
& + \sum_{t|\beta_{t,s(i(g))}^{Sub}=1} \sum_{g|s(i(g)) \in S^*} \delta_{s(i(g))}^{Sub} (-\bar{\pi}_{t,g}^G \gamma_{(t,g)_1}^{GS} - \bar{\pi}_{t,g}^G \gamma_{(t,g)_3}^{GS}) + \sum_{t|\beta_{t,s(i(g))}^{Sub}=1} \sum_{g|s(i(g)) \in S^*} \bar{\pi}_{t,g}^G \gamma_{(t,g)_3}^{GS} \\
& + \sum_{t|\beta_{t,j}^{Line}=1} \sum_{ll \in L^*} \bar{\pi}_{t,l}^A (\gamma_{(t,l)_3}^{A^-} - \gamma_{(t,l)_3}^{A^+}) + \sum_{t|\beta_{t,i}^{Bus}=1} \sum_{l,i \in I^*, l \in L_i^{Bus}} \bar{\pi}_{t,l}^A (\gamma_{(t,l)_3}^{BA^-} - \gamma_{(t,l)_3}^{BA^+}) \\
& + \sum_{t|\beta_{t,s}^{Sub}=1} \sum_{l,s \in S^*, l \in L_s^{Sub}} \bar{\pi}_{t,l}^A (\gamma_{(t,l)_3}^{SA^-} - \gamma_{(t,l)_3}^{SA^+}) + \sum_{t|\beta_{t,ll}^{Line}=1} \sum_{l,ll \in L^*, ll \in L_l^{Par}} \bar{\pi}_{t,l}^A (\gamma_{(t,l)_3}^{LA^-} - \gamma_{(t,l)_3}^{LA^+}) \\
& + \sum_{t|\beta_{t,j}^{Line}=1} \sum_{l \in L^*} \bar{\pi}_{t,l}^L (\gamma_{(t,l)_3}^{L^-} - \gamma_{(t,l)_3}^{L^+}) + \sum_{t|\beta_{t,i}^{Bus}=1} \sum_{l,i \in I^*, l \in L_i^{Bus}} \bar{\pi}_{t,l}^L (\gamma_{(t,l)_3}^{LB^-} - \gamma_{(t,l)_3}^{LB^+}) \\
& + \sum_{t|\beta_{t,s}^{Sub}=1} \sum_{l,s \in S^*, l \in L_s^{Sub}} \bar{\pi}_{t,l}^L (\gamma_{(t,l)_3}^{LS^-} - \gamma_{(t,l)_3}^{LS^+}) + \sum_{t|\beta_{t,ll}^{Line}=1} \sum_{l,ll \in L^*, ll \in L_l^{Par}} \bar{\pi}_{t,l}^L (\gamma_{(t,l)_3}^{LL^-} - \gamma_{(t,l)_3}^{LL^+}) \\
& + \sum_{t \in T} \sum_{l \in L^*} \bar{\pi}_{t,l}^A (\eta_{(t,l),k'}^{A^+} - \eta_{(t,l),k'}^{A^-}) + \sum_{t|\beta_{t,j}^{Line}=1} \sum_{l \in L^*} \bar{\pi}_{t,l}^L (\eta_{(t,l),k'}^{L^+} - \eta_{(t,l),k'}^{L^-}) + \sum_{t|\beta_{t,i}^{Bus}=1} \sum_{l,i \in I^*, l \in L_i^{Bus}} \bar{\pi}_{t,l}^L (\eta_{(t,l,i),k'}^{LB^+} - \eta_{(t,l,i),k'}^{LB^-}) \\
& + \sum_{t|\beta_{t,s}^{Sub}=1} \sum_{l,s \in S^*, l \in L_s^{Sub}} \bar{\pi}_{t,l}^L (\eta_{(t,l,s),k'}^{LS^+} - \eta_{(t,l,s),k'}^{LS^-}) + \sum_{t|\beta_{t,ll}^{Line}=1} \sum_{l,ll \in L^*, ll \in L_l^{Par}} \bar{\pi}_{t,l}^L (\eta_{(t,l,ll),k'}^{LL^+} - \eta_{(t,l,ll),k'}^{LL^-}) \\
& + \sum_{t|\beta_{t,g}^{Gen}=1} \sum_{g \in G^*} (-\bar{\pi}_{t,g}^G \eta_{(t,g),k'}^G) + \sum_{t|\beta_{t,i(g)}^{Bus}=1} \sum_{g \in I^*} (-\bar{\pi}_{t,g}^G \eta_{(t,g),k'}^{GB}) + \sum_{t|\beta_{t,s(i(g))}^{Sub}=1} \sum_{s(i(g)) \in S^*} (-\bar{\pi}_{t,g}^G \eta_{(t,g),k'}^{GS}) \\
& + \sum_{t \in T} \sum_g D_t h_g P_{(t,g),k'}^G + \sum_{t \in T} \sum_{i,c} D_t f_{i,c} S_{(t,i,c),k'} \quad \forall k' = 1, 2, \dots, k
\end{aligned}$$

THIS PAGE INTENTIONALLY LEFT BLANK

APPENDIX C: LINEARIZATION OF CROSS-PRODUCTS

This is an explicit list of constraints for the three-bus example in Chapter IV. γ, η represent the dual variables for the linearizing constraints.

$$v_{12}^{L^+} - \bar{\pi}_{12}^{L^+} \delta_{12}^L \leq 0 \quad (\gamma_{121}^{L^+})$$

$$v_{12}^{L^+} - \pi_{12}^{L^+} \leq 0 \quad (\gamma_{122}^{L^+})$$

$$v_{12}^{L^+} - \pi_{12}^{L^+} - \bar{\pi}_{12}^{L^+} \delta_{12}^L \geq -\bar{\pi}_{12}^{L^+} \quad (\gamma_{123}^{L^+})$$

$$v_{13}^{L^+} - \bar{\pi}_{13}^{L^+} \delta_{13}^L \leq 0 \quad (\gamma_{131}^{L^+})$$

$$v_{13}^{L^+} - \pi_{13}^{L^+} \leq 0 \quad (\gamma_{132}^{L^+})$$

$$v_{13}^{L^+} - \pi_{13}^{L^+} - \bar{\pi}_{13}^{L^+} \delta_{13}^L \geq -\bar{\pi}_{13}^{L^+} \quad (\gamma_{133}^{L^+})$$

$$v_{23}^{L^+} - \bar{\pi}_{23}^{L^+} \delta_{23}^L \leq 0 \quad (\gamma_{231}^{L^+})$$

$$v_{23}^{L^+} - \pi_{23}^{L^+} \leq 0 \quad (\gamma_{232}^{L^+})$$

$$v_{23}^{L^+} - \pi_{23}^{L^+} - \bar{\pi}_{23}^{L^+} \delta_{23}^L \geq -\bar{\pi}_{23}^{L^+} \quad (\gamma_{233}^{L^+})$$

$$v_{12}^{L^-} + \bar{\pi}_{12}^{L^-} \delta_{12}^L \geq 0 \quad (\gamma_{121}^{L^-})$$

$$v_{12}^{L^-} - \pi_{12}^{L^-} \geq 0 \quad (\gamma_{122}^{L^-})$$

$$v_{12}^{L^-} - \pi_{12}^{L^-} + \bar{\pi}_{12}^{L^-} \delta_{12}^L \leq \bar{\pi}_{12}^{L^-} \quad (\gamma_{123}^{L^-})$$

$$v_{13}^{L^-} + \bar{\pi}_{13}^{L^-} \delta_{13}^L \geq 0 \quad (\gamma_{131}^{L^-})$$

$$v_{13}^{L^-} - \pi_{13}^{L^-} \geq 0 \quad (\gamma_{132}^{L^-})$$

$$v_{13}^{L^-} - \pi_{13}^{L^-} + \bar{\pi}_{13}^{L^-} \delta_{13}^L \leq \bar{\pi}_{13}^{L^-} \quad (\gamma_{133}^{L^-})$$

$$v_{23}^{L^-} + \bar{\pi}_{23}^{L^-} \delta_{23}^L \geq 0 \quad (\gamma_{231}^{L^-})$$

$$v_{23}^{L^-} - \pi_{23}^{L^-} \geq 0 \quad (\gamma_{232}^{L^-})$$

$$v_{23}^{L^-} - \pi_{23}^{L^-} + \bar{\pi}_{23}^{L^-} \delta_{23}^L \leq \bar{\pi}_{23}^{L^-} \quad (\gamma_{233}^{L^-})$$

$$v_{12}^{LCap^+} - \bar{\pi}_{12}^{LCap^+} \delta_{12}^L \leq 0 \quad (\gamma_{121}^{LCap^+})$$

$$v_{12}^{LCap^+} - \pi_{12}^{LCap^+} \leq 0 \quad (\gamma_{122}^{LCap^+})$$

$$v_{12}^{LCap^+} - \pi_{12}^{LCap^+} - \bar{\pi}_{12}^{LCap^+} \delta_{12}^L \geq -\bar{\pi}_{12}^{LCap^+} \quad (\gamma_{123}^{LCap^+})$$

$$v_{13}^{LCap^+} - \bar{\pi}_{13}^{LCap^+} \delta_{13}^L \leq 0 \quad (\gamma_{131}^{LCap^+})$$

$$v_{13}^{LCap^+} - \pi_{13}^{LCap^+} \leq 0 \quad (\gamma_{132}^{LCap^+})$$

$$v_{13}^{LCap^+} - \pi_{13}^{LCap^+} - \bar{\pi}_{13}^{LCap^+} \delta_{13}^L \geq -\bar{\pi}_{13}^{LCap^+} \quad (\gamma_{133}^{LCap^+})$$

$$v_{23}^{LCap^+} - \bar{\pi}_{23}^{LCap^+} \delta_{23}^L \leq 0 \quad (\gamma_{231}^{LCap^+})$$

$$v_{23}^{LCap^+} - \pi_{23}^{LCap^+} \leq 0 \quad (\gamma_{232}^{LCap^+})$$

$$v_{23}^{LCap^+} - \pi_{23}^{LCap^+} - \bar{\pi}_{23}^{LCap^+} \delta_{23}^L \geq -\bar{\pi}_{23}^{LCap^+} \quad (\gamma_{233}^{LCap^+})$$

$$v_{12}^{LCap^-} + \bar{\pi}_{12}^{LCap^-} \delta_{12}^L \geq 0 \quad (\gamma_{121}^{LCap^-})$$

$$v_{12}^{LCap^-} - \pi_{12}^{LCap^-} \geq 0 \quad (\gamma_{122}^{LCap^-})$$

$$v_{12}^{LCap^-} - \pi_{12}^{LCap^-} + \bar{\pi}_{12}^{LCap^-} \delta_{12}^L \leq \bar{\pi}_{12}^{LCap^-} \quad (\gamma_{123}^{LCap^-})$$

$$v_{13}^{LCap^-} + \bar{\pi}_{13}^{LCap^-} \delta_{13}^L \geq 0 \quad (\gamma_{131}^{LCap^-})$$

$$v_{13}^{LCap^-} - \pi_{13}^{LCap^-} \geq 0 \quad (\gamma_{132}^{LCap^-})$$

$$v_{13}^{LCap^-} - \pi_{13}^{LCap^-} + \bar{\pi}_{13}^{LCap^-} \delta_{13}^L \leq \bar{\pi}_{13}^{LCap^-} \quad (\gamma_{133}^{LCap^-})$$

$$v_{23}^{LCap^-} + \bar{\pi}_{23}^{LCap^-} \delta_{23}^L \geq 0 \quad (\gamma_{231}^{LCap^-})$$

$$v_{23}^{LCap^-} - \pi_{23}^{LCap^-} \geq 0 \quad (\gamma_{232}^{LCap^-})$$

$$v_{23}^{LCap^-} - \pi_{23}^{LCap^-} + \bar{\pi}_{23}^{LCap^-} \delta_{23}^L \leq \bar{\pi}_{23}^{LCap^-} \quad (\gamma_{233}^{LCap^-})$$

$$\pi_{12}^{L^+} \leq \bar{\pi}_{12}^{L^+} \quad (\eta_{12}^{L^+})$$

$$\pi_{13}^{L^+} \leq \bar{\pi}_{13}^{L^+} \quad (\eta_{13}^{L^+})$$

$$\pi_{23}^{L^+} \leq \bar{\pi}_{23}^{L^+} \quad (\eta_{23}^{L^+})$$

$$\pi_{12}^{L^-} \geq -\bar{\pi}_{12}^{L^-} \quad (\eta_{12}^{L^-})$$

$$\pi_{13}^{L^-} \geq -\bar{\pi}_{13}^{L^-} \quad (\eta_{13}^{L^-})$$

$$\pi_{23}^{L^-} \geq -\bar{\pi}_{23}^{L^-} \quad (\eta_{23}^{L^-})$$

$$\pi_{12}^{LCap^+} \leq \bar{\pi}_{12}^{LCap^+} \quad (\eta_{12}^{LCap^+})$$

$$\pi_{13}^{LCap^+} \leq \bar{\pi}_{13}^{LCap^+} \quad (\eta_{13}^{LCap^+})$$

$$\pi_{23}^{LCap^+} \leq \bar{\pi}_{23}^{LCap^+} \quad (\eta_{23}^{LCap^+})$$

$$\begin{array}{ll}
\pi_{12}^{LCap^-} \geq -\bar{\pi}_{12}^{LCap^-} & (\eta_{12}^{LCap^-}) \\
\pi_{13}^{LCap^-} \geq -\bar{\pi}_{13}^{LCap^-} & (\eta_{13}^{LCap^-}) \\
\pi_{23}^{LCap^-} \geq -\bar{\pi}_{23}^{LCap^-} & (\eta_{23}^{LCap^-})
\end{array}$$

THIS PAGE INTENTIONALLY LEFT BLANK

INITIAL DISTRIBUTION LIST

1. Defense Technical Information Center
Ft. Belvoir, Virginia
2. Dudley Knox Library
Naval Postgraduate School
Monterey, California
3. Professor Javier Salmeron, Code OR/Wd
Department of Operations research
Naval Postgraduate School
Monterey, California
4. Professor R. Kevin Wood, Code OR/Wd
Department of Operations research
Naval Postgraduate School
Monterey, California
5. Professor Ted Lewis, Code CS/Lt
Department of Computer Science
Naval Postgraduate School
Monterey, California
6. Professor Paul Stockton
Center of Homeland Security
Naval Postgraduate School
Monterey, California
7. Professor Ross Baldick
Department of Electrical Engineering
University of Texas at Austin
Austin, Texas,
8. LCDR Rogelio Alvarez
NAVICP Philadelphia
Philadelphia, Pennsylvania